1985

Synthesis and characterization of new reduced scandium chlorides stabilized by interstitial atoms

Shiou-Jyh Hwu
Iowa State University

Hwu, Shiou-Jyh

SYNTHESIS AND CHARACTERIZATION OF NEW REDUCED SCANDIUM CHLORIDES STABILIZED BY INTERSTITIAL ATOMS

Iowa State University PH.D. 1985

PLEASE NOTE:

In all cases this material has been filmed in the best possible way from the available copy. Problems encountered with this document have been identified here with a check mark __√__.

1. Glossy photographs or pages _____
2. Colored illustrations, paper or print _____
3. Photographs with dark background _____
4. Illustrations are poor copy _____
5. Pages with black marks, not original copy _____
6. Print shows through as there is text on both sides of page _____
7. Indistinct, broken or small print on several pages __✓__
8. Print exceeds margin requirements _____
9. Tightly bound copy with print lost in spine _____
10. Computer printout pages with indistinct print _____
11. Page(s) _____ lacking when material received, and not available from school or author.
12. Page(s) _____ seem to be missing in numbering only as text follows.
13. Two pages numbered _____. Text follows.
14. Curling and wrinkled pages _____
15. Dissertation contains pages with print at a slant, filmed as received _____
16. Other _____

_____

_____

University
Microfilms
International

Synthesis and characterization of new reduced scandium chlorides stabilized by interstitial atoms

by

Shiou-Jyh Hwu

A Dissertation Submitted to the
Graduate Faculty in Partial Fulfillment of the
Requirements for the Degree of
DOCTOR OF PHILOSOPHY

Department: Chemistry
Major: Inorganic Chemistry

Approved:

Signature was redacted for privacy.

In Charge of Major Work

Signature was redacted for privacy.

For the Major Department

Signature was redacted for privacy.

For the Graduate College

Iowa State University
Ames, Iowa

1985

TABLE OF CONTENTS

CHAPTER I. INTRODUCTION

Scandium, the first element in 3d series, displays unique chemistry. During the last decade research on binary ($Sc-ScX_3$) and ternary ($M^IX-Sc-ScX_3$) chlorides and bromides has shown the inability of scandium to keep one valence electron and simply make coordination compounds with isolated scandium(II) cations. However, in the heavier rare earth metal halides, compounds with an oxidation state of +2 are found in a number of systems, e.g., $EuCl_2$, $YbCl_2$, $SmCl_2$, and $TmCl_2$, in the order of decreasing in stability. The phase Sc_xI_2,[1] $x\sim0.93$, has a CdI_2-type layer structure which is evidently stabilized by the large iodine anion. The analogous chloride does not exist as the solid phase, yet it was assumed to be the intermediate phase during a vapor transport process.[2] In M^IScX_3 (M = Rb, Cs; X = Cl, Br),[3,4] where scandium has a formal oxidation state of +2, the shortest scandium separation suggests strong metal-metal bonding, e.g., 3.02 A in $CsSc_xCl_3$ (x = 0.79).

A series of metal-rich scandium halides varying in halogen-to-metal ratio, $1 \leq X/Sc < 2$, has been prepared and structurally characterized, namely Sc_7Cl_{12},[5] Sc_2X_3 (X = Cl, Br),[6] Sc_5Cl_8,[2] Sc_7Cl_{10},[7] and ScCl.[8] All these phases except Sc_2X_3 (which has an unknown structure) contain octahedral Sc_6 units which are discrete for X/Sc = 1.71 (Sc_7Cl_{12}), condensed into chains for X/Sc = 1.60 (Sc_5Cl_8), double chains for X/Sc = 1.43 (Sc_7Cl_{10}), or layers for X/Sc

= 1.00 (ScCl). The arrangement of X atoms around the Sc_6 units is equivalent to that in the M_6X_8 (6-8) or M_6X_{12} (6-12) clusters. The X/Sc ratio decreases as more reduced compounds are formed with more cluster condensation. Their crystal structures have revealed the existence of short and presumably strong metal-metal bonding within the octahedral clusters. This stabilizes these solid compounds via a contribution of lattice energy.

In Figure 1, both the 6-8 and 6-12 types of coordinated octahedral clusters (M_6) with their cubic close packed nonmetal atoms (eight and twelve, respectively) are shown. The 6-8 type (top) has face-capping nonmetal atoms while 6-12 type (bottom) has edge-bridging nonmetals. The smaller crowding inherent in 6-8 type is represented by the ideal values of $\sqrt{2}$ and 1 for d_{X-X}/d_{M-M} in 6-8 and 6-12 types, respectively, when X atoms are in contact. However, strong metal-metal bonding together with the larger matrix effect (anion-anion repulsion) in real 6-12 examples results in a configuration in which the metals are often drawn inside the cube on which the nonmetal atoms lie, as shown; in other words, the distortion is probably always a manifestation of nonmetal crowding.[9]

These two types of isolated metal octahedral clusters are well-known in many binary metal halide compounds. The 6-8 parentage evidently exists only with smaller metals (Mo_6Cl_8) or large anions (Nb_6I_8) where 12-coordination of

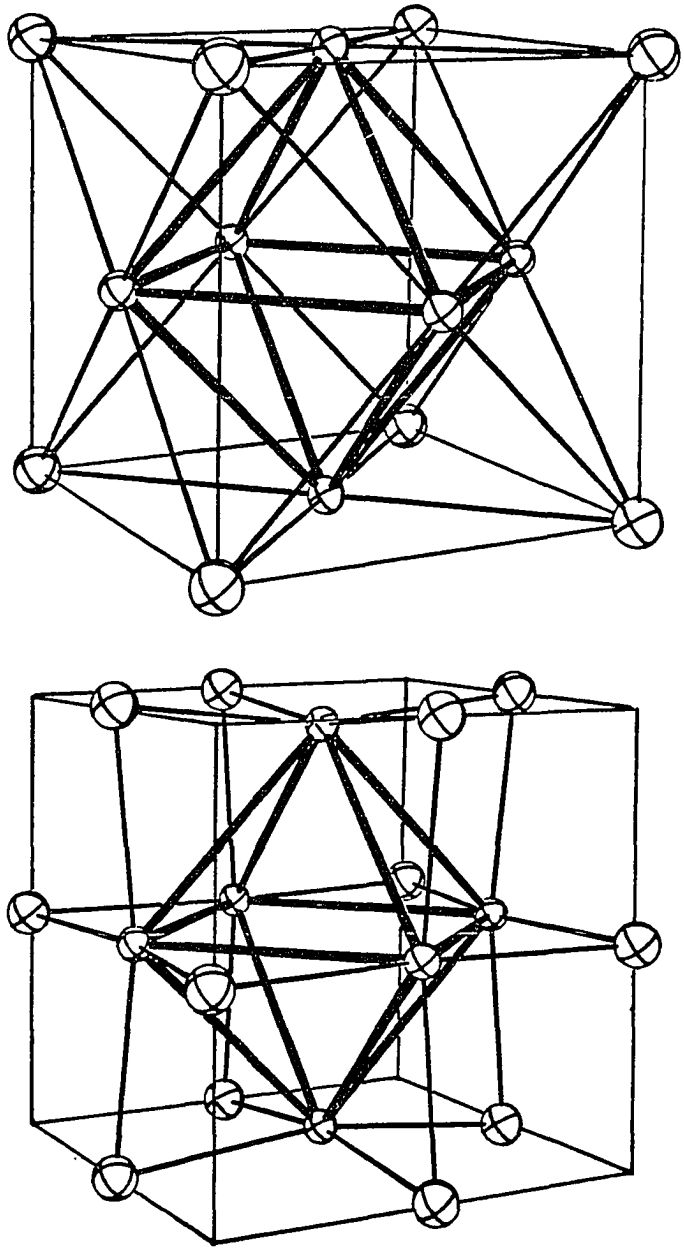

Figure 1. M_6X_8 (top) and M_6X_{12} (bottom) types clusters viewed as metal octahedra face-capped and edge-bridged by nonmetal atoms, respectively.

the metal octahedron by halide appears to unstable because of strong X-X repulsion and the resultant loss of M-M bonding.[9] The compounds with these cluster types receiving the most attention have been those of the group V and VI transition metals located in the second and third row of the periodic table, namely Nb, Ta, Mo and W. In fact, the 6-8 type isolated cluster is known only for $\geq$19 electrons, e.g., $Nb_6I_{11} \equiv Nb_6I_8I_{6/2}$[10] with 5 x 6 - 11 = 19 d electrons, so that too must be a factor in cluster formation.

Values of the average Pauling metal-metal bond order, n, per metal valence electron (PBO/e) for the scandium chlorides mentioned above suggest the presence of strong metal-metal interactions.[9] Why nature chooses 6-12 type, e.g., Sc_7Cl_{12} and Sc_5Cl_8, with an inherently larger matrix effect rather than 6-8 type, e.g., Sc_7Cl_{10} and ScCl, is not always clearly understood.[11] But condensed clusters of 6-8 and 6-12 parentage can be considered to also result from a lack of valence electrons in the metal, especially for group III and lanthanide elements. However, binary zirconium chlorides with 1.0 < Cl:Zr < 3.0 have shown no evidence whatsoever of cluster condensation presumably because zirconium metal has more valence electrons for the same stoichiometry than any of these group III elements.

The number of electrons available for metal cluster bond formation in $Sc_5Cl_8 \equiv (ScCl_2)^+(Sc_4Cl_6)^-$ is 7 per formula unit. Another structurally well-characterized

compound, $Sc_7Cl_{12} \equiv Sc(Sc_6Cl_{12})$, has as few as nine electrons per Sc_6 cluster. Both compounds were reported[2,5] to be the two least reduced binary phases. Yet, the structural study of Sc_7Cl_{12} showed a residual electron density in the center of the Sc_6 cluster amounting to Z = 7.6 based upon refinement of oxygen in this position. In addition, these two phases have presented synthetic problems, namely nonreproducible and low yield results.[2,5,11] Other compounds in the lanthanide or early transition metal halides systems, e.g., Er_7I_{10},[12,13] Ln_7I_{12} (Ln = La, Tb, Er),[13] Zr_6Cl_{15},[5] Zr_6I_{12},[14] and $CsZr_6I_{14}$[15], have had similar problems with low yields, unreproducible syntheses or residual electron densities. The yield could have been low because of the kinetic problem, surface blockage for example. At the time these structures were reported, possibilities cited for the source of residual peaks included interstitial atoms or errors in the X-ray diffraction data.

However, the inclusion of nonmetals in the centers of metal clusters has been recently reported for a number of reduced metal halides that contain either isolated clusters or clusters in the condensed arrays noted above. The first well-characterized example of a nonmetal in the center of an octahedral cluster was the compound $Nb_6I_{11}H$.[10] Reports of other examples of hydrogen in metal-metal bonded arrays have more recently appeared, i.e., MXH_x (M = Y[16] or Zr;[17,18] X =

Cl or Br) and $CsNb_6I_{11}H$.[19] The first well-characterized example of a second period metal in such an array was reported by Seaverson and Corbett,[20] who found that oxygen occupied tetrahedral sites between the double metal layers of $ZrClO_{0.4}$. Other examples followed rapidly. Warkentin and coworkers reported a number of rare earth metal halides that contained carbon, nitrogen or dicarbon units in the centers of metal-metal bonded clusters.[21,22] It was also found that carbon could be included in the octahedral interstices between the double metal layers of the yttrium monohalide structure to give compound of the composition Y_2Cl_2C.[23]

These results suggested previously described structures with residual electron densities in the center of the clusters might really have contained small interstitial elements. Very recently, syntheses in the other systems with potential interstitial elements purposely added have also given products in high yields, namely $Zr_6I_{12}C$, $Zr_6I_{14}C$, $MZr_6I_{14}C$ (M = K, Rb, Cs), and $Zr_6Cl_{15}N$.[24,25] Ziebarth[26] has currently expanded this area of synthesis by presenting a number of structurally related new compounds in Zr-Cl system containing interstitials, namely Be, B, C, or N. The single crystals of interstitially-stabilized phases obtained before in low yields probably formed because of trace impurities in the pseudo-binary syntheses.

In the course of this work, number of pseudo-binary phases were serendipitously found in the Sc-Cl system, e.g., "1T-ScCl", "β-Sc_2Cl_3", and "Sc_7Cl_{10}". At the end of each single crystal study, a residual peak (Z = 5-7) in the center of the scandium octahedron appeared in the final electron density difference maps. Then, deliberate attempts to prepare these compounds with the potential second period interstitials, e.g., B, C and N, gave nearly quantitative yields. The compound $ScClH_x$ with hydrogen in Sc-Sc bonded arrays has also been synthesized in this system. Reactions that were conducted in conjunction with either negative results or low yield reactions directly related to $ScClH_x$ problems also demonstrated that some alkali metal atoms could intercalate into the chlorine octahedral interstices in the van der Waals gap in the compounds such as $M^I_zScClH_x$ (M^I = Li, Na, K, etc.). Also, results and some indirect evidence have suggested that the materials reported as "Sc_7Cl_{12}",[5] "Sc_5Cl_8",[2] and "ScCl"[8] might be $Sc_7Cl_{12}O$, Sc_5Cl_8C and $ScClH_{0.3}$, respectively. The isostructural phases, $Sc_7Cl_{12}X$ (X = B, N) and Sc_5Cl_8N were also prepared.

The number of isostructural phases that have been prepared and structurally characterized also allows a careful examination of factors that have a pronounced effect on the degree of metal-metal bonding of these materials. Besides, several physical measurements that were restricted by the quantities of the products obtained before, have been

carried out to further reveal some physical properties of these materials. It is hoped that the reader will gain some insight and guidance for further investigations of this unique element scandium and its extensive chemistry.

CHAPTER II. EXPERIMENTATION

Materials

Scandium metal

The metal used was available within the Ames Laboratory. It was prepared by metallothermic reduction of ScF_3 by triply distilled calcium metal. The purity was of the order >99.9 at.% with the typical impurities (ppm atomic) of O-90, N-10, H-320, C-236, F-185, Fe-39, W-15, Y-2, Ce-3, Nd-7, other lanthanide, <2. However, some variability among the batches was unavoidable.

The material used in the syntheses of reduced chlorides was either in the form of rolled strips about 1.0 x 0.5 x 0.02-cm or 100-mesh powder produced by decomposition of the ground hydride in high vacuum at 700-750°C (H:Sc = 0.09:1 by vacuum fusion). In the dehydrogenation of scandium dihydride, a liquid nitrogen trap was placed between the apparatus and vacuum line to minimize contamination by moisture or hydrocarbons. Otherwise these gas species will react with powdered metal at the dehydrogenation temperature and produce contaminating products. Metal turnings, which ordinarily give more surface area than strips, were used to synthesize trichloride.

Both strips (electropolished) and turnings were stored in a canning jar inside an Ar-filled dry box equipped with a tray of P_2O_5 and constantly purged with dry nitrogen or argon that was recirculated through a Molecular Sieve

column. The moisture level was maintained <1 ppm. The oxygen level was improved by a second column containing Ridox. A 25 watt light bulb without glass burned for 3-4 hours inside the dry box atmosphere. Powdered metal was stored in sealed ampules.

Scandium trichloride

Anhydrous scandium trichloride was prepared by the reaction of scandium metal with electronic grade HCl gas in a modified flow system of the design described by Löchner.[27] Scandium metal (turnings and/or strips) used in the trichloride synthesis was recovered from previous binary systems. The crude scandium trichloride was purified by four sublimations (ca. 10^{-5} to 10^{-6} torr, dynamic vacuum; 750°C). A two-compartment tantalum apparatus[27] was used for the sublimation to condense the scandium trichloride at the cold end as well as keep it from reacting with the fused silica jacket. The color of the final product is off-white.

Some special precautious should be followed when working with highly hygroscopic materials such as this. Since powder has a great surface area, it tends to pick up moisture even while exposed to the dry box atmosphere. Chunks and/or macrocrystalline material are preferred to reduce the problem. These materials should be stored in individual evacuated Pyrex ampules with enough quantity to load several reactions at once, ca. 1.5 to 2.0 grams total. Water and/or Sc_2O_3 react with $ScCl_3$ to form, on heating,

ScOCl as a white powder or transparent purple red flakes. Repeated exposure of $ScCl_3$ to the dry box atmosphere invariably produces some ScOCl contaminant in the products. Therefore, $ScCl_3$ should be the last reactant loaded in a reaction tube in order to minimize the problem.

Interstitial elements

A 95% purity amorphous boron (325 mesh, Alpha) was kindly supplied by M. Ziebarth, University of Wisconsin. Crystallized boron was obtained from Dr. R. N. Shelton of Ames Laboratory. The lattice parameters of borides prepared from either source of boron did not differ significantly. The amorphous boron gave more nearly complete reactions, presumbly because of its much higher surface area.

Spectroscopic grade powdered graphite (National brand, Union Carbide Corp.) was obtained from E. Dekalb of Ames Laboratory. It was degassed at 850°C for a few hours under dynamic vacuum and then stored in tightly stoppered vials in the dry box. Both nitrogen and hydrogen gas reactant (Air Products, Allentown PA.) were in 99.5% purity.

The NaN_3 (99%, Aldrich Chemical Co., Milwaukee, WIS.) used in nitride synthesis was as a white powder.

General Synthetic Techniques

The reactions were carried out in sealed tantalum or niobium containers since scandium trichloride and its reduction products readily attack Pyrex or fused silica under the conditions used. The reaction tubes were cleaned

in tantalum cleaning solution (55% conc. H_2SO_4, 25% conc. HNO_3, and 20% conc. HF, by volume). One end of the tube then was crimped and welded. It is not desirable to use cleaning solution after the first weld. Otherwise, the white residue that may be left in the crimped end has been suggested to be a possible source of the interstitial impurities in the original syntheses of some of these phases.[26]

Next the reaction mixtures were loaded. The specific conditions and techniques used in the preparation of different reduced ternary scandium chlorides will be dealt with separately in the chapters III and IV. Since the materials are all hygroscopic and/or air sensitive, especially $ScCl_3$ and the reduced chlorides, manipulations were performed in the dry box.

The loaded and crimped shut reaction containers (two to three at a time) were then transferred quickly through the air into a heliarc welder and sealed off under 500 mm of helium. Reaction tubes were held in place by brass heat sinks. Use of a high current prevented heating and loss of volatile reactants.

Reaction tubes (0.95-cm o.d.) were 5-cm in length for isothermal equilibration and 8-13-cm in length for temperature gradient reactions. These containers were sealed in a fused silica jacket in order to prevent atmospheric oxidation of the tubes at reaction temperature. Prior sealing the jacket, the containers were briefly washed with tantalum

cleaning solution to remove any tantalum or niobium oxide formed during the glass blowing. Also, the jacket was flamed under dynamic vacuum at red hot temperature (ca. 800°C)[28] to hinder oxygen and hydrogen contamination of the products. Chromel-alumel thermocouples were placed on the outside of the jacket to monitor reaction temperatures.

To make a high yield of a powdered product, about 150 to 200 mg of $ScCl_3$ and excess scandium strips, or a stoichiometric amount of metal powder, were loaded into a niobium tube along with proper amount of any interstitial element. To separate the interstitial elements or scandium powder from trichloride, the metal tube was sometimes lightly crimped once or twice at the middle prior to heating. The reaction period was as short as one week at 860 to 1000°C. Trace amounts of ScOCl were occasionally found in the reaction products besides the excess scandium strips. Vapor transport reactions usually take a long period of time (4-6 weeks) to grow crystals large enough for crystallographic examination. Transport is a very good way of separating products from each other as well as from any of the melts in this type of research. For example, in the $Sc/ScCl_3/B$ system with a 940/900°C gradient, three different phases were found, namely melts, Sc_4Cl_6B and $Sc_7Cl_{12}B$ distributed from the high to low temperature regions, respectively.

Nitride syntheses used nitrogen gas or NaN_3 powder. The former gave better yields in making $Sc_7Cl_{12}N$, Sc_5Cl_8N and Sc_4Cl_6N. However, these products were not formed quantitatively, primarily because of the small volume of nitrogen gas that can be enclosed into the reaction tubes. The tubes contained elemental nitrogen (1 atm) from the dry box. Instead of pumping out the N_2 completely, the welder system was barely pumped to just hold the door shut. The parallel reaction with thorough pumping before welding gave no nitride compounds at all but $ScCl_x$ melts.

Reactions were air-quenched unless otherwise noted. All reaction containers were opened in a dry box designed for crystal mounting. The latter was filled with dry N_2 and equipped with a nearly horizontal window. A binocular microscope mounted above the window allowed careful optical examination of reaction products. When appropriate, single crystals for X-ray diffraction were then mounted in 0.2-0.5-mm o.d. glass capillaries. The crystals were kept stationary in the capillary with Vaseline grease. Most reaction products were stored under vacuum in sealed glass ampules.

Characterization

Powder X-ray diffraction

Guinier diffraction was used to identify reaction products, occasionally to judge relative yields, and to obtain precise lattice parameters. Patterns were

photographically recorded using a Hägg-Guinier camera equipped with a silicon monochromator to give only Cu $K\alpha_1$ (λ = 1.54056 A) radiation. A rotating circular sample holder was used to give sharp patterns. Samples were mounted between layers of Scotch tape in a nitrogen-filled dry box. NBS (National Bureau of Standards) silicon was mixed with the sample as an internal standard as previously described.[29] This calibration method gave a and c lattice constants for NBS α-Al_2O_3 that agreed with the reported values within 0.8 and 2.5 parts in 10^4, respectively. Most of the samples did not diffract very strongly. One of the reasons was that the heaviest elements in the structure, Sc and Cl, were not good scatterers. Therefore, four to five hour exposures were often employed. The diffraction maxima were measured with a Nonius Guinier Viewer to an uncertainty of ±0.005 mm. These were converted to 2θ values by applying a quadratic equation obtained from the least-square fit of the positions of the six silicon lines to known diffraction angles using the program GUIN.[30] The patterns were indexed and lattice parameters obtained from the least squares program LATT[31] with constraint to the indicated crystal system.

Cell parameters of the compounds investigated are listed in Table I. Calculated powder patterns of known or postulated structures were obtained from the program POWD[32] and were automatically plotted on the scale of the Guinier

Table I. Cell parameters of reduced ternary scandium chlorides stabilized by interstitial atoms

Compound	a (A)	b (A)	c (A)
$Sc_7Cl_{12}B$	13.0145(9)		8.899(1)
$Sc_7Cl_{12}N$	12.990(2)		8.835(1)
Sc_4Cl_6B	11.741(1)	12.187(1)	3.5988(3)
$Sc_4Cl_6N(1)$[b]	11.634(4)	12.144(3)	3.550(3)
$Sc_4Cl_6N(2)$[b]	11.625(4)	12.118(3)	3.5447(7)
$Sc_4Cl_6N(3)$[b]	11.625(6)	12.094(4)	3.543(2)
Sc_5Cl_8C	17.80(1)	3.5259(7)	12.052(7)
Sc_5Cl_8N	17.85(1)	3.5505(7)	12.090(8)
$Sc_7Cl_{10}C_2(1)$[b]	18.634(2)	3.5131(4)	11.834(1)
$Sc_7Cl_{10}C_2(2)$[b]	18.620(4)	3.4975(6)	11.810(2)
$Sc_7Cl_{10}C_2(3)$[b]	18.613(5)	3.4960(7)	11.806(2)
Sc_2Cl_2C	3.3997(8)		8.858(3)
Sc_2Cl_2N	3.3495(4)		8.808(1)
ScClH	3.4785(8)		26.531(8)

[a]The number of lines from Guinier powder pattern to use in LATT (reference 31) calculation, unless otherwise noted. AL = Ames Laboratory diffractometer. [b]The number in the parentheses indicates as the phase number; see text.

α (deg.)	β (deg.)	γ (deg.)	V (A^3)	# lines[a]
90.0	90.0	120.0	1305.4(2)	27
90.0	90.0	120.0	1291.1(4)	27
90.0	90.0	90.0	514.9(1)	30
90.0	90.0	90.0	501.5(3)	24
90.0	90.0	90.0	499.3(2)	15(AL)
90.0	90.0	90.0	498.0(4)	18
90.0	130.11(4)	90.0	578.6(4)	20
90.0	130.13(4)	90.0	585.9(4)	21
90.0	99.77(1)	90.0	763.4(1)	14
90.0	88.81(2)	90.0	757.9(2)	18
90.0	99.78(2)	90.0	757.1(3)	21
90.0	90.0	120.0	88.66(7)	11(AL)
90.0	90.0	120.0	85.58(3)	10(AL)
90.0	90.0	120.0	277.0(2)	9

camera by the program PPPLOT.[26] The powder patterns of many well-characterized materials were obtained from standard diffraction files.[33] Appendix A provides both the calculated and observed Guinier powder patterns of the phases under consideration.

Single crystal X-ray diffraction

Single crystal x-ray diffraction was used as a tool to reveal accurate molecular geometries and stoichiometries.

A summary of crystallographic data is listed in Table II. The first R/R_w values are for the refinements with unit occupancy of corresponding interstitial atoms. The refined occupancies and their isotropic B values are listed separately at the bottom of the table while the R/R_w values are reported right underneath them. In some cases, the isotropic temperature factor B could not be refined simultaneously with the corresponding occupancy. Therefore, a fixed B was obtained from mean anisotropic temperature factors (B) of Sc and Cl atoms by the program GEOMK.[34]

Oscillation photographs were often used to determine if a crystal was single. Both zero-level and first-level Weissenberg photographs (Charles Supper Co.) were taken to obtain cell constants and symmetry information. These also served as checks for superlattice reflections.

Three automatic four-circle diffractometers were used in this reaearch, namely the Ames Laboratory diffractometer,[35,36] a commercial SYNTEX $P2_1$, and a DATEX

Table II. Crystallographic data for single crystal investigations

	$Sc_7Cl_{12}B$	$Sc_7Cl_{12}N$	Sc_4Cl_6B	Sc_4Cl_6N (1)[a,b]	Sc_4Cl_6N (2)[a,b]	Sc_5Cl_8C	Sc_5
Space group	$R\bar{3}$	$R\bar{3}$	Pbam	Pbam	Pbam	C2/m	C
Z	3	3	2	2	2	2	
Crystal dimensions (mm)	0.46 0.30 0.25	0.26 0.20 0.14	0.40 0.02 0.02	1.50 0.02 0.04	1.50 0.03 0.06	0.30 0.01 0.01	0. 0. 0.
Diffractometer[c] Scan mode[d]	S T	D W	D W	D W	A W	D W	
$2\theta_{max}$ (deg.)	55	60	60	50	50	60	
Reflections measured[e] observed independent	966 846 589	3071 2060 621	1770 1134 580	2130 1713 468	1899 1426 464	2070 554 305	13 9 6
R_{ave} (%)	1.6	6.1	3.0	6.5	6.5	5.4	3
R/R_w (%)[f]	3.2/4.0	4.2/4.9	3.5/4.1	8.4/15.1	7.7/11.1	7.2/8.1	5.4
2nd extinction coeff. (10^{-5})	10.0(1)	3.2(3)	—	—	—	—	
Absorption coeff. (cm^{-1})	44	44	40	41	41	46	
Range of trans	0.75-1.00	0.88-1.00	0.89-1.00	0.57-1.00	0.81-0.99	0.83-1.00	0.9 1.
Interstitial							
Occupancy (%)	100(4)	80(2)	105(4)	102(8)	96(6)	120(2)	8
Iso. $B(A^2)$[g]	0.1(1)	0.23[h]	0.9(2)	0.5(5)	1.1(4)	4(2)	0.02
R_w (final %)	3.0/3.8	4.0/4.7	3.4/4.0	8.4/15.1	7.5/11.0	7.1/8.1	5.4

[a]Residual electron densities at 1/2,0,1/2 were 1.2 and 2.5 e/A^3 for cry
A=Ames Laboratory Diffractometer. [d]T = 2θ/θ-scan, W = ω-scan. [e]Reflections
are reported with interstitial atoms at unit occupancy. [g]Isotropic temperat
[h]The fixed B is an average of the isotropic values for Sc and Cl, see text.

c_5Cl_8N	$Sc_7Cl_{10}C$ (1)[b]	$Sc_7Cl_{10}C_2$ (2)[b]	$Sc_7Cl_{10}C_2$ (3)[b]	Sc_2Cl_2C (1T-)	Sc_2Cl_2N (1T-)	ScClH (3R)
C2/m	C2/m	C2/m	C2/m	$P\bar{3}m1$	$P\bar{3}m1$	$R\bar{3}m$
2	2	2	2	2	2	6
0.40	0.50	0.40	0.50	0.20	0.20	0.25
0.03	0.05	0.04	0.06	0.16	0.18	0.20
0.02	0.02	0.02	0.03	0.05	0.05	0.02
D W	A W	A W	S T	A W	A W	D T
60	50	50	55	50	50	60
1364	1733	1708	1820	436	424	596
942	1287	1398	670	362	374	464
683	630	676	426	73	76	73
3.0	4.2	2.4	2.4	5.3	4.9	7.8
5.4/8.5	3.6/4.8	2.9/4.7	3.8/4.1	3.5/5.3	5.0/6.2	9.0/10.7
–	–	–	–	–	–	–
45	41	47	47	50	53	49
).93-1.00	0.87-0.98	0.83-1.00	0.75-1.00	0.70-1.00	0.77-0.98	0.64-0.98
89(4)	123(3)	109(3)	129(4)	118(7)	110(4)	–
02(24)	1.0(1)	1.2(2)	3.8(5)	2.1(4)	1.7(4)	–
5.4/8.5	3.5/4.6	2.9/4.6	3.8/4.1	3.2/5.0	5.0/6.0	–

crystal 1 and 2, respectively. [b]See text. [c]S = SYNTEX $P2_1$, D = DATEX, ons with $F_{obs} \geq 3\sigma_F$ and $I_{obs} > 3\sigma_I$ were considered observed. [f]Values ature factor B was varied simultaneously with occupancy, unless noted.

diffractometer, which was used the most. The details of each instrument, indexing procedure and their software are described by Smith[37] and elsewhere.[38]

All data sets were collected with the maximum $2\theta = 50^{o}$ to 60^{o}. Three standard reflections ($2\theta > 25^{o}$) were rechecked every 75 reflections to monitor instrument and crystal stability. No significant decay was observed in any of the data sets. At least two octants of data were taken for centric space group. The PHI scan for absorption correction (tuned peaks with $\chi = 90\pm10^{o}$ or 270 ± 10^{o} and moderate intensity) and LATT (tuned Friedel-related peaks for cases that lacked an acceptable Guinier powder pattern) were run after finishing data collection.

The poorer quality single crystals (mostly the plate or needle shaped crystals) often had streaked spots on the Weissenberg photographs. If the normal ω-scan was chosen for data collection, rather high background was obtained because of the broadening of the peaks. Increasing the scan steps to cover whole width of peaks or changing to $2\theta/\theta$-scan improved the results significantly. Experience showed the latter method gave more accurate peak maxima since peaks were scanned normal to the streaking direction. For example, least-square refinement of data for a plate of 3R-ScClH (ZrCl-type), gave R/R_w values of 0.171/0.163 (ω-scan), 0.093/0.112 (increasing scan steps), and 0.090/0.107 ($2\theta/\theta$-scan).

Empirical absorption corrections, using the diffractometer ψ-scan data and the program ABSN,[39] were applied to all data sets. The data were then reduced using DATRD[40] with the appropriate extinction conditions applied where necessary, and the observed reflections ($I > 3\sigma(I)$) were corrected for Lorentz-polarization[39] effects, and their standard deviations were calculated as usual. The data sets were averaged using FDATA.[41] Any reflection which differed from the average of its symmetry equivalent set by more than 6σ was omitted. Structure factor calculations and least squares refinement using only neutral atom scatterers were done using the full matrix program ALLS.[42] The residual indices $R = \Sigma||F_o| - |F_c|| / |F_o|$ and $R_w = [\Sigma\omega(|F_o| - |F_c|)^2 / \Sigma\omega|F_o|^2]^{1/2}$ with $\omega = \sigma_F^{-2}$ are reported. Fourier syntheses were accomplished with FOUR.[43] All calculations were carried out on a VAX 11-780 computer.

Since most of these phases, except Sc_4Cl_6X (X = B, N), $Sc_7Cl_{10}C_2$ and 1T-Sc_2Cl_2X (X = C, N), were isotypic with materials whose structures had been previously determined, structure refinements were started with scandium and chlorine positions from known structures. The Sc_4Cl_6X (X = B, N) structure was found to be isomorphous with "β-Tb_2Br_3"[44] by comparison of observed with calculated powder patterns. Initial coordinates for the scandium and chlorine atoms were based on the latter. For $Sc_7Cl_{10}C_2$,[45] a sharpened Patterson map showed that many of the same

structural features of Sc_7Cl_{10} remained according to the u,o,w and u,1/2,w sections. The atomic coordinates for the related structure of Er_7I_{10}[12] provided the correct model.

In general cases, after the anisotropic refinement of heavy atoms, difference Fourier syntheses gave residuals of 5 to 7 e/A^3 in the center of the metal clusters. Interstitial hydrogen could not be located because of its small scattering power. It was believed, because of the high yield in the synthesis using purposely added interstitial elements, that the corresponding atom did occupy the center of the cluster and gave the residual density. Isotropic refinement with an interstitial atom at unit occupancy lowered the R factor by about five percent. In addition, there is no synthetic or X-ray evidence for substoichiometric phases in any of these cases except the scandium monochloride hydrides. The structural refinement of the multiplicity of each interstitial atom gave unit occupation within 3σ except for $Sc_7Cl_{12}N$, Sc_5Cl_8C, $Sc_7Cl_{10}C_2$ (crystals 1 and 3) probably due to the crystallographic problems (Table II).

In rare cases, as with $Sc_7Cl_{12}X$ (X = B, N) gems, a secondary extinction correction was necessary to clarify the status of the cluster centers. Inclusion of a correction resulted a better agreement of F_{calc} and F_{obs} particularly with high intensity reflections which had larger F_{calc} values before the extinction correction was applied.

Whether this was a result of the "perfectness" of the crystal is uncertain.[37] Yet, the secondary extinction correction was sometimes not necessary or even important, especially for the needle-shaped crystals. The final difference Fourier synthesis map showed <1 e/A^3 in all regions, except for Sc_4Cl_6N (1 and 2), see Chapter III. The general temperature-factor expression of an atom for a given set of planes (hkl) is $\exp[-\frac{1}{4}(B_{11}h^2a^{*2} + B_{22}k^2b^{*2} + B_{33}k^2c^{*2} + 2B_{12}hka^*b^*\cos\gamma^* + 2B_{13}hla^*c^*\cos\beta^* + 2B_{23}klb^*c^*\cos\alpha^*)]$, where the B_{ij} are the thermal parameters in the same units as the conventional isotropic thermal parameter B.

The calculated and observed structure factors for all phases under consideration are listed in Appendixes B-K.

Analytical data, especially the quantitative analysis for interstitial elements, are not available because of a lack of large crystals to give representative samples. Analysis on a powder product would only give an analytical result of what was put into the reaction mixture. For these reasons, the single crystal structure refinements not only gave the molecular dimensions, but also revealed the important structure compositions to a reasonable extent for atoms heavier than lithium.

All drawings of the structures were produced using the program ORTEP,[46] with thermal ellipsoids drawn at the 50% probability level unless otherwise indicated.

Photoelectron emission spectroscopy

Both XPS and UPS spectra were collected using an AEI-200B spectrometer and Al Kα X-ray radiation at 1486.6 eV or the He(I) line at 21.2 ev, respectively. In order to prevent the surface contamination by oxidation, the unopened metal reaction tubes with the products were introduced into a dry box (<1 ppm H_2O, O_2) attached directly to the spectrometer. The tubes were opened immediately prior to mounting. After being ground in an agate mortar, the samples were evenly spread on double-sided cellophane-tape or on an indium substrate. The inevitably adventitious carbon was used for calibration (≡ 285.0 eV). Data were obtained by signal averaging using a Nicolet 1180 computer system.

Magnetic susceptibility

Magnetic susceptibility measurements were done with a SQUID (Superconducting Quantum Interference Device) magnatometer equipped with an HP85B computer and HP82901M flexible disc drive for data processing. Powdered samples (ca. 14 to 35 mg) were packed into the long, uniform, 3 mm-o.d. fused silica tubes to about 0.5 to 0.7-cm height under vacuum and sealed. The sample tube was then glued (with GE 7030 glue) into a plastic tube which was connected to the metal suspension rod. The magnetic moment was measured at 4K and extended to 340K with a fixed magnetic field.

Electron microprobe analyses

Microprobe analyses were conducted on "$K_xSc_4Cl_6$" and $Sc_7Cl_{10}C_2$ samples by F. Laabs using an Applied Research Laboratories Model EMX electron microprobe, formerly available in Ames Laboratory. Samples were transferred by attaching a plastic glove bag flushed by dry nitrogen to the entry port of the spectrometer.

Extended Hückel calculations

Theoretical band and molecular orbital calculations were done by the extended Hückel method that has been previously described.[47,48] The atomic orbital energies not included in these programs were obtained elsewhere.[49] Geometries of clusters and atomic orbital parameters are given in Appendix L.

CHAPTER III. RESULTS: M_6X_{12}-TYPE CLUSTER COMPOUNDS STABILIZED BY THE INTERSTITIAL ELEMENTS B, C, N

Interstitial-Centered, Discrete Cluster Compounds. The Synthesis and Characterization of $Sc_7Cl_{12}X$, (X = B, N)

Introduction

The compositions Sc_7Cl_{12} and Zr_6Cl_{15} were the first discrete cluster compounds of the group III and IV metals.[5] These early transition metal chlorides have isolated 6-12 type clusters and are formed in chemical transport reactions at 880/900°C and 750/600°C, respectively, as black, truncated blocks with well-formed faces.

The orginal crystal structure determinations of Sc_7Cl_{12} and Zr_6Cl_{15} had shown residual electron density in the center of both clusters, amounting to Z = 7.6 (Sc) and 6 (Zr) based on refinement of oxygen in these positions. These would be, otherwise, novel compounds in terms of the presence of strong metal-metal bonds for metals that have enough radial extension of their outermost valence orbitals to overcome the matrix effect from anion-anion repulsion. The yields of these products were low and not reproducible, raising suspicions about the presence of a real impurity atom in the center of the clusters which stabilizes compound formation. After the later discovery of Sc_2Cl_2C (see following) which was abundantly synthesized with graphite in a ternary system, the interstitial compounds $Sc_7Cl_{12}X$ (X = B, N) and $Zr_6Cl_{15}N$ were prepared. The "Zr_6Cl_{15}" has since

been confirmed to actually be $Zr_6Cl_{15}N$.[25]

In this section, the synthesis and characterization of $Sc_7Cl_{12}X$ will be discussed. The interstitial-centered, discrete $Sc_6(X)$ cluster of these compounds provides a very good model for MO calculations which allow the qualitative descriptions of the bonding character of interstitial in the metal octahedra.

Experimental

Synthesis The polycrystalline $Sc_7Cl_{12}B$ was synthesized at 860°C (two weeks) using stoichiometric amounts of Sc, $ScCl_3$, B powders. The yield was larger than 95%. With the same conditions but scandium strips, the yield was 80% with the coexistence of the $ScCl_{1.5}$ (mouse fur) phase. At a reaction temperature of 740°C, the $ScCl_{1.5}$ was the dominant product with a small portion of an unknown powder. The single crystals of $Sc_7Cl_{12}B$ were found in a higher temperature gradient reaction, 900/940°C, in which the scandium strips were used and placed at the hot end of the tube. These gem-like crystals (25% yield, visual estimation) were at the cold end of the tube while Sc_4Cl_6B (70% yield, as fat needles) were at the hot end.

Attempts to prepare quantitative yield of $Sc_7Cl_{12}N$ however, were not very successful. The main problem was the choices of the source of nitrogen. At first, elemental nitrogen gas was sealed in the reaction container as described in Chapter II. This method turned out to give at

most ca. 10% yields from stoichiometric amounts of $ScCl_3$ and Sc powders at 860°C or 950°C reaction temperatures. The "low" yield results from the small amount of nitrogen which can be sealed in the reaction tube. In the other reactions with NaN_3 powder as the source of nitrogen, the products were 1T-Sc_2Cl_2N (see following) at reaction temperatures as low as 735°C. The single crystals of $Sc_7Cl_{12}N$ studied (5% yield) were obtained at 950°C (5 weeks) in the nitrogen-filled ternary reaction using Sc, $ScCl_3$ powders, and the co-products were Sc_5Cl_8N (5%), ScOCl (5%), and melts, $ScCl_x$.

Single crystal examination The title compounds are all isomorphous with "Sc_7Cl_{12}"[5], in the space group $R\bar{3}$, Z = 3. The lattice parameters and the crystallographic data are in Tables I and II, respectively.

$Sc_7Cl_{12}B$ One octant, a total of 981 reflections, was collected in primitive rhombohedral cell with 2θ between 5.83 and 54.90°. Two PHI scans were taken at 2θ = 13.87 and 23.63° for absorption correction at φ angles that were not evenly divided by 10. Since the ABSN program for absorption correction was written to expect φ value evenly divisible by 10, all these reflections and their intensities were converted to those appropriate for ABSN by linear interpolation using program PHINUM.[50] It turned out that the PHI scan did not give too much of the correction because the crystal was somewhat symmetrical (Table II).

In order to use the atom positions from the hexagonal setting as in reported "Sc_7Cl_{12}" and to make a comparison with it, the rhombohedral setting was transferred to equivalent trigonal setting ($-h + k + l = 3n$) by using the transformation matrix: $h_H = h_R - k_R$, $k_H = k_R - l_R$ and $l_H = h_R + k_R + l_R$. Only 14% of the reduced reflections (846 with 3σ cut off) were duplicate which gave $R_{ave} = 0.016$.

The structure was first solved with a fully occupied boron position with isotropic B = 1.5 at center of the cluster where extra electron density appeared in original structure.[5] The difference Fourier synthesis map at this stage of refinement was flat at both atom sites and elsewhere. The secondary extinction correction was applied and dropped R/R_w to 0.034/0.041. Then, the isotropic B for the boron atom was refined to 0.10(9) (Table II). The occupancy and the temperature factor, B, of interstitial boron atom were refined simultaneously, resulting in a composition $Sc_7Cl_{12}B_{1.00(3)}$ (Table II). The thermal parameter of the boron atom was varied anisotropically to give a small spherical thermal ellipsoid and with no change in the positional and thermal parameters for the other atoms. Reweighting the averaged data set[37] to make the best quality of fit had no effect. The final positional and thermal parameters for $Sc_7Cl_{12}B_{1.0}$, as well as for $Sc_7Cl_{12}N_{1.0}$ (see below), are listed in Table III.

Table III. Positional and thermal parameters for $Sc_7Cl_{12}X$ (X = B, N) and "Sc_7Cl_{12}"[a]

	x	y	z
$Sc_7Cl_{12}B$			
Sc1	0.0	0.0	0.5
Sc2	0.1630(1)	0.0439(1)	0.1502(1)
Cl1	0.3106(1)	0.2295(1)	0.0058(1)
Cl2	0.1292(1)	0.1791(1)	0.3354(1)
B[b]	0.0	0.0	0.0
$Sc_7Cl_{12}N$			
Sc1	0.0	0.0	0.5
Sc2	0.1616(1)	0.0438(1)	0.1492(1)
Cl1	0.3104(1)	0.2292(1)	0.0051(1)
Cl2	0.1300(1)	0.1803(1)	0.3351(1)
N[b]	0.0	0.0	0.0
"Sc_7Cl_{12}"			
Sc1	0.0	0.0	0.5
Sc2	0.1608(1)	0.0435(1)	0.1476(1)
Cl1	0.3103(1)	0.2290(2)	0.0052(1)
Cl2	0.1298(2)	0.1801(1)	0.3340(1)
Cl3[a,c]	0.0	0.0	0.0

[a]References 5 and 10. [b]Occupancy = 1.0. [c]Occupancy = 0.46(1), see text.

B_{11}	B_{22}	B_{33}	B_{12}	B_{13}	B_{23}
1.31(3)	B_{11}	4.89(6)	$1/2B_{11}$	0.0	0.0
0.66(2)	0.77(2)	0.90(2)	0.35(1)	-0.12(1)	-0.05(1)
0.69(2)	1.10(2)	1.16(2)	0.24(1)	-0.16(1)	0.23(1)
1.11(2)	1.26(2)	0.96(2)	0.67(1)	-0.12(1)	-0.16(1)
0.10(9)					
0.83(5)	B_{11}	6.20(15)	$1/2B_{11}$	0.0	0.0
0.78(3)	0.77(3)	1.12(3)	0.38(2)	-0.03(2)	-0.04(2)
0.75(3)	1.17(4)	1.46(4)	0.27(3)	-0.14(2)	-0.24(3)
1.20(4)	1.31(4)	1.29(4)	0.71(3)	-0.13(2)	-0.20(2)
1.02(12)					
0.95(6)	B_{11}	6.52(17)	$1/2B_{11}$	0.0	0.0
0.88(4)	0.79(4)	1.10(5)	0.41(3)	-0.01(1)	-0.02(1)
0.94(6)	1.25(6)	1.49(7)	0.36(2)	-0.12(1)	0.23(3)
1.42(5)	1.14(6)	1.37(7)	0.66(14)	0.24(3)	0.11(3)
1.25(19)	B_{11}	1.34(25)	$1/2B_{11}$	0.0	0.0

$Sc_7Cl_{12}N$ Three octants of 3071 reflections were collected in hexagonal cell. Only one PHI-scan with θ = 26.13° was collected and used in ABSN. It also gave only a small absorption correction since the crystal was nearly spherical. About 92% of the duplicate data set were averaged to give R_{ave} = 0.061.

During the structure determination, all the heavy atoms were refined anisotropically to the result R/R_w = 0.107/ 0.130. A residual peak ca. 5/A^3 was left in the center of the Sc_6 cluster based on a difference Fourier synthesis map. With isotropic refinement for nitrogen as the interstitial at the center, the results in Table II were obtained. Atomic positions and the thermal parameters are in Table III. Refinement with the secondary extinction factor made no improvement at all. The occupancy of nitrogen atom could not be refined simultaneously with its temperature factor. A reliable B value for the refinement of the occupancy of nitrogen atom site was obtained with the program GEOMK[34] which calculates the mean anisotropic B values of the other atoms. The structure was refined with this calculated B(0.23) to give an empirical composition $Sc_7Cl_{12}N_{0.80(2)}$.

The calculated and observed structure factor tables for $Sc_7Cl_{12}X$ (X = B, N) are in Appendices B and C, respectively.

Results and discussions

Structure description The Guinier powder patterns (Table A1) have shown that these interstitial-stabilized

phases, $Sc_7Cl_{12}X$ (X = B, N), are isomorphous with the previously reported "Sc_7Cl_{12}",[11] and that all the lines can be indexed accordingly to the rhombohedral lattice (hexagonal setting) to give the lattice parameters in Table I. Oscillation and Weissenberg photographs were rarely obtained because of the crystal orientation problems associated with gem-like crystals. Their reciprocal axes do not often lie near that of the capillaries making an alignment difficult. However, one of the non-data crystals of $Sc_7Cl_{12}N$ phase was fortunately aligned on the Weissenberg camera and gave photographs showing the symmetry elements were consistent with the $R\bar{3}$ space group and no extra reflections due to a supercell. Therefore, the heavy atoms are isostructural with Sc_7Cl_{12} and the additional interstitial atom is in the center of the Sc_6 cluster. The [110] projection of the whole unit cell of $Sc_7Cl_{12}N$ is in Figure 2. No terminal chlorine bonds are drawn for simplicity in order to show the Sc_6 clusters and the isolated scandium along the $\bar{3}$ axis, the body diagonal of the rhombohedral unit cell. The formula unit of these compounds can be rewritten as $Sc^{3+}[Sc_6(X)Cl^i_6Cl^i_{6(2/3)}Cl^a_{6(1/3)}]^{3-}$, (i = inner, a = ausser). The first six chlorines (Cl2) in Figure 2 bridge the edges of threefold scandium faces of the trigonal antiprism (TAP) and bond to isolated Sc1 as well. The other six inner-outer chlorine atoms (Cl1) bridge the waist edges of the TAP and connect to the other six clusters (Fig. 2) through bonding

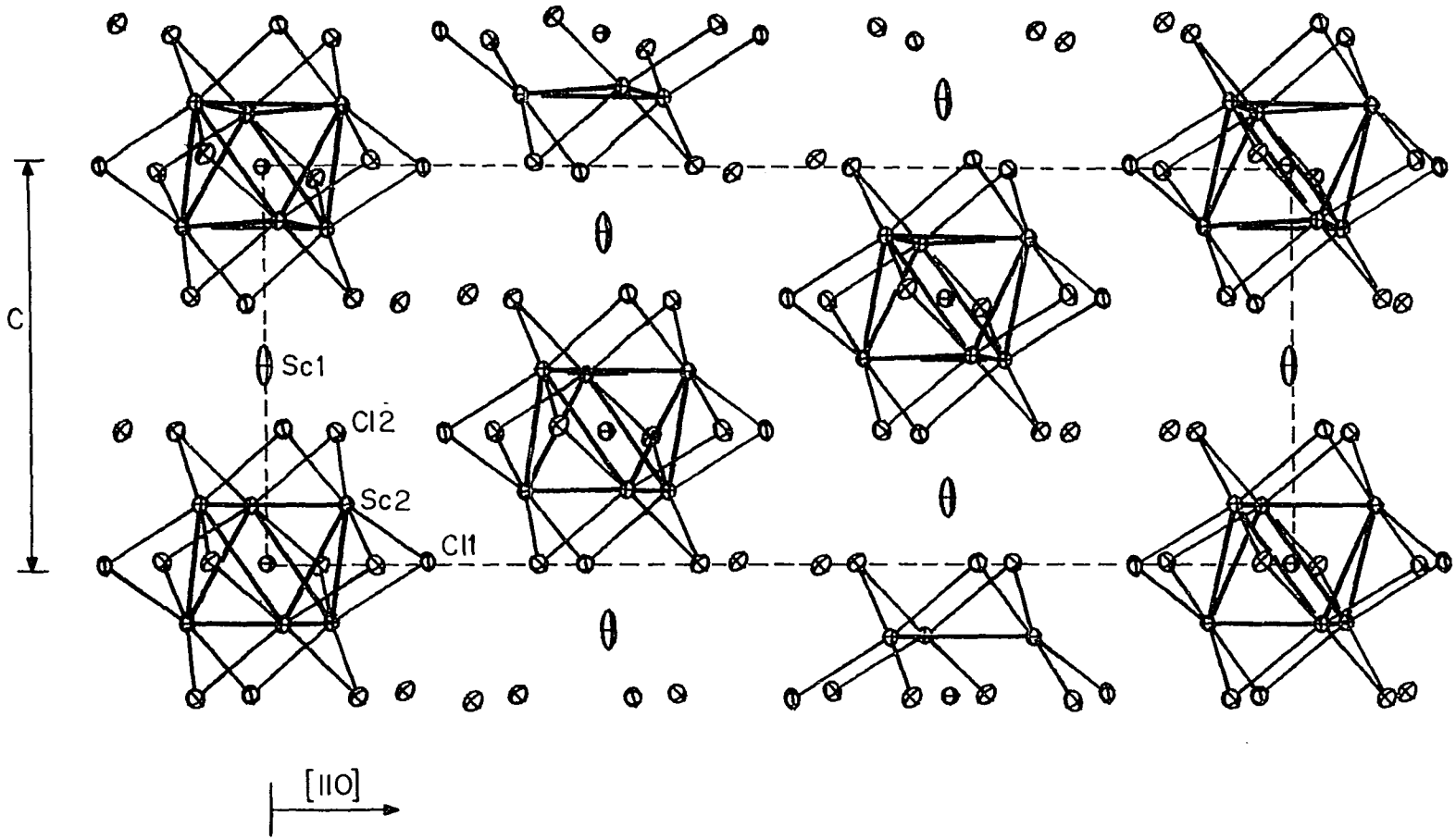

Figure 2. [110] projection of unit cell of $Sc(Sc_6Cl_{12})N$ with no terminal chlorine bonds drawn for simplicity.

to the apex scandium atoms. The isolated scandiums (Sc1) are in TAP interstices of close packed chlorine layers that alternate with Sc_6 clusters.

The boride, and presumably the nitride as well, gives a finely divided powder probably through a vapor phase reaction. The single crystal was found to be a transported product. The whiskers, $ScCl_{1.45}$, on which the Sc_7Cl_{12} gems in the pseudo binary preparations grew,[5] have not been produced in reactions with interstitial atoms added. This probably indicates that the former compound is interstitial free. However, according to differential thermal analysis,[11] $ScCl_{1.45}$ is only stable in very narrow temperature range, e.g., 877-890°C. Hence, it might be missed by using the wrong temperature.

Because no quantitative analyses were obtained, the structure refinements included occupancy variation and gave a fully occupied boron and only 80% of a nitrogen in the boride and nitride compounds, respectively (Table II). The fractional occupancy for the nitrogen may be real or caused by a crystallographic effect. The latter could be too "perfect", in which case the secondary extinction correction should be able to compensate, as in Zr-X systems.[37] However, as noted above, secondary extinction made no improvement. The nitride crystal had a smaller percentage of observed reflection (67%, in Table II) than the boride (88%), suggesting that the former crystal might be either

too small or a poorer diffractor. There is no experimental evidence to show substoichiometry which would cause lattice constant variations, based on Guinier powder patterns. Therefore, the apparent non-unity occupancy could be caused by the smaller data set and errors which are reflected in the high R_{ave} value and R/R_w (Table II) and somewhat larger standard deviations on thermal parameters (Table III). This occupancy could also result from a mixed interstitial compound, e.g., Sc_7Cl_{12} (NX) where X = B and/or C. Yet the $Sc_7Cl_{12}B$ and $Sc_7Cl_{10}C_2$ were found to be dominant in attempted preparations of B-N and C-N mixed interstitials, respectively.

Table IV provides the distances and angles for the compound $Sc_7Cl_{12}X$ (X = B, N), as well as "Sc_7Cl_{12}"[5] for comparison. In Figure 3, only two scandium clusters and one isolated cation along the 3-fold axis are shown for further discussion.

The Sc_6 metal clusters are distorted octahedra. They are compressed along $\bar{3}$ axis to give a longer Sc2-Sc2 bond distance on the threefold planes and a shorter one around the waist. The differences of these two types Sc2-Sc2 bond length are 0.012 A and 0.019 A for boride and nitride, respectively, and 0.030 A for "Sc_7Cl_{12}", i.e., the latter has the most distorted octahedra. The sizes of the interstitial-centered scandium octahedra vary from one interstitial to another with the smaller atomic number

Table IV. Distances (A) and angles (deg) for $Sc_7Cl_{12}X$ (X = B, N) and "Sc_7Cl_{12}"[a]

	$Sc_7Cl_{12}B$	$Sc_7Cl_{12}N$	"Sc_7Cl_{12}"
Metal cluster			
Sc1-Sc2	3.647(1)	3.625(1)	3.627(1)
Sc2-Sc2	3.293(1)	3.256(1)	3.234(1)
Sc2-Sc2	3.281(1)	3.237(1)	3.204(1)
Isolated Sc			
Sc1-Cl2	2.547(1)	2.550(1)	2.549(1)
Metal cluster to chlorine			
Sc2-Cl1(i)	2.557(1)	2.550(1)	2.540(1)
Sc2-Cl1(i)	2.594(1)	2.587(1)	2.576(1)
Sc2-Cl1(a)	2.730(1)	2.744(1)	2.755(1)
Sc2-Cl1-Sc2	79.13(2)	78.12(4)	77.54(4)[b]
Sc2-Cl2-Sc2	78.96(3)	78.10(4)	77.67(4)[b]
Metal cluster to bridging chlorines			
Sc2-Cl2	2.577(1)	2.573(1)	2.566(1)
Sc2-Cl2	2.603(1)	2.595(1)	2.591(1)
Interstitials			
Sc2-X	2.324(1)	2.296(1)	2.276(1)
Cl1(i)-X	3.632(1)	3.622(1)	3.610(1)[b]
Cl2-X	3.639(1)	3.626(1)	3.611(1)[b]

[a]References 5 and 11. [b]Calculated from atom coordinates of "Sc_7Cl_{12}" by a program DAPT, reference 51.

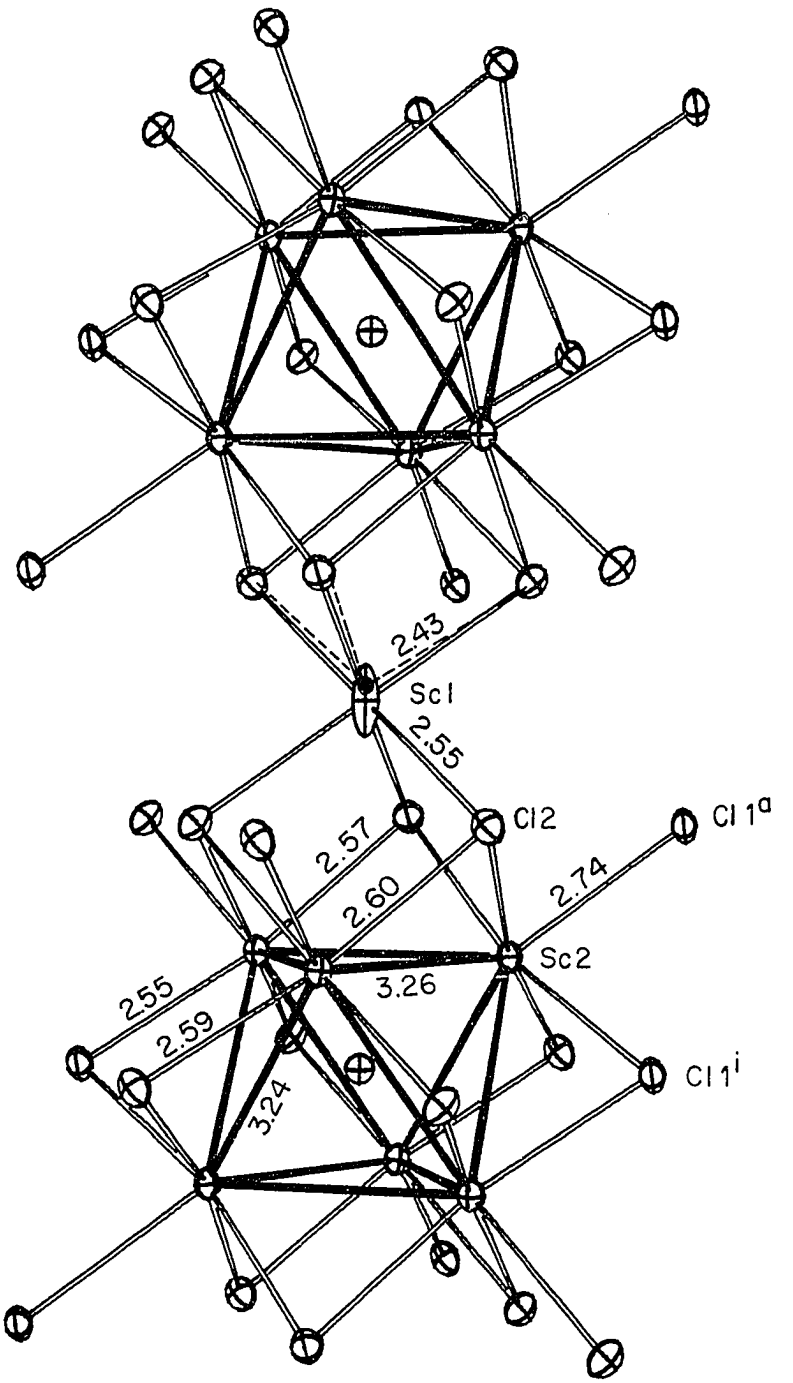

Figure 3. Two clusters and an isolated scandium from $Sc_7Cl_{12}N$ are drawn along c, a threefold, axis.

interstitial giving the larger cluster. The size of the octahedral hole is represented by the bond distance of interstitial to scandium, 2.324(1) A for boride, 2.296(1) A for nitride and 2.276(1) A for "Sc_7Cl_{12}",[5] the smallest in the series. There is indeed a very interesting comparison in terms of the cell parameters of these three phases. A plot of cell parameters against the atomic number of the corresponding interstitial atoms shows "Sc_7Cl_{12}" has an interstitial with an atomic number greater than 7 (Figure 4). The cell volume and the cluster center to scandium distances of "Sc_7Cl_{12}" are linear related with those for boride and nitride. The distances suggest the previously reported compound might be an "oxide", however, attempted syntheses such a phase have not been successful. In these attempts, Sc_2O_3 or ScOCl were the sources of oxygen and failed to give "$Sc_7Cl_{12}O$" but rather gave ScOCl. This strongly suggests that the former phase is thermodynamically less stable than the latter and should not be formed in the first place. In fact, there are only 483 independent reflections for the "Sc_7Cl_{12}" crystal data set ($2\theta_{max} = 50^{o}$) while the R/R_w for the last refinement are 5.6/6.4 larger than those for boride and nitride (Table II). The standard deviations of the thermal parameters for "Sc_7Cl_{12}" are larger than those for the title compounds (Table III) suggesting the former data crystal is poorer.

The Sc-Cl (bridging) distances in the boride versus the

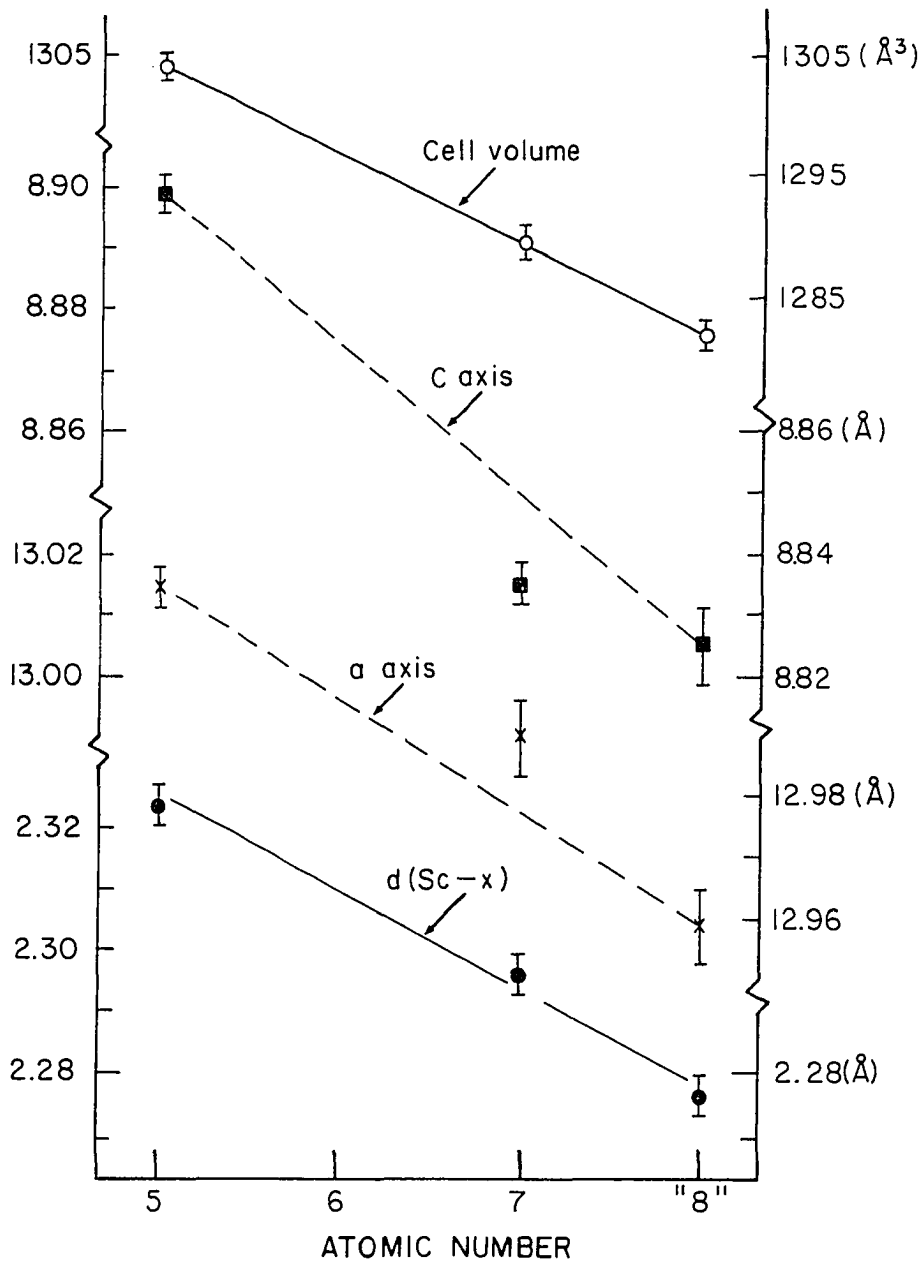

Figure 4. Cell parameters (±3σ) of $Sc_7Cl_{12}X$ (X = B, N) and "Sc_7Cl_{12}" (ref. 5) are plotted against the corresponding atomic numbers of their interstitial elements.

nitride differ by only 0.010-0.017A. The difference in bridging distances within the same structure vary by a larger amount, 0.036-0.037 A (Table IV), resulted from the distortion of the metal octahedron. The terminal chlorine to scandium distances, Sc2-Cl1[a], only increase from 2.731(1) A in boride to 2.744(1) A in nitride and 2.755(1) A in "Sc_7Cl_{12}". This variation presumably results from different orbital overlap populations between scandium and interstitial atoms (see later discussion). The isolated Sc1 to Cl2 distances are not affected by the different interstitial atoms and are constant, 2.55 A, which is nearly the sum of the Shannon crystal radii,[52] e.g., $r_{Sc^{3+}} + r_{Cl^-}$ = 0.885 A + 1.67 A = 2.555 A. The Sc(III)-Cl bond distances in other compounds are 2.54 A for Sc_5Cl_8C (see next), 2.54-2.56 A for $Sc_7Cl_{10}C_2$,[45] and 2.50 A to 2.57 A for Sc_7Cl_{10}.[7] The nonbonded chlorine to interstitial as well as Sc1 to Sc2 separations are 3.62-3.65 A which are similar to the Cl to Cl separations distances, 3.48-3.66 A (Table IV).

As the final least square refinements showed (Table III and Fig. 4) both of these $Sc_7Cl_{12}X$ interstitial compounds have elongated thermal ellipsoids (TE) for Sc1 as in the "Sc_7Cl_{12}" structure. In $R\bar{3}$, these atoms occur on the special position (0,0,1/2) and therefore are evenly spaced along the c axis and in the chains displaced by the R-centering operation. In "Sc_7Cl_{12}", the special position (0,0,z) for Sc1 in space group R3 was used, neither the z

parameters nor the large B_{33} changed significantly.[11] Therefore, the large B_{33} term was suggested as a systematic displacement and not just anisotropic thermal motion.[11] The refinements of their occupancies, 0.942(1) and 1.01(1) for boride and nitride, respectively, suggest the scandium site is nearly fully occupied. The vertical separation between neighboring Cl2 layers is 0.03 A longer than between Cl1 layers for both boride and nitride, but 0.05 A for "Sc_7Cl_{12}". In other words, the chlorine close packed layers are not planar but rather puckered. Therefore, if the TE elongation were due to this puckering, the elongation should be the same, but it is in fact much worse in the nitride than in the boride. In addition, the puckering of the chlorines is somehow associated with the size of the Sc_6 TAP and results in a variation in the Sc2-Cl-Sc2 angles. As the cluster contracts, the bridging angles get smaller (Table IV), i.e., the angles at Cl2 are decreased by 0.9-1.0^{o} for the nitride but the Sc1-Cl2 distances are retained the same.

As mentioned above, Sc1 in the nitride structure has a more elongated TE than in the boride. It was successfully refined as two different sites along 3-fold axis, each with an occupancy of 50% possibility (Figure 3). The two new sites for Sc1 are 0.45 A apart and to the nearest Cl2 distance is 2.43 A. The distance seems too short even for the scandium(III) compared with 2.58 A for $ScCl_3$. Therefore, crystallographically, Sc1 is apparently not

alternatively occupying at two different sites to result in an elongated TE.

In fact, the same thermal elongation has occurred in Ln_7I_{12}[13] (Ln = La, Tb, etc.). The only exception is in the case of Er_7I_{12} which has rather squashed TE for the isolated Er cation with a B_{11}/B_{33} ratio of 1.6:1 whereas the ratios are 1:6.6 and 1:9.0 in Ln = La and Tb, respectively. In boride and nitride, the TE ratios are 1:3.7 and 1:7.5, respectively. However, the B_{33}(nitride)/B_{33}(boride) ratios are essentially constant for a given atom in the two structures. Thus, for Sc2 this ratio is 1.24 while it is 1.30 for the chlorines or Sc1. This result is applicable to Ln_7I_{12} (Ln = La, Tb, not Er). Therefore, the different elongation (B_{11}/B_{33}) among these derivatives could reflect the lack of the crystal quality rather than the different degrees of the puckered chlorine layers. In fact, "Sc_7Cl_{12}" has the most puckered layers but not the most elongated TE (Table III).

So far, experiments with different space groups have also been tried. None of these has solved the elongated TE problem, except for $Sc_7I_{12}C$[53] in which the refinement was done in the acentric space group (R3). The TE of Sc1 in the latter compound was elongated (B_{11}/B_{33} = 1:26) in $R\bar{3}m$ but reasonable in R3 (1:1.7).

The interstitial atoms are fixed in the center of the Sc_6 cluster by symmetry, and correspond to crystal radii of

1.44 A and 1.41 A of boride and nitride, respectively. The averaged boron radius in $MM'Zr_6Cl_{15}B$ (M = K; M' = Cs)[25] is 1.44 A while the matrix effect should be very much the same in $Sc_7Cl_{12}X$. The $Zr_6I_{12}B$ shows a longer Zr-B distance, resulting in a longer boron crystal radius,[37] 1.51 A, because the iodine atoms are expected to have a larger matrix effect than chlorine. The scandium to nitrogen distance in ScN (rock salt)[54] is 2.25 A and the crystal radius for nitrogen is 1.37 A. The nitrogen crystal radius observed in $Sc_7Cl_{12}N$ is 0.04 A larger than it is in ScN, perhaps because the matrix effect limits the cluster contraction.

Extend HUckel MO calculations To gain the understanding of bond interactions for qualitative arguments, molecular orbital (MO) calculations for $Sc_6Cl_{18}^{9-}$ and $Sc_6Cl_{18}B^{9-}$ (isoelectronic with the cluster in $Sc_7Cl_{12}B$) with D_{3d} group symmetry have been done utilizing the extended HUckel method. The atom coordinates used in these calculations are from single crystal data of $Sc_7Cl_{12}B$ and are listed in Appendix L along with valence orbital ionization energies and zetas. MO diagrams from these calculations are in Figure 5.

The symmetry of the empty cluster, $Sc_6Cl_{18}^{9-}$, used for the calculations is D_{3d}, nearly O_h group symmetry. Using the O_h symmetry descriptions, scandium metal bonding orbitals are broken down to a_{1g} (-8.5 eV), t_{1u} (-7.6 eV), t_{2g} (-7.5 eV), and a_{2u} (-6.5 eV) orbitals as shown in the

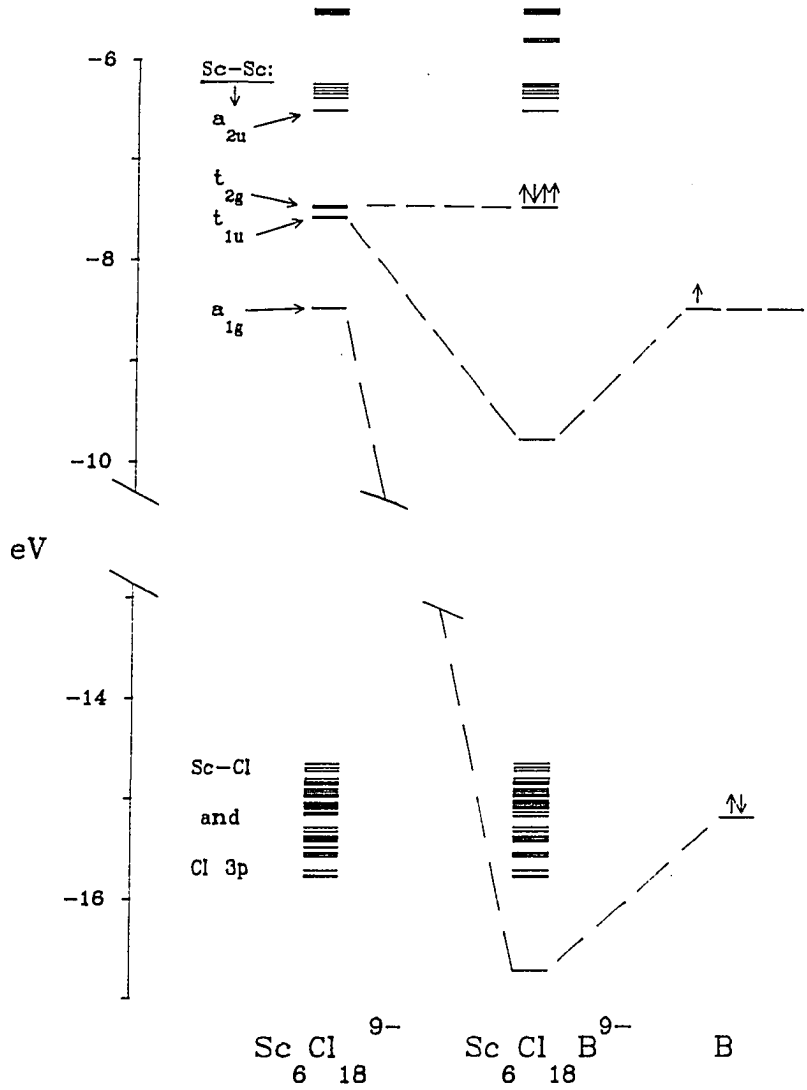

Figure 5. Molecular orbital diagram from extended HUckel calculations, $Sc_6Cl_{18}^{9-}$ with D_{3d} symmetry (left), atomic B (right), and $Sc_6Cl_{18}B^{9-}$ with D_{3d} symmetry (center). Orbital labels refer to irreducible representations in O_h symmetry. The HOMO of $Sc_6Cl_{18}B^{9-}$ is the partially (2/3) occupied t_{2g} set.

left column of Figure 5. However, orbitals that belong to these previously degenerate sets differ in energy only slightly, in no case by more than 0.1 eV. The Sc-Sc bonding orbitals transform in D_{3d} symmetry as a_{1g}, a_{2g}, a_{1u}, a_{2u}, e_g, and e_u but to simplify discussion of these orbitals they will continue to be referred to in their O_h-equivalent description. At energy levels between -15.8 to -14.7 eV, the orbitals are primarily Sc-Cl and Cl 3p. When interstitial boron is introduced into the empty cluster, its 2s (-15.2 eV) and 2p (-8.5 eV)[49] valence orbitals interact with the $a_{1g}(z^2)$ and $t_{1u}(xz, yz)$ sets to give four new Sc-B bonding orbitals below the remaining Sc-Sc orbitals at a_{1g} (-16.7 eV) and t_{1u} (-9.8 eV), respectively, that are primarily in boron s and p in character.

Rigid structure calculations for nitride result in lower energy Sc-N a_{1g} and t_{1u} orbitals, -26.7 and -13.9 eV, respectively, primarily because the valence orbitals of the nitrogen atom are lower in energy.[49]

In Table V, selected details from extended Hückel calculations for $Sc_6Cl_{18}X^{9-}$ (X = empty cluster, B, N) are listed. An inspection of Sc-Sc reduced overlap population shows the filled clusters, $Sc_7Cl_{12}B$ vs empty cluster for example, has significantly lost Sc-Sc bonding to partially contribute to Sc-interstitial bonding. The rigid structure calculations give very similar values with the ones from actual geometry. They are also consistent in the increasing

Table V. Selected details from extended Hückel calculations of $Sc_6Cl_{18}X^{9-}$ (X= empty,[a] B, and N)

	Charge on interstitial	Number of cluster electrons	Average Sc-Sc distance (A)	Occupation[b] of interstitial s orbital in a_{1g}	Occupation[b] of interstitial p orbital in t_{1u}	Sc-Sc reduced overlap population[c]
empty cluster	–	9	3.287[a]	–	–	0.19
$Sc_7Cl_{12}B$	-1.92	12	3.287	1.45	1.16	0.07
$Sc_7Cl_{12}N$	-1.91	14	3.247	1.74	1.72	0.07

[a]The atom coordinates are those of $Sc_7Cl_{12}B$. [b]The fraction of the two electrons in the s, or p orbital that are occupied. Occupation of orbital $i = \sum_{\alpha} Q_{i\alpha}$, where $Q_{i\alpha} = 2C_{i\alpha} \sum_j C_{j\alpha} S_{ij}$ and S_{ij} = overlap integrals. [c]The average sum of the overlap of atomic orbitals on pairs of adjacent scandium atoms for all occupied molecular orbitals.

order of fractional occupation of interstitial orbitals in Sc-interstitial a_{1g} and t_{1u} sets from boron to nitrogen. Calculated charges on these interstitial atoms show they are nowhere near ionic in character. In fact, interstitial compounds found so far all prove to be largely covalent in terms of metal-interstitial bonding.[24,25,45]

If we formally assign B(5-) and N(3-), we will then conclude the numbers of electrons left in scandium metal cluster bonding are 4 and 6, repectively. The small number of metal bonding electrons seem to suggest the weakening of the total Sc-Sc bondings. The crystal structures however show that the Sc-Sc bond distances are indeed nearly as short as in a real binary compound, 3.15-3.27 A in Sc_7Cl_{10},[7] on account of the strong Sc-interstitial bonding.

The metal orbitals that interact with interstitial s and p are $z^2(a_{1g})$ and xz, yz(t_{1u}). The former have greater overlap with interstitials than with the terminal chlorine p, resulting in longer terminal Sc-Cl distances, e.g., 2.73 A (boride) and 2.74 A (nitride). This increasing order is presumably related to the increasing overlap between scandium and the interstitial.

Magnetic susceptibility In the boride, there are twelve electrons in the valence orbitals $a_{1g}^2\ t_{1u}^6\ t_{2g}^4$. The t_{2g} orbitals are partially (2/3) occupied with two unpaired electrons, which should generate the magnetic susceptibility. This was measured on 14 mg ground $Sc_7Cl_{12}B$ crystals,

at different magnetic fields, H = 250, 500, 1,000, 2,000 and 10,000G. In Figure 6, three representative data sets (Curve a, b, c) are plotted as χ (emu/mole of $Sc_7Cl_{12}B$) vs. T (K) with H = 1,000G, 2,000G, and 5,000G, respectively. These curves imply an antiferromagnetic ordering below the Néel transition temperature (~180K) reduces the magnetic moment. If one fits the susceptibility data of curve b at the Curie tail below 50K to the equation $\chi = \chi_o + C/(T-\theta)$ (where χ is molar susceptibility, χ_o is from the contribution of temperature-independent paramagnetism and core diamagnetism, C is Curie constant, and θ is Weiss constant), one can get $\chi_o = 1.56 \times 10^{-3}$ emu/mole, $C = 2.10 \times 10^{-3}$ emu K/mole and $\theta = 0.6$K. If the Curie tail is due to a Gd^{3+} impurity, 20ppm (atomic) in each formula unit would do. The possible Néel transiton apparently is field independent. If one sights along the raw data on curve a, one could imagine another possible transition occurring at T = ~120K. Since the magnetic susceptibilities are too complicated to be understood, one should run additional experiments, e.g., low temperature powder diffraction, to see whether possible phase transition may occur at ca. 120K and 180K. Single crystal neutron diffraction may clarify the process of the magnetic ordering. If the magnetic ordering occurs among the clusters through the isolated scandium atom, one would see a doubled magnetic unit cell at below the spin-ordering temperature, 180K, by the latter method.

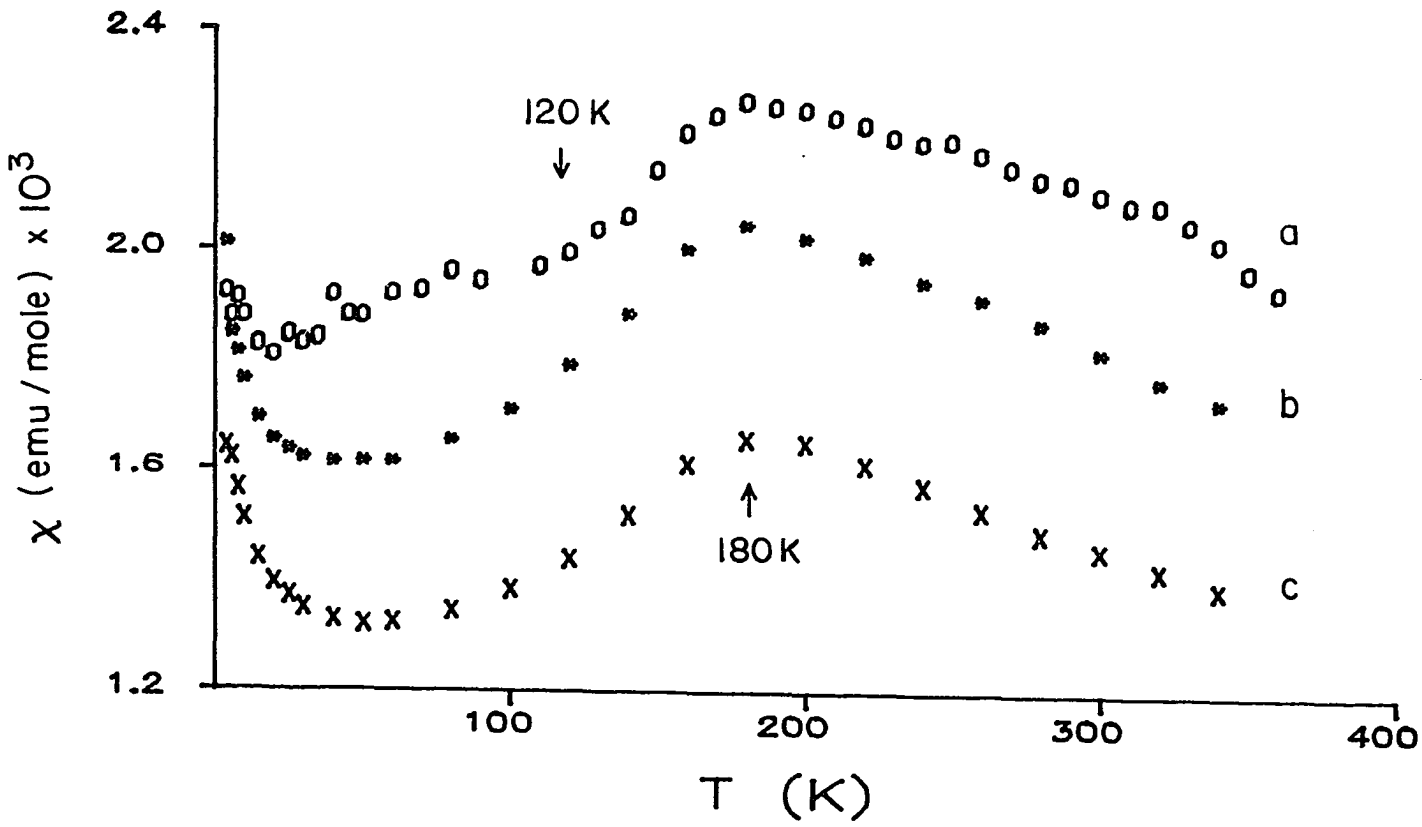

Figure 6. Magnetic susceptibility for $Sc_7Cl_{12}B$ with a) H = 1,000G, b) 2,000G, and c) 5,000G.

Unsuccessful reactions Attempts to make $ZrSc_6Cl_{12}X$ (X = Be, B, C) at 900/880°C (13 days) using stoichiometric amount of $ZrCl_4$, $ScCl_3$, X powders and excess (2x) scandium strips, failed. The products were zirconium metal plus unknown powder in beryllium reaction, $Sc_7Cl_{12}B$ (85% yield) in boron reaction, and Sc_5Cl_8C (70% yield, hot end) + "$Sc_7Cl_{12}N$" (<5%, cold end; according to the lattice parameters) in carbide reaction. Apparently, the excess scandium strips reduced the $ZrCl_4$ to form zirconium metal. The other elements from the second period, X = Be, C, F, were used to attempt to make $Sc_7Cl_{12}X$ at 860°C, but this also failed. The graphite reaction produced Sc_5Cl_8C, while the others gave unknown powder patterns.

With the iodine anion, similar clusters have been prepared with heavier interstitials, e.g., $Cs_aZr_6I_{14}X$ (a = 0.30, 0.68; X = Si, Al, respectively).[24] But the scandium experiment with a stoichiometric amount of starting materials with Si or Al ($AlCl_3$) powder at 860°C gave no evidence that large interstitial elements exist in this phase. The large iodine has more of a matrix effect, and presumably creates more room for large intercalated cations.

Infinite Single Chain Structures Derived by Cluster Condensation and Stabilized by Interstitial Elements. Synthesis and Characterization of Sc_4Cl_6X (X = B, N) and Sc_5Cl_8Y (Y = C, N)

Introduction

Condensation of clusters of M_6X_8 (6-8) or M_6X_{12} (6-12) parentage evidently occurs in many reduced early transition metal chalcogenides or the rare earth metal halides. The rationale for the condensation, besides the low X:M ratio, is the lack of metal-metal bonding electrons either because the metals have few valence electrons, such as in Ln_5Br_8 (Ln = Gd, Tb)[55], La_2Cl_3[56] (Gd_2Cl_3[57] type), Sc_7Cl_{10},[7] etc., or that the nonmetals (O, S) take two electrons away from the metal in forming metal-nonmetal bonds, e.g., $NaMo_4O_6$.[58]

The new infinite single chain compounds described here consist of edge-sharing scandium octahedra centered by interstitial elements B, C, or N. The scandium-interstitial bonds stabilize the metal cluster formation from scandium octahedra to derive a 6-12 type parentage. Such phenomena have been described for discrete cluster compounds in the previous section and for the double chain compound $Sc_7Cl_{10}C_2$.[45] In this section the specific examples of single chain compounds, the "transition" stage of condensation between isolated clusters of former type and the double chain of the latter, are shown for Sc_4Cl_6X (X = B, N) and Sc_5Cl_8Y (Y = C, N).

The heavy atom structure in the Sc_4Cl_6X phase is isomorphous with β-Tb_2Br_3.[44] Several factors for β-Tb_2Br_3, however, e.g., low yield product, extra electron density in the center of the cluster, suggest this structure is also stabilized by an impurity atom, silicon perhaps.

The compound Sc_5Cl_8Y is isomorphous with the previously reported "Sc_5Cl_8"[2] which in fact might have been an impurity-stabilized carbide based on the similar lattice parameters to those of Sc_5Cl_8C. Since the structure of the former has been described in great detail before,[2] it will only be used as a comparison in the discussion.

Experimental

Synthesis

Sc_4Cl_6X The polycrystalline boride was synthesized in high yield (85%, visual estimation) at 950°C (two weeks) from stoichiometric amounts of Sc, $ScCl_3$ and B powders. The by-product was 5-10% of plate crystals, "3R-$Sc_2Cl_2B_x$" by Guinier powder pattern. (However the lattice parameters of these plate crystals are too small to be a boride of this kind, a = 3.4117(6) A, c = 26.435(9) A. The compound was not formed reproducibly.) In order to get nearly 100% yields of the title compound, the same conditions with excess (3x) boron were needed. At this reaction temperature no other identifiable boride was reproducibly formed, suggesting that the Sc_4Cl_6B is more stable than any other borides. On the contrary, a

stoichiometry to make Sc_4Cl_6B at 860°C gave only $Sc_7Cl_{12}B$ with, presumably, an excess of elemental boron or ScB_x. At reaction temperatures above 860°C and below 950°C, the products were two phase mixtures, and the higher yield of Sc_4Cl_6B was produced at the higher reaction temperature. The Sc_4Cl_6B phase can also be formed by decomposition of $Sc_7Cl_{12}B$ at 950°C. However, a mixed interstitial reaction to make $Sc_2Cl_2B_{0.5}N_{0.5}$ (where the Cl/B ratio was 4:1) at 855°C gave Sc_4Cl_6B and ScN_x suggesting that besides the temperature dependence, the chlorine to boron ratio certainly is an important factor in the formation of Sc_4Cl_6B at lower temperatures where the kinetics need to be favorable. Therefore, $Sc_7Cl_{12}B$ was not observed from quenched Sc_4Cl_6B at 950°C to 860°C. The single crystal of Sc_4Cl_6B was obtained from a reaction with scandium strips reaction in an attempt to make "3R-$Sc_2Cl_2B_2$" at 950°C. The yield of the former phase was 95% and excess boron probably remained unreacted. The strips from the reaction tube were not brittle as they would have been if ScB_x formed.

The Sc_4Cl_6N synthesis was the most studied but least successful in terms of a high yield. The reason for this is the same as $Sc_7Cl_{12}N$, i.e., elemental nitrogen gave the best yield but could not be sealed in the reaction tube in quantitative amounts. So, based on the amount of nitrogen in the reaction container, the yield of product was nearly 100%. The reactions with NaN_3 added and with the wide

temperature range, 780-960°C, gave at least an 80% yield of 1T-Sc_2Cl_2N instead (see following). The fat needle crystals of Sc_4Cl_6N (5% yield) were obtained from a nitrogen-added reaction with KCl, $ScCl_3$ powders and scandium strips. The crystals, however, were not single (see below). The major product of this reaction was a melt, $ScCl_x$. The parallel reaction without added N_2 gave mainly melts again but with 5% of "Sc_5Cl_8C", the identity of the latter being based on its indexed Guinier powder pattern.

Sc_5Cl_8Y The carbide, but not nitride, of Sc_5Cl_8Y can be synthesized in a nearly 100% yield as a green-hued, black powder at 860°C (12 days) from stoichiometric amounts of Sc, $ScCl_3$ and C powders. Single crystals (thick fibers) of Sc_5Cl_8C (5% yield) were found in the incomplete reaction of an attempt to synthesize "Sc_4Cl_6C" in three days at 940°C. They were easily distinguishable from the very fine needles of the major product, $Sc_7Cl_{10}C_2$ (95% yield). The Guinier powder pattern of the single crystals of the Sc_5Cl_8C gave a very similar set of cell parameters to those of the above described high yield product. The single crystal of Sc_5Cl_8N for a structure determination was produced in a 900/950°C (4 weeks) temperature gradient from a quaternary reaction, $Sc/ScCl_3/NaN_3$, where both excess scandium strips (5x) and NaN_3 were at the hot end and $ScCl_3$ at the cold end with Cl/N ratio of 6/1. The yield of this Sc_5Cl_8N phase was as low as 5-10%; in addition, Na_3ScCl_6

formed evidently as the "sink" for the $ScCl_3$.

Single crystal results The single crystal data collection and structure refinement procedures and results were stated in Chapter II and also in Tables I and II. The atomic positions and the thermal parameters of Sc_4Cl_6X and Sc_5Cl_8Y are listed in Tables VI and VII, respectively.

Sc_4Cl_6X This phase crystallizes in the orthorhombic space group Pbam (No.55) with two very similar axial lengths in a and b. An oscillation photograph taken around one of the reciprocal axes, c^*, showed mirror symmetry perpendicular to the needle axis c. The first and zero-level Weissenberg photographs showed a ninety degree angle between a^* and b^* reciprocal axes, a two-fold axis along c^*, and extinction conditions in hol (h = 2n + 1) and okl (k = 2n + 1).

Crystallographic twinning in terms of the microscopic intergrowth of two crystals along the common c-axis, but with ninety degree phase differences in the ab plane, appeared for crystals 1 and 2 (Table II) as two sets of festoons on the Weissenberg photographs. The hkl and $k'h'l'$ festoons are close to each other because of approximately equal cell dimensions a and b. This situation sometimes generates an unresolvable problem in crystal orientation because the tuning procedure was not able to pick up reflections from only one crystal. The only crystal of Sc_4Cl_6N phase (crystal 3) found in a nitrogen-added reaction

Table VI. Atom positions and the thermal parameters of Sc_4Cl_6X (X = B, N)

	x	y	z	B_{11}[a]	B_{22}	B_{33}	B_{12}
Sc_4Cl_6B							
Sc1	0.3745(1)	0.3521(1)	0.5	1.32(6)	1.06(5)	0.91(5)	-0.14(5)
Sc2	0.3948(1)	0.5830(1)	0.0	1.08(5)	0.86(5)	0.86(5)	-0.04(4)
Cl1	0.4794(2)	0.2407(2)	0.0	1.4(1)	1.13(5)	1.20(5)	-0.01(5)
Cl2	0.2400(2)	0.4297(2)	0.0	1.23(7)	1.53(7)	1.16(6)	-0.06(6)
Cl3	0.2326(2)	0.1814(2)	0.5	1.74(8)	1.65(7)	1.08(6)	-0.77(6)
B	0.5	0.5	0.5	0.7(1)			
Sc_4Cl_6N (K, crystal 1)							
Sc1	0.3770(3)	0.3522(3)	0.5	1.6(2)	1.0(1)	1.8(2)	0.1(1)
Sc2	0.3950(3)	0.5799(3)	0.0	1.2(2)	1.1(2)	1.9(2)	-0.2(1)
Cl1	0.4844(4)	0.2409(4)	0.0	1.6(2)	1.3(2)	1.8(2)	-0.2(1)
Cl2	0.2401(3)	0.4270(3)	0.0	1.1(2)	1.1(2)	1.7(2)	-0.1(1)
Cl3	0.2370(4)	0.1781(4)	0.5	1.9(2)	1.5(2)	1.9(2)	-0.2(1)
N	0.5	0.5	0.5	0.5(4)			
"K"[b]	0.5	0.0	0.5	2(2)			

Sc_4Cl_6N (Cs, crystal 2)							
Sc1	0.3767(2)	0.3537(2)	0.5	2.7(1)	1.3(1)	1.2(1)	-0.04(8)
Sc2	0.3970(2)	0.5803(2)	0.0	2.5(1)	1.2(1)	1.2(1)	-0.06(8)
Cl1	0.4828(3)	0.2416(3)	0.0	2.9(2)	1.5(1)	1.3(1)	0.1(1)
Cl2	0.2404(3)	0.4294(3)	0.0	2.7(1)	1.7(1)	1.2(1)	-0.1(1)
Cl3	0.2340(3)	0.1790(3)	0.5	3.0(2)	1.9(1)	1.2(1)	-0.6(1)
N	0.5	0.5	0.5	1.1(4)			
"Cs"[b]	0.5	0.0	0.5	2.4(5)			

[a] $B_{13} = B_{23} = 0$, by symmetry. [b] The further refinement for the residual electron density at this special position resulted in partially K and Cs occupancy in the amount of 0.08(2) and 0.055(5), respectively; see text.

Table VII. Atom positions and the thermal parameters of Sc_5Cl_8Y (Y = C, N)

	x	y	z	B_{11}[a]	B_{22}	B_{33}	B_{13}
Sc_5Cl_8C							
Sc1	0.0	0.0	0.0	1.2(3)	2.5(5)	0.8(3)	0.8(3)
Sc2	0.4881(5)	0.0	0.6134(7)	1.4(3)	0.4(3)	1.6(3)	1.0(2)
Sc3	0.3355(5)	0.5	0.3219(7)	1.5(3)	1.7(4)	1.2(3)	1.1(3)
Cl1	0.2990(7)	0.0	0.4321(9)	1.6(4)	1.1(4)	1.3(3)	0.9(3)
Cl2	0.1325(7)	0.5	0.1044(10)	1.3(3)	1.2(4)	1.7(3)	0.8(3)
Cl3	0.3291(7)	0.0	0.1644(10)	1.3(3)	1.1(3)	1.2(3)	0.8(2)
Cl4	0.5297(7)	0.5	0.2367(10)	3.1(5)	1.1(4)	2.2(4)	2.2(4)
C	0.5	0.5	0.5	3.4(6)			
Sc_5Cl_8N							
Sc1	0.0	0.0	0.0	1.4(1)	1.3(1)	1.1(1)	0.92(9)
Sc2	0.4875(1)	0.0	0.6151(2)	1.01(7)	1.13(9)	1.20(7)	0.73(6)
Sc3	0.3346(2)	0.5	0.3212(2)	1.48(8)	0.67(8)	1.38(7)	1.07(7)
Cl1	0.2973(2)	0.0	0.4310(3)	1.26(9)	0.8(1)	1.55(9)	1.08(8)
Cl2	0.1324(2)	0.5	0.1031(3)	1.3(1)	0.8(1)	1.6(1)	0.87(8)
Cl3	0.3271(2)	0.0	0.1626(3)	1.46(9)	0.78(9)	1.09(8)	0.85(8)
Cl4	0.5300(2)	0.5	0.2372(3)	2.2(1)	1.0(1)	1.7(1)	1.47(9)
N	0.5	0.5	0.5	0.5(2)			

[a] $B_{12} = B_{23} = 0$ by symmetry.

had a serious twinning problem. Therefore, only Guinier data are reported in Table I. Crystals 1 and 2 mentioned above were obtained earlier in the study of $MCl/ScCl_3/Sc$ systems with M = K and Cs, respectively. They had very similar cell dimensions with that of the known interstitial phase Sc_4Cl_6N (3), especially crystal 2, and are probably the impurity-stabilized Sc_4Cl_6N phases. Therefore, single crystal structure refinements for these phases were tentatively accomplished with nitrogen as the interstitial atom (Table II) for later comparisons.

Boride crystals on the other hand, had no problem with twinning and gave sharp spots and a resulting low R_{ave}, Table II.

In order to confirm the identity of interstitial elements in Sc_4Cl_6X, the occupancies were varied simultaneously with the isotropic B's resulting in a nearly unit occupancy for the boride. Crystal 1 and 2 were refined with nitrogen as the interstitial atom to give nearly unit occupancies (Table II). However, the data showed residual electron densities of ca. 1.2 e/A^3 for crystal 1 and 2.5 e/A^3 for crystal 2 at the (1/2, 0, 1/2) position where cations (M^I = K, Cs) are possible. These residual electron densities were not observed in the boride structure refinement, however, so those in crystal 1 and 2 might be real. Further, these residual electron densities when refined as potassium and cesium atoms resulted in the

compositions of 0.08(2) and 0.055(5), respectively with the corresponding isotropic B's 2(2) and 2.4(5). The parameters for the scandium and chlorine atoms did not vary significantly. The occupancy and the B value of the nitrogen in crystal 1 were 0.98(8) and 0.3(5), respectively, with R/R_w 0.079/0.148, while crystal 2 gave the corresponding values 0.85(1), 0.8(3) and 0.045/0.078.

The final difference Fourier syntheses of boride and nitride crystals (except the metal cation positions) are <1 e/A^3 at both atom sites and elsewhere. In addition, the boride single crystal refinement showed a good agreement with the model to give lower R/R_w values which are consistent with the good quality of the crystal (Table II).

Sc_5Cl_8Y Weissenberg photographs showed poor quality crystals for both the carbide and nitride as reflected by streaked spots. However, the former had poorer crystallinity resulting in rather high peak background which consequently gave fewer observed reflections (27% observed in carbide crystal vs 69% in nitride) and higher R_{ave} (Table II). Notably, the carbide crystal was ca. one-eighth as large as the nitride, also leading to fewer reflections in the unique data set of the former.

The heavy atom positions for the structures of these phases were obtained from "Sc_5Cl_8"[2] and refined accordingly. The difference Fourier syntheses map of each crystal structure refinement at this stage showed a sizable peak at

the (0, 0, 1/2) special position. Addition of interstitial atoms at this position caused the R values to drop from the original of 11.2 and 10.6 percent in Sc_5Cl_8C and Sc_5Cl_8N, respectively, to 7.2 and 5.4 percent (Table II). The occupancies of these interstitials were also varied to give the empirical formula $Sc_5Cl_8C_{1.20(2)}$ and $Sc_5Cl_8N_{0.89(4)}$ with B's equal to 4(2) and 0.02(24), respectively. The lattice constants of the former matches with the ones from its high yield product suggesting more than unit occupancy of carbon in the former structure was not due to the mixed interstitial C and N, for example. However, the small thermal ellipsoid of the nitrogen interstitial atom for the latter, and the high standard deviations of the thermal parameters as well as some other positional parameters of the heavy atoms (especially for carbide, Table VII) were presumably caused by the poor crystallinity.

Magnetic susceptibility measurement The magnetic susceptibility of Sc_5Cl_8C was measured by a SQUID method utilizing a 25 mg polycrystalline sample. The measurements were done in the temperature range of 4 to 340K at the magnetic fields of 2,000 and 5,000 G.

Results

Structure description In Figure 7, both structures of Sc_4Cl_6B and Sc_5Cl_8N are shown as viewed down the shortest neddle axes b and c, respectively, and parallel to the metal chain directions. These two types of compounds have similar

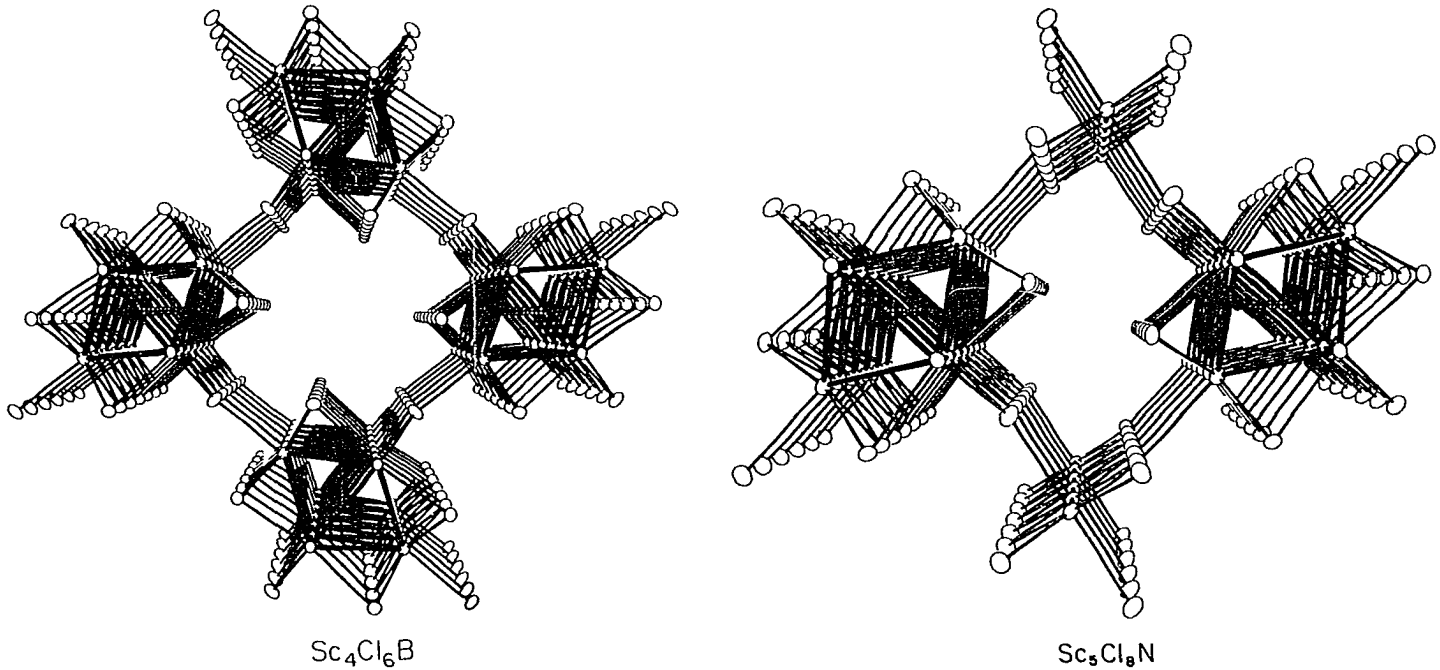

Figure 7. Structure of I) Sc_4Cl_6X, (X = B), and II) Sc_5Cl_8Y (Y = N) viewed down the short axes, c and b, respectively. Both structures have $Sc_4Cl_6^{n-}$ infinite chains where in the former case they are interconnected by inner-outer chlorines and in the latter, through parallel $ScCl_2^+$ chain. The atoms are drawn at 50% probability.

structures such that M_6 clusters are linked through shortened trans edges to form infinite chains running parallel to the shortest crystal axis, as in Gd_2Cl_3.[57] Chlorine atoms bridge all edges of the metal octahedra to give Sc_4Cl_4 chain units while two additional chlorines per repeat unit bridge between metal vertices in separate chains to form sheets (in the plane of the page) and to give the empirical formula, with interstitial atoms in the center of all metal octahedra, of Sc_4Cl_6X. In the compound Sc_5Cl_8Y, a second, parallel chain consists of edge-shared octahedra of chloride about isolated scandium(III) atoms, i.e., $(ScCl_2^+)_\infty$, connects to the $(Sc_4Cl_6Y^-)_\infty$ chains. In Figure 7, the connectivity of the infinite chains is presented to show the similarity between these two structures. Also, the metal chain appears to be quite well-sheathed by chloride, all Cl-Cl nearest neighbor separations thereabout ranging between 3.5 and 3.7 A, these being close to the customary sum of van der Waals radii.

In Figures 8 and 9, the unit cell projections of Sc_4Cl_6B and the C-centered Sc_5Cl_8N are viewed along the metal chain, e.g., along [001] and [010] directions, respectively. The important interatomic distances and angles of Sc_4Cl_6X and Sc_5Cl_8Y phases are given in Tables VIII and IX, respectively. Structure factor results of Sc_4Cl_6X (X = B and N crystal 1 and 2) and Sc_5Cl_8Y (Y = C, N) are available in Appendices D-H, respectively.

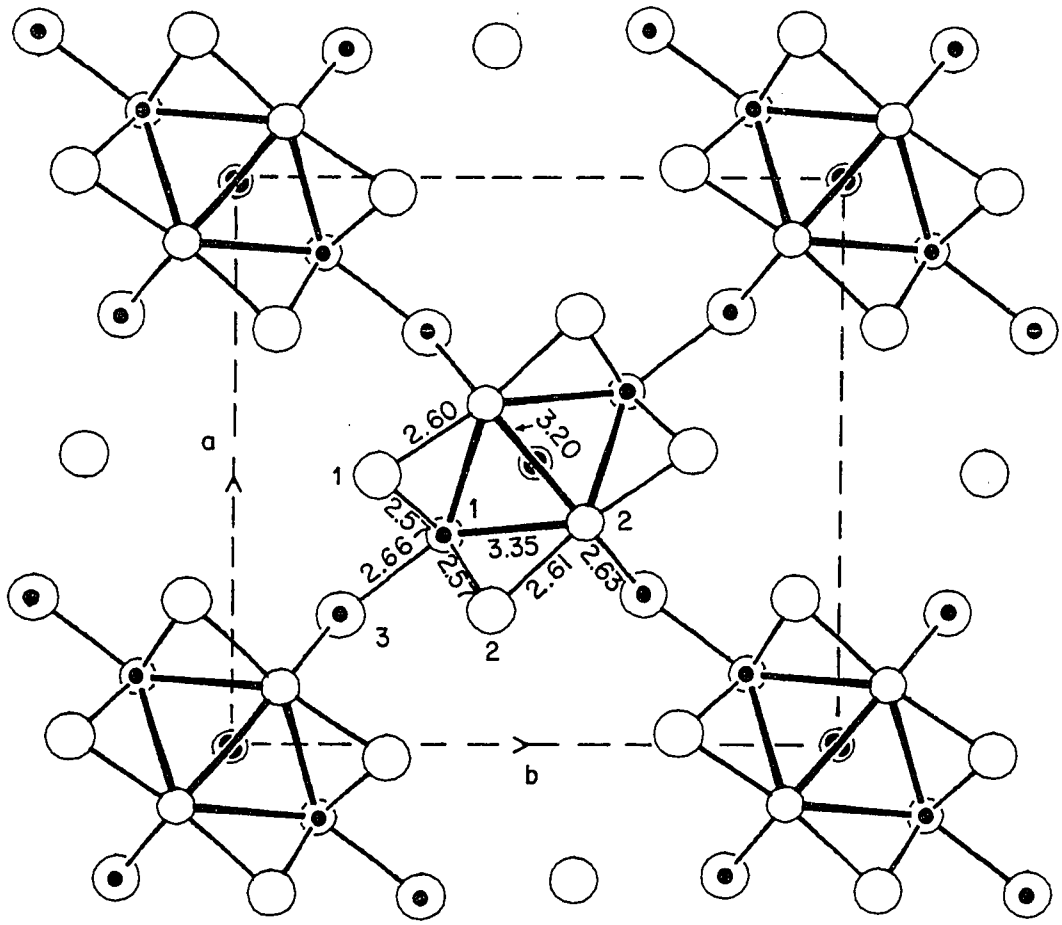

Figure 8. A unit cell projection of Sc_4Cl_6B viewed along the metal chain [001] plus the bond distances and the atom numbering system. Heavy lines interconnect the metal atoms (small spheres). The dotted atoms are separated by c/2 from the remainder. Interstitial atoms are in the centers of the scandium octahedra, boron in this case.

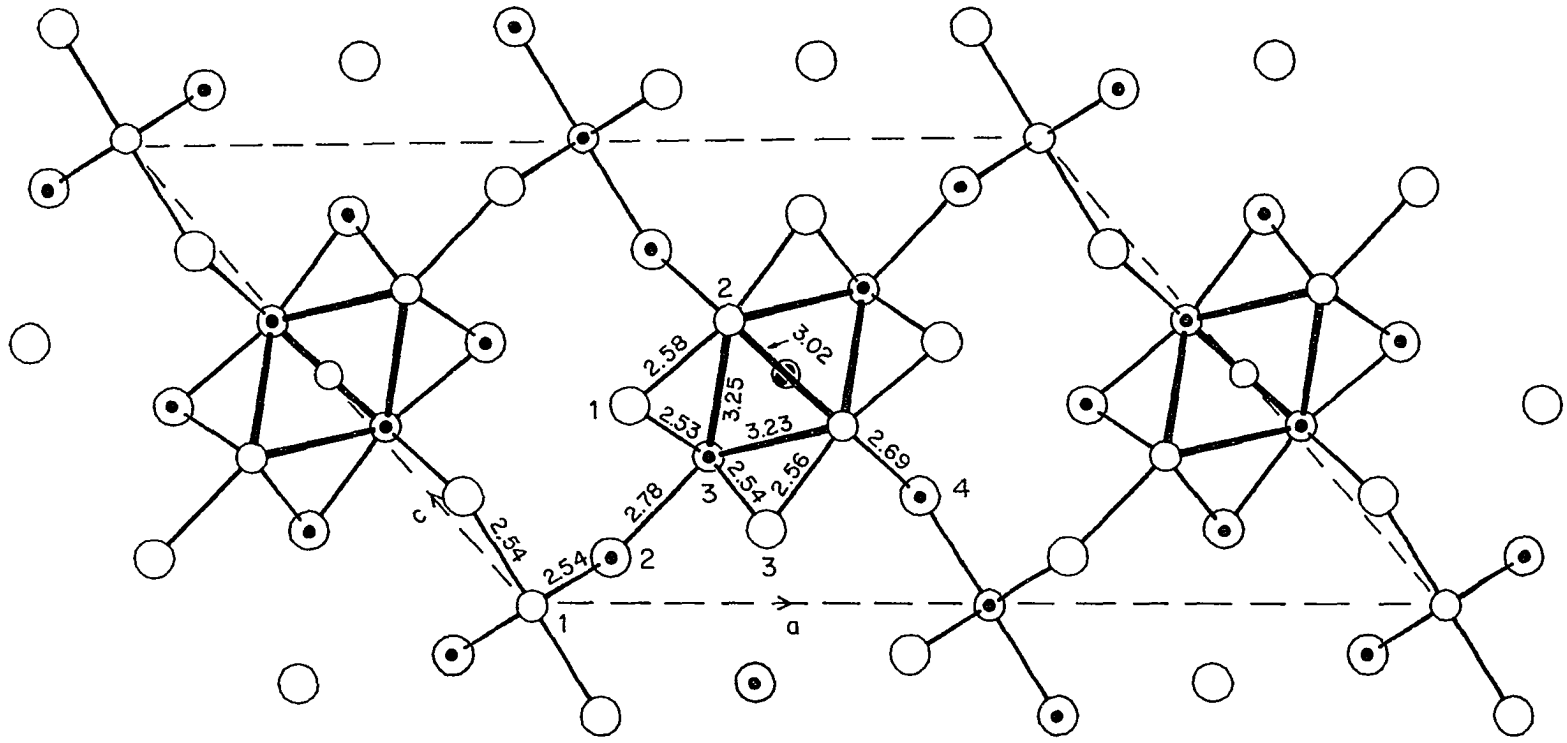

Figure 9. A C-centered unit cell of Sc_5Cl_8C viewed along the metal chain [010] plus the bond distances and the atom numbering system. Heavy lines interconnect the metal atoms (small spheres). The dotted atoms are separated by b/2 from the remainder. Interstitial atoms (Y) are in the center of the scandium octahedra, nitrogen in this case.

Table VIII. Selected bond distances (A) and angles (deg.) for Sc_4Cl_6X, (X = B, N)

	Sc_4Cl_6B	Sc_4Cl_6N (1)	Sc_4Cl_6N (2)
	Distances		
Metal array			
Sc1-Sc2	3.351(1)	3.293(4)	3.277(3)
Sc1-Sc2a	3.348(1)	3.296(4)	3.271(3)
Sc2-Sc2a	3.197(2)	3.120(7)	3.086(5)
Sc2-Sc2b	3.5988(3)	3.550(3)	3.545(1)
Chlorine atoms on metal array			
Sc1-Cl1	2.570(1)	2.557(4)	2.551(3)
Sc1-Cl2	2.572(1)	2.552(4)	2.548(3)
Sc2a-Cl1	2.604(2)	2.589(5)	2.571(4)
Sc2-Cl2	2.606(2)	2.587(5)	2.580(4)
Sc2-Cl3c(inner)	2.628(1)	2.632(4)	2.625(3)
Sc1-Cl3(outer)	2.664(2)	2.669(6)	2.690(3)
Interstitials in metal array			
X-Sc1 (x2)	2.329(1)	2.295(4)	2.279(3)
X-Sc2 (x4)	2.4069(7)	2.363(3)	2.350(1)
Nonbonded distances (<3.65A)			
Cl1-Cl2	3.634(2)	3.607(6)	3.622(5)
Cl1-Cl2d	3.697(2)	3.631(6)	3.642(5)
Cl1-Cl3	3.488(2)	3.467(5)	3.475(4)
Cl1-Cl3d	3.602(2)	3.571(5)	3.550(4)
Cl2-Cl3	3.523(2)	3.505(5)	3.515(4)
Cl2-Cl3c	3.569(2)	3.538(5)	3.518(4)
X-Cl1	3.644(1)	3.617(4)	3.604(3)
X-Cl2	3.644(1)	3.617(4)	3.603(3)
X-Cl3	3.514(1)	3.504(5)	3.479(4)

Table VIII. (Continued)

Angles			
Metal array			
Sc1-Sc2-Sc2a	61.45(3)	61.8(1)	61.78(8)
Sc2-Sc1-Sc2a	57.01(3)	56.5(1)	56.25(9)
Sc1-Sc2-Sc2b	57.52(1)	57.38(5)	57.26(3)
Sc2-Sc1-Sc2b	64.96(3)	65.2(1)	65.49(7)
Sc1-Sc2a-Sc2e	57.49(1)	57.42(5)	57.19(4)
Sc2a-Sc1-Sc2e	65.02(3)	65.2(1)	65.62(7)
Chlorine atoms on metal array			
Sc1-Cl1-Sc2a	80.65(4)	79.7(2)	79.4(1)
Sc1-Cl1-Sc1f	88.88(5)	87.9(2)	88.0(1)
Sc1-Cl2-Sc2	80.65(4)	79.7(1)	79.4(1)
Sc1-Cl2-Sc1f	88.78(5)	88.1(2)	88.1(1)
Sc2-Cl3c-Sc2b	86.41(5)	84.8(2)	85.0(1)
Bridging chlorines			
Sc2-Cl3c-Sc1c	135.31(3)	135.6(1)	135.75(7)
Interstitials in metal array			
Sc2-X-Sc2a	83.23(4)	82.6(1)	82.1(1)
X-Sc2-Sc2a	41.62(2)	41.32(6)	41.05(5)

a = 1-x, 1-y, z
b = x, y, 1+z
c = 1/2-x, 1/2+y, z
d = 1/2+x, 1/2-y, z
e = 1-x, 1-y, 1+z
f = x, y, z-1

Table IX. Selected bond distances (A) and angles (deg.) for Sc_5Cl_8Y (Y = C , N), and Sc_5Cl_8[a]

	Sc_5Cl_8	Sc_5Cl_8C	Sc_5Cl_8N
	Distances		
Metal array			
Sc2-Sc2a	3.021(7)	3.02(1)	3.090(4)
Sc3-Sc2a	3.213(5)	3.228(8)	3.268(3)
Sc2-Sc3	3.222(5)	3.245(8)	3.275(3)
Chlorine atoms on metal array			
Sc2-Cl1	2.578(6)	2.58(1)	2.596(4)
Sc3-Cl1	2.530(4)	2.530(8)	2.549(2)
SC3-CL2	2.799(6)	2.78(1)	2.777(4)
Sc3-Cl3	2.554(4)	2.538(8)	2.552(2)
Sc2a-Cl3	2.572(6)	2.56(1)	2.591(4)
Sc2a-Cl4	2.667(4)	2.686(8)	2.675(3)
Chlorine atoms around isolated metal atoms			
Sc1-Cl2	2.538(4)	2.536(7)	2.548(2)
Sc-Cl4e	2.563(5)	2.544(9)	2.555(3)
Nonbonded distances (<3.6A)			
Cl1-Cl1f	3.517(7)	3.54(2)	3.524(5)
Cl1g-Cl4e	3.541(6)	3.56(1)	3.579(4)
Cl1-Cl2	3.528(6)	3.52(1)	3.534(4)
Cl2-Cl3	3.527(6)	3.55(1)	3.538(4)
Cl3-Cl3g	3.481(7)	3.52(2)	3.498(5)
Cl3-Cl4	3.551(6)	3.55(1)	3.589(4)
Interstitial atoms to nonbonded chlorines			
X-Cl1	–	3.578(9)	3.612(3)
X-Cl3	–	3.587(9)	3.618(3)
Interstitials in metal array			
X-Sc3 (x2)	–	2.254(6)	2.273(1)
X-Sc2 (x4)	–	2.322(4)	2.353(1)

[a]Reference 2.

Table IX. (Continued)

	Angles		
Metal array			
Sc2-Sc3-Sc2b	66.3(1)	65.8(2)	65.64(7)
Sc3-Sc2-Sc2b	56.86(5)	57.09(9)	57.18(4)
Sc2a-Sc3-Sc2c	66.5(1)	66.2(2)	65.81(7)
Sc3-Sc2a-Sc2c	56.75(6)	56.89(9)	57.09(3)
Sc2-Sc3-Sc2a	56.0(1)	55.7(2)	56.36(8)
Sc2-Sc2a-Sc3	62.2(2)	62.5(2)	61.94(7)
Chlorine atoms on metal array			
Sc2-Cl1-Sc3	78.2(1)	78.9(3)	79.07(9)
Sc3-Cl1-Sc3d	88.3(2)	88.3(3)	88.3(1)
Sc3-Cl3-Sc2a	77.6(2)	78.6(3)	78.90(9)
Sc3-Cl3-Sc3d	87.2(2)	88.0(4)	88.2(1)
Sc2a-Cl4-Sc2c	82.7(2)	82.1(3)	83.1(1)
Chlorine atoms around isolated metal atoms			
Cl2-Sc1-Cl2d	87.9(2)	88.1(3)	88.33(9)
Cl2-Sc1-Cl4e	89.7(1)	89.4(3)	89.63(8)
Bridging chlorine atoms			
Sc1-Cl2-Sc3	133.96(8)	134.1(2)	133.82(6)
Sc2a-Cl4-Sc1b	136.16(9)	136.5(2)	135.95(6)
Interstitial atoms in metal array			
Sc2-X-Sc2a	–	81.2(2)	82.07(8)
X-Sc2-Sc2a	–	40.6(1)	41.03(4)

a = 1-x ,y, 1-z; g = 1/2-x, 1/2+y, -z
b = x, 1+y, z h = 1/2+x, 1/2+y, z
c = 1-x, 1+y, 1-z i = -x, -y, -z
d = x, y-1, z j = 1/2-x, y, -z
e = x-1/2, y-1/2, z k = -x, y, -z
f = 1/2-x, 1/2+y, 1-z

In Figures 8 and 9, all the atoms are so arranged either at z = 0 (single circle) or ±1/2 (double circles). Crystallographically, in the Sc_4Cl_6X structure there are two independent scandiums, three chlorines and one interstitial element. Twofold axes are vertical to the mirror planes (ab-planes at z = 0 or ±1/2) at the origin and the inversion center where the interstitial is. With additional $[ScCl_2^+]_\infty$ chain, there is one more independent scandium and chlorine in Sc_5Cl_8Y. Thereby, the connectivity scheme for discrete clusters of the Sc_4Cl_6X structure is $[Scl_2Sc2_{4/2}(X)Cl1^i{}_{4/2}Cl2^i{}_{4/2}Cl3^{i-a}{}_{2(1/3)}Cl3^{a-i}{}_{2(2/3)}]_\infty$ vs $[SclCl2_{4/3}Cl4_{2/3}]_\infty$ $[Sc2_{4/2}Sc3_2(Y)Cl1^i{}_{4/2}Cl3^i{}_{4/2}Cl4^a{}_{2(2/3)}Cl2^a{}_{2(1/3)}]_\infty$ for Sc_5Cl_8Y. The scandium atoms (small circles) are interconnected to one another with heavy lines but with light lines to chlorine atoms. The shortest axis in each structure is the repeat distance of van der Waals contacts within the parallel and commensurate chlorine strings. The Sc-Sc repeat distances along the chain also appear to be governed by the Cl-Cl separation such that the longest Sc_2 waist distances are betwen 3.55 and 3.60 A in Sc_4Cl_6X or 3.53 and 3.55 A in Sc_5Cl_8Y (Table VIII and IX). In fact, the nominal metal octahedra in this chain are distorted, and the other scandium bond distances among the octahedra are in the range between 3.09 and 3.35 A for the Sc_4Cl_6X structure vs. 3.02 and 3.28 A for the Sc_5Cl_8Y. The related bond distances in the isolated but more nearly regular Sc_6

cluster of $Sc_7Cl_{12}X$ (in the previous section) are in the range between 3.20 and 3.29 A vs. 3.07 and 3.30 A, etc. in $Sc_7Cl_{10}C_2$[45] with a double chain of condensed clusters. The feature of distortion is common to all of these compounds with a relatively low electron count.

As in other interstitially stabilized chlorides with M_6X_{12} parentage, the outward edges of scandium octahedra are bridged by chlorine atoms. In fact, they are all three coordinate to scandium atoms, i.e., chlorine 1 and 2 in Sc_4Cl_6X (Figure 8) cap "triangular faces" between the condensed clusters.[2,45] The corresponding chlorines in Sc_5Cl_8Y are Cl1 and 3 in Sc_5Cl_8Y (Figure 9). In the former structure, two inner-outer chlorines (Cl3) bridge the waist edges of the scandium octahedron and also connect to the other parallel chains at the apex scandium atoms (Sc1). In the latter, however, Cl2 and Cl4 in the octahedrally coordinated scandium (Sc1) make the connection between metal cluster chains. The bridging Sc-Cl distances for both structures are in the range between 2.53 and 2.69 A (Table VIII and IX). These, in fact, are very typical bond distances for bridging chlorines in scandium compounds, e.g., 2.55 to 2.59 A in $Sc_7Cl_{12}X$ and 2.51 to 2.66 A in $Sc_7Cl_{10}C_2$.[45] Finally, in Sc_5Cl_8Y, the chlorine (Cl2) bonds to the metal cluster at the apices in an exo fashion at a distance of 2.78 to 2.80 A, somewhat longer than the bridging chlorine to scandium distances mentioned above, but

comparable with those of the same kind, 2.73 to 2.74 A in $Sc_7Cl_{12}X$ and 2.80 A in $Sc_7Cl_{10}C_2$.

Scandium octahedra are centered by boron or nitrogen in the Sc_4Cl_6X structure and carbon or nitrogen in Sc_5Cl_8Y. The interstitial atoms are covalently bonded with six scandium atoms and the mean Sc-interstitial bond distances are 2.38 A for boron, 2.30 A for carbon, and 2.33 A or 2.34 A for nitrogen (Tables VIII and Table IX).

Interestingly, the Sc-Sc and Sc-Cl bond distances in Sc_5Cl_8C are very similar to (within 3σ of) those of "Sc_5Cl_8"[2] (Table IX). The lattice parameters of the former (a = 17.80(1) A, b = 3.5259(2) A, c = 12.052(7) A and β = 130.11(4)°) are in fact identical within 2σ to those of the latter (a = 17.78(2) A, b = 3.523(8) A, c = 12.04(1) A and β = 130.10(6)°). Also the "Sc_5Cl_8" compound was reported as a low-yield transported product with a 6-12 type structure but a somewhat less satisfactory crystal refinement resulted as the R and R_w were 0.115 and 0.136, respectively. In addition, reactions with purposely adding carbon successfully gave Sc_5Cl_8C. More strikingly, the sizes of the scandium octahedral interstices are very similar with each other (Table X). Therefore, it is very probable that the earlier compound was actually stabilized by carbon. The missed interstitial peak in the earlier structure refinement might have been the result of crystallographically disorder, lack of a second extinction correction,[37] or just poorer data.

Discussion Compounds with the composition X:M = 1.5:1 derived from 6-8 type parentage are numerous, e.g., Y_2Cl_3, La_2Cl_3 and Gd_2Cl_3. The single crystal structure determinations of Sc_4Cl_6X (X = B, N), on the other hand, show a 6-12 type cluster. The latter structure type is usual for halides of group III and rare earth metals stabilized by interstitials (B, C, N).

Second, if all valence orbitals of the interstitials are occupied as B^{5-} or N^{3-} in Sc_4Cl_6X, the electrons left available for metal bonding in the scandium octahedra are (3 x 4 - 6 - 5 (or 3) =) 1 and 3, respectively. These infinite chains of octahedra are achieved with ratios of electron per scandium of 0.25 and 0.75, respectively, while the Cl/Sc ratio is 1.5. In Sc_5Cl_8Y, the e/Sc ratios are 0.6 for the carbide and 0.8 for the nitride with Cl/Sc = 1.6. The attempt to make "Sc_4Cl_6Be" failed probably because of no electrons left in the Sc-Sc bonding orbitals. (The oxidation state of beryllium presumably would be minus six.) On the other hand, the structural chemistry of clusters derived from the group IV and group V elements to date appears to be devoid of these chains. For interstitial-free zirconium and niobium chains at a similar nonmetal/metal ratio of 1.5, the bonding in halides would involve 2.5 and 3.5 e/metal, respectively.[59]

Besides "Sc_4Cl_6Be", "Sc_4Cl_6C" is also missing as well as $Sc_7Cl_{12}C$. However, the Sc_5Cl_8C carbide with the

intermediate Cl/Y ratio of 8 can be synthesized at 860°C, which is also the formation temperature for the $Sc_7Cl_{12}X$ compounds. This suggests the former phase is more stable around this temperature. Likewise, $Sc_7Cl_{10}C_2$[45] has been obtained at 950°C and its Cl/C ratio of five is very close to that for the missing Sc_4Cl_6C. Therefore, the thermal stability of the species such as $Sc_7Cl_{10}C_2$ and Sc_5Cl_8C within the reaction temperature range of 860 to 1000°C perhaps accounts for the missing carbide compositions. Reactions below 860°C produce $ScCl_{1.5}$ (mouse fur) instead with a peritectic decomposition temperature of 877°C.[11]

Since the single crystal of Sc_5Cl_8C was found in an incomplete reaction intended to make "Sc_4Cl_6C" (940°C) and since all the carbide phases, including Sc_2Cl_2C, can be made using excess scandium metal and stoichiometric amounts of graphite, the kinetic stability is also an important factor.

The crystal radii for the interstitials in both Sc_4Cl_6X and Sc_5Cl_8Y structures are 1.50 A for boron, 1.41 A for carbon, and 1.44 or 1.46 A for nitrogen, if one takes 0.885 A as the six-coordinate Sc(III) crystal radius from Shannon.[52] In general, the interstitial boron always has the largest radius among those in the same structure type in which any matrix effect is basically constant. The second period elements have some size variability as shown in the cases of Sc_4Cl_6B and $Sc_7Cl_{12}B$ where the boron crystal radii are 1.44-1.52 A and 1.44 A, respectively, however. The

tightness of the close packed layers is a factor which should be taken into account for differences in crystal radii of interstitial atoms. Intuitively, the Sc-B distances should decrease with more valence electrons per metal cluster. Experimentally, the Sc-interstitial distances vary inversely with the number of electrons per Sc_6 cluster, i.e., the more the electron count, the smaller the Sc-B distances, e.g., 1.5 e/Sc_6 in Sc_4Cl_6B vs. 4 e/Sc_6 in $Sc_7Cl_{12}B$ with the smaller Sc-B distance.

The valence orbitals of carbon and nitrogen are smaller giving rise to shorter scandium-interstitial bond distances. The reverse order of observed carbide and nitride radii in Sc_5Cl_8Y can not be understood in terms of number of electrons per Sc_6 available for metal bonding, 4.5 for Sc_5Cl_8C which has less than 6 e's for Sc_5Cl_8N. On the other hand, the Sc-N bond distance in Sc_5Cl_8N is nearly the same as observed in Sc_4Cl_6N. The nitride radii are 0.03-0.05 A larger than those for the carbide in Sc_5Cl_8Y, which is in the opposite order, however. The refinement of Sc_5Cl_8N was very good and the bond distances are significantly different from those in Sc_5Cl_8C (Table IX). Thus, it appears the larger cell parameters of the nitride relative to the carbide are real in terms of the given interstitial element. Since the former phase was obtained from a quaternary reaction, $NaN_3/ScCl_3/$ Sc, the expanded lattice parameters

might originate from an intercalate, Na^+ in this case. The structure refinement, however, showed no residual electron density whatsoever, indicating this is a pure ternary compound. The other possibility for a rather large cell is the presence of larger interstitials, e.g., Be or B. In fact, there was no success in attempts to make these phases. Since these possibilities are excluded, it seems there is something related to the tightness of the close packing causing the difference in cell size.

The Sc_4Cl_6X unit cell can be viewed as an orthorhombic version of the tetragonal $NaMo_4O_6$ structure but lacking the intercalated sodium in the channel surrounded by chlorine atoms. The chains are slightly tilted so as to give rather nonplanar bridging chlorine atoms between chains versus the coplanar oxygen in $NaMo_4O_6$. The angle defined by the atoms of 1c, 3c and midway between 2 and 2b is 167.4^o and is depicted in the top structure of Figure 10. There are two types of connectivities in the Sc_5Cl_8C structure, through either the outer-inner chlorines (Cl4) or the inner-outer chlorines (Cl2), as in the bottom of Figure 10. These two strings formed intersecting zig-zag chains in a two dimensional network in the ac plane. The angle about Cl4 is 163.9^o while that about Cl2 is 163.8^o. The nonplanar Sc_3Cl configuration is a feature of all these single or double chain compounds in either 6-12 or 6-8 type structure. The

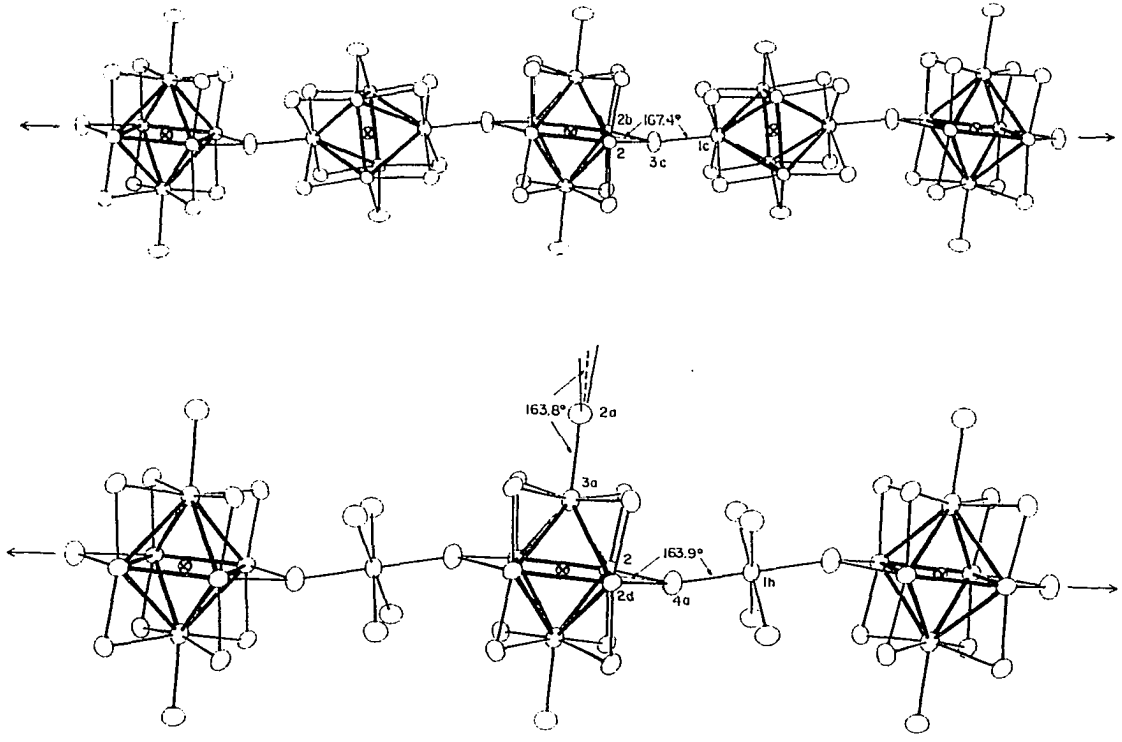

Figure 10. Two strings of interconnected infinite single chains running perpendicular to this plan, Sc_4Cl_6B (top) and Sc_5Cl_8N (bottom), which lie along [110] and [200], respectively. The metal octahedra are in heavy lines and all the atoms are drawn at 90% probability. The labels for atoms in Sc_4Cl_6B and Sc_5Cl_8N phases are as defined in Tables VIII and IX, respectively.

tilting may result from hybridization of the chlorine atoms, but more likely from the filling of space to reasonable Cl-Cl van der Waals separations.

It seems that the Sc_4Cl_6X structure type has the least packing efficiency with an empty chanel surrounded by chlorines, Figure 7. Electronically, the extended HÜckel band calculations[60] show a partially filled band at the Fermi level favoring the intercalation of either of these Sc_4Cl_6X compounds. The distances from the intercalate center to the eight nearest chlorines in Sc_4Cl_6B are 3.43-3.77 A. The sum of Shannon crystal radii of K^+(VIII) and Cl^- is 3.32 A also suggesting these "holes" are certainly big enough for the alkali metals (except for Rb and Cs). Therefore, experiments with high temperature synthetic routes in the quaternary systems $MCl_x/ScCl_3/Sc/X$ (M = Na, K, Ba; X = B, C, N) at 860-950°C and intercalation of Sc_4Cl_6B in liquid ammonia with Li, Na, or K were tried but were unsuccessful. In addition, the crystals 1 and 2 originally were solved as quaternary compounds with unreasonably small amounts of intercalates, potassium and cesium, respectively (see the section of single crystal results). The microprobe analysis on the boundle-like phase of crystal 1 gave an averaged 0.13 K per "$Sc_4Cl_{5.78}$" which did not immediately suggest the examined species had potassium in the structure. There is some possibility of a trace amount of "KCl"

deposited on the surface of the crystal, yet that is unlikely because the chlorine composition is low (less than 6). Thus, there may be a trace amount of potassium in the structure as the structure determinations showed.

Magnetic susceptibility The magnetic susceptibility data for Sc_5Cl_8C was measured on 25 mg of polycrystalline sample with H = 2,000 G (crosses) and 5,000 G (asterisks) (Figure 11). A fit of magnetic data with H = 2,000 G at below 50K to the Curie-Weiss equation, gives $C = 2.13 \times 10^{-3}$ emu K/(mole of Sc_5Cl_8C), $\theta = -4K$ and $\chi_o = 4.58 \times 10^{-4}$ emu/(mole of Sc_5Cl_8C). (The formula weight of Sc_5Cl_8C is 520.41 g/mole.) The $\mu_{eff} = (8 \times 2.13 \times 10^{-3})^{1/2} = 0.13\ \mu_B$. This is much less than the spin-only value for an electron ($1.73\mu_B$) per formula unit. According to experience, this Curie tail is most likely due to a paramagnetic impurity and would correspond to only 13 ppm (atomic) per formula unit of Gd^{3+} ($\mu_{eff} = 7.94\mu_B$). The data are corrected for the impurity for the whole temperature range (4-340K) and plotted in curve with open circles. The corrected χ gives a temperature-dependent paramagnetism with two phase transition points at both ~75K and ~200K. The corrected magnetic data above 50K were fitted with the Curie-Weiss equation to give $C = 1.37 \times 10^{-1}$ emu K/mole, $\theta = -370K$, $\chi_o = 1.46 \times 10^{-4}$ emu/mole, and $\mu_{eff} = 1.05\ \mu_B$. The raw data sets (H = 2,000G and 5,000G) show a field-dependent paramagne-

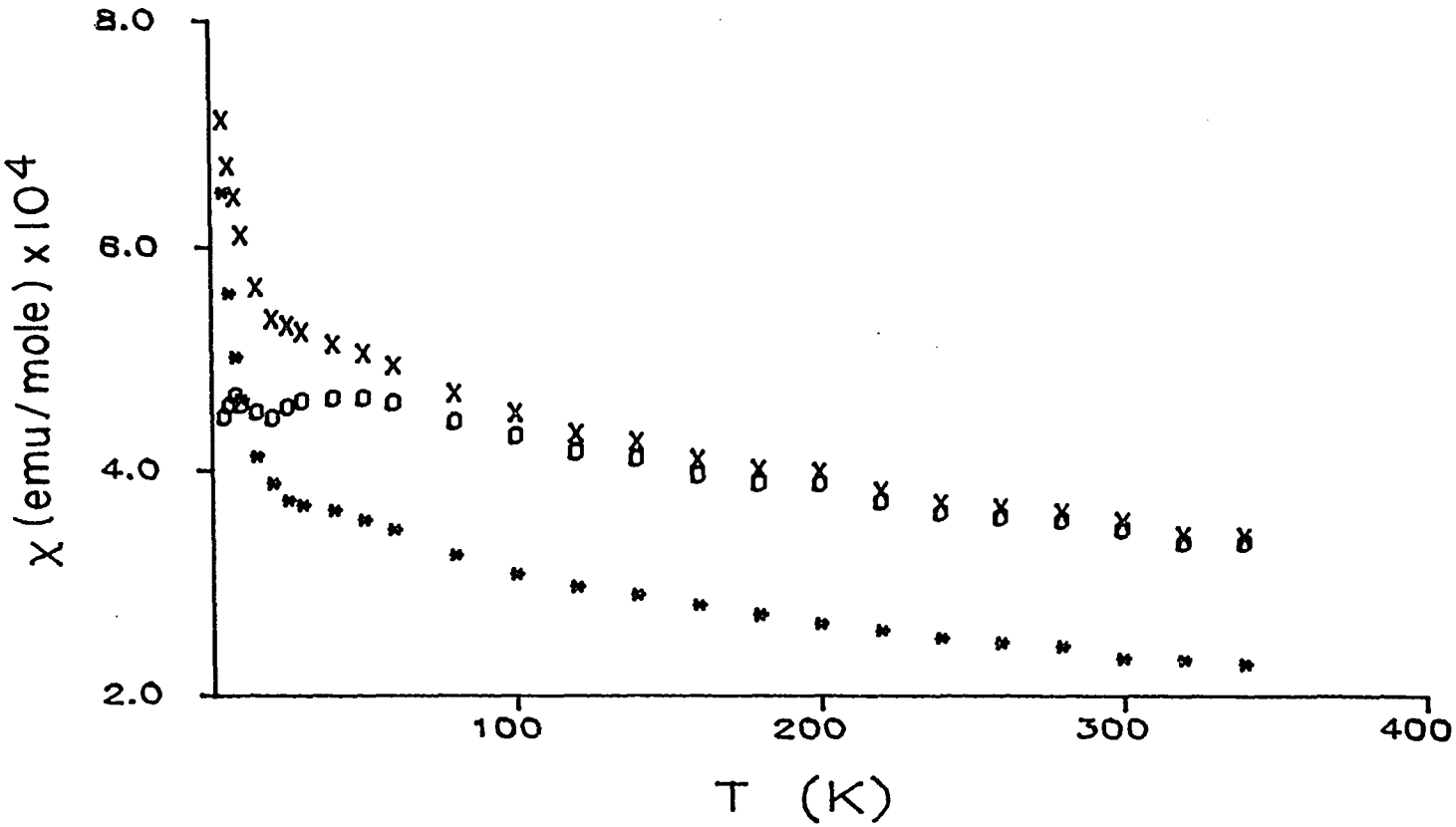

Figure 11. Magnetic susceptibility data for Sc_5Cl_8C with (x) H = 2,000G, (o) corrected for Curie tail, and (*) H = 5,000G.

tism. The UPS data (see below) show a small density of states at the Fermi edge, suggesting this black, air sensitive material probably has delocalized electrons to contribute to a temperature-independent Pauli paramagnetism, in contrast to the observed magnetic data.

The similarities in terms of the density of states curves of infinite metal chains of Sc_4Cl_6X and Sc_5Cl_8Y is shown by the band calculations which were done with the extended HÜckel method and the geometry from the single crystal data.[60] The conduction band of the Sc_4Cl_6B is also partially filled. Together with the magnetic susceptibility results of Sc_5Cl_8C, these two structure types compounds should be very interesting in their physical properties, conductivity for example. Therefore, the single crystal conductivity measurement should be conducted as soon as large enough crystals, e.g., 2-3—mm in length, are obtained. These might be produced by long reaction times, ca. two months or more, through vapor transport process.

Interstitial Atoms in Double Chain Structures. The Synthesis and Characterization of Heptascandium Decachlorodicarbide, $Sc_7Cl_{10}C_2$[1]

Introduction

The evidence absence of interstitials in clusters composed of molybdenum and niobium family elements (except for hydrogen in the niobium iodies) probably results because of the small size of the metal and thenceforth of the cavity available. On the other hand, the sizes of the d orbitals increase to the left in the periodic table and with a diminished number of cluster-based electrons for bonding, the clusters of earlier transition elements are larger and better able to accommodate small nonmetals without a great loss of metal-metal bonding through expansion. Actually, this chemistry is not altogether unprecedented when considered in light of the properties of the metals themselves. Substantial amounts of these interstitials occur in α-phase (metal) solid solutions for some of the same group III and IV elements, for example, in $YH_{0.2}$, $ZrO_{0.4}$ and $ZrN_{0.3}$,[61] and many more binary but still metallic compounds are formed by these elements with a structural rearrangement of the parent metal. All of these reactions evidence strong metal-

---

[1]This material has been published: Hwu, S.-J.; Corbett, J. D.; Poeppelmeier, K. R. J. Solid State Chem. 1985, 57, 43. The content has been modified to fulfill the needs for continuity in this dissertation.

nonmetal interactions with substantial covalency, as has been demonstrated for the hydrides[62] and the carbides,[63] for example.

Not surprisingly, some examples of interstitials within metal-bonded halide phases have been discovered serendipitiously. The most likely circumstances are the accidental inclusion of a sufficient amount of an unexpected impurity, carbonaceous for instance, together with the formation of a well-crystallized product that can be readily recognized and separated even in low yield. A residual electron density in the middle of a cluster following an otherwise satisfactory crystallographic solution is often the first hint that something may be amiss. Although X-ray diffrac-tion is somewhat insensitive for the precise identifiction of the interstitial atom involved, synthesis of crystals of the same phase in high yield can invariably be accomplished by the purposeful addition of the correct nonmetal provided some mechanism for crystal growth is available.

The present section describes the discovery and characterization of such a phase $Sc_7Cl_{10}C_2$ in which single carbon atoms are bound in the middle of all of the nominal Sc_6 octahedra that make up infinite double chains generated by sharing trans and some side edges of the simple clusters. The carbon-free analog Sc_7Cl_{10} is already known[7] and exhibits virtually identical chains but with a distinctly different arrangement of chlorine and of a separate

scandium(III) chain. A better formation that reflects the last feature is $^{1}_{\infty}[Sc^{III}Cl_2^{+}\ Sc_6Cl_8^{-}]$ when some approximations are made regarding the assignment of bridging chlorines between the units.

The title compound has been recognized as isomorphism with "Er_7I_{10}".[12,44] The latter does not immediately require a presence of an interstitial impurity, however some factors, e.g., residual electron density, low yield, nonreproducible product, and 6-12 type condensed cluster with a large hole size, have suggested this may be true.

Experimental

Synthesis The phase was ultimately identified as $Sc_7Cl_{10}C_2$ was first seen as needles with a ruby red reflectance that were obtained in low yield during an attempt to synthesize the composition "$RbSc_4Cl_6$" through reaction of RbCl, Sc strips and $ScCl_3$ at $1000^{o}/960^{o}C$ for 5 weeks. The moisture-sensitive crystals were found in the hot end of the tube in a 10-15% yield. The principal new material otherwise was $Rb_3Sc_2Cl_9$ while ScOCl was not evident. Weissenberg photos together with the initial tuning procedures on the diffractometer showed these new crystals to be quite similar to Sc_7Cl_{10}[7] with the same space group (C2/m) but with somewhat different values for one axis length and the monoclinic angle. The Guinier powder pattern of the new phase was quite different (Table A4).

The crystal structure solution (below) showed this new phase had a Sc_7Cl_{10}-like double metal chain structure but a distinctly different arrangement of both the chlorine atoms and the scandium(III) side chain and with a clear electron density residual in the center of each metal cluster within the chain. The last was initially taken to represent oxygen (and was refined as such) because of the rather pervasive character of ROCl oxychloride in this and other rare earth metal-rich systems where it is thought to come both from the reactions and from some outgassing of the silica jacket[28] unless this is flamed especially well before sealing. Microprobe analyses of three single crytals supported on a carbon plate gave good agreement for the chlorine to scandium ratio, 1.42(3):1 vs. 1.43:1 for Sc_7Cl_{10}, but the O:Cl values ranged between 0.06 and 0.48:1. More importantly, attempts at direct synthsis in which ScOCl was purposely included gave inconsistent results, the "$Sc_7Cl_{10}O_2$" being found in some instances but not in many others. ScOCl was clearly mobile at these temperatures so a kinetic explanation for the lack of success did not seem approriate. A second structure result was meanwhile obtained for a crystal from a 5-10% yield in a reaction that also produced another interstitial phase Sc_5Cl_8C.

A clue to the correct identity of the interstitial atoms came from another reaction in which crystals of the

phase in question were found together with single crystals of what was subsequently structurally refined as shown to be Sc_2Cl_2C by its direct synthesis in high yield from metal, trichloride and graphite.[23] Reactions aimed at the synthesis of $Sc_2Cl_2C_x$ from the same reactants (excess Sc strips) at 1010°C gave a mixture of the intended phase together with $Sc_7Cl_{10}C_2$ for $x \leq \sim 0.8$, with a quantitative yield of large crystals of the latter with correct chlorine-to-carbon stoichiometry ($x = 0.4$). A third set of diffraction data was collected and refined for a single crystal from the last reaction to confirm that the known phase was the same as studied twice before.

Reaction of the above starting materials for a week at 860°C is sufficient to give microcrystalline products of $Sc_7Cl_{10}C_2$, with transport yielding nice single crystals over a longer period near 1000°C. Powdered metal gives Sc_2Cl_2C and unreacted $ScCl_3$ after six weeks at 860°C, presumably representing a nonequilibrium situation. It appears that $Sc_7Cl_{10}C_2$ and Sc_2Cl_2C are adjacent line phases, with the yields at 1000°C depending principally on the relative amount of carbon present; characteristically, scandium strips in excess are needed for good yields. The preparation of Sc_5Cl_8C is generally carried out at lower temperatures, 860-900°C.

Structure solutions Although the cell parameters of the new phase were clearly different from those Sc_7Cl_{10}, a

sharpened Patterson map showed that many of the same structural features remained according to the u,o,w and u,1/2,w sections. The atomic coordinates for the related (see below) structure of Er_7I_{10}[12] provided the correct model, and this refined uneventfully to a very satisfactory result. Crystal parameters and some refinement results for this and two crystals subsequently studied (and referred to in the previous section) are given in Table II. Absorption corrections were applied to all using a ψ-scan method and the program ABSN,[39] with scans being made at two different values of θ for the first two crystals (μ = 47 cm^{-1}, 0.83 < T < 0.99 for crystal two). Secondary extinction corrections were found to be unnecessary. The final different maps were flat to well less than 1 e/A^3 at all positions.

Refinement of diffraction data from a third crystal was completed in order to establish that the product made in high yield by the purposeful introduction of carbon was identical to those twice studied that contained uncertain interstitials (though clearly the occupancies in the latter cases refined to close to the correct values for carbon). The last study accomplished this purpose well although the standard deviations of the positional and thermal parameters were two to four times greater than obtained with either of the other crystals. The poorer result likely arose from somewhat lower crystal perfection relative to crystal two and, more importantly, because fewer reflections were

observed when a 2θ/θ-scan mode and no monochrometer were used (Table II). Weissenberg photos indicated the crystal quality was 2 > 3 > 1 although the differences were not large and all would be characterized as satisfactory as to peak size and freedom from more than slight streaking. The question of different cell sizes will be considered later.

The refined structural parameters for the second crystal of $Sc_7Cl_{10}C_2$, which appears to be the best result of the three studied by all criteria, are listed in Table X. The observed and calculated structure factor data appeared in the paper.[45]

The composition of $Sc_7Cl_{10}C_2$, especially the identity and amount of the carbon interstitial, was established principally by the synthesis of the phase in substantially quantitative yield (>95%, with no other phases detected in Guinier patterns) by the on-stoichiometry reaction:

$$10\ ScCl_3 + 6\ C + 11\ Sc\ (excess,\ strips) \longrightarrow 3\ Sc_7Cl_{10}C_2.$$

The X-ray refinements agreed with this fairly well (Table II). In addition, the presence of a carbide-like C 1s emission from the compound was established by photoelectron spectroscopy (see following). Powder pattern data show that the same phase had been seen earlier[2] and identified to have Cl:Sc = 1.40(7) on the basis of microprobe analyses.

Magnetic susceptibility Polycrystalline samples were sealed in high purity fused silica tubes under a helium atmosphere for the susceptibility measurements which were

Table X. Atom parameters for $Sc_7Cl_{10}C_2$, (crystal 2)

	x	y	z	B_{11}[a]	B_{22}	B_{33}	B_{13}
Sc1	0.0	0.0	0.0	0.76(6)	1.49(8)	0.86(7)	0.19(5)
Sc2	0.3464(1)	0.0	0.2676(1)	0.85(5)	0.63(5)	0.88(5)	0.25(4)
Sc3	0.2004(1)	0.5	0.2768(1)	0.75(5)	0.58(5)	0.79(5)	0.17(3)
Sc4	0.3190(1)	0.5	0.4928(1)	0.70(5)	0.41(5)	0.79(5)	0.19(4)
Cl1	0.4284(1)	0.5	0.3742(1)	0.88(6)	0.90(6)	1.23(6)	0.18(5)
Cl2	0.0956(1)	0.5	0.3843(1)	0.79(6)	0.96(7)	1.03(6)	0.18(4)
Cl3	0.1239(1)	0.0	0.1336(1)	1.37(6)	0.91(7)	1.32(6)	-0.24(5)
Cl4	0.2871(1)	0.5	0.1255(1)	1.17(6)	0.78(6)	0.92(6)	0.20(4)
Cl5	0.4519(1)	0.0	0.1243(1)	1.63(7)	0.91(7)	1.55(6)	0.72(5)
C[b]	0.2613(3)	0.0	0.3745(5)	1.2(2)			

[a] $B_{12} = B_{23} = 0$, by symmetry. [b] Occupancy of 2.17(5).

done at Bell Laboratories down to 4.2K by Farady method.[64]

Results

Structure description Figure 12 shows the contents of approximately one-half of the C-centered unit cell as viewed along the short b axis but with the cell tilted slightly so the clusters and bridging functions may be discerned. All atoms occur at y = ±1/2 (double circles) or y = 0 (single). The scandium atom arrangement, basically the same as in Sc_7Cl_{10}, can be viewed as first generating elongated octahedra which share trans edges (Sc3-Sc4) so to form chains parallel to b. In addition, parallel pairs of these chains are fused through sharing of a pair of cis edges in each octahedron (Sc4-$Sc4^b$) to yield double chains. Carbon is near the center of each octahedron. Side and top views of the metal chain (plus carbon) are shown in Figure 13 with all of the shared edges in heavy outline in the bottom drawing. One octahedron can be described as $(Sc2)_2(Sc3)_{2/2}(Sc4)_{2/3}(Sc4)_{1/3}$.

Two additional features define the structure, the halogen placement about both metal chain and the isolated Scl atoms which are located at the corners and at the center of the (001) face. These arrangements are significantly different from those in Sc_7Cl_{10}. As can be seen in Fig. 12, chlorine bridges all exposed edges of the octahedra that comprise the chains to produce a $^1_\infty[Sc_6Cl_6]$ unit. Second, the isolated Scl atoms which are again taken to be

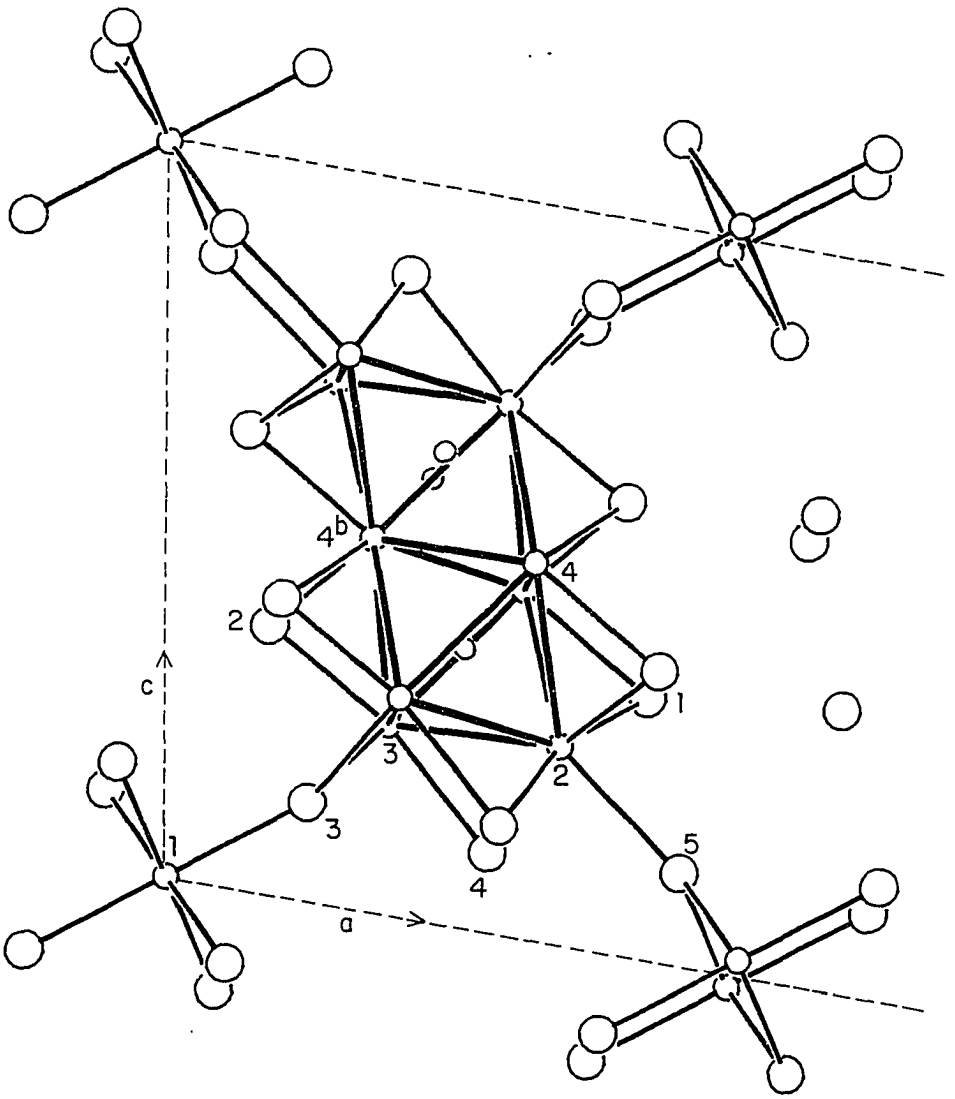

Figure 12. A section of the $Sc_7Cl_{10}C_2$ structure viewed approximately along the metal chain [010] plus the atom numbering system. All atoms occur at y = 0 or 1/2, with pairs of circles corresponding to those with y = ±1/2. Heavy lines interconnect the metal atoms (small spheres). The remainder of the cell is generated by a C-centering condition (x + 1/2, y + 1/2, z); an inversion center occurs at the midpoint of the $Sc4-Sc4^b$ connections.

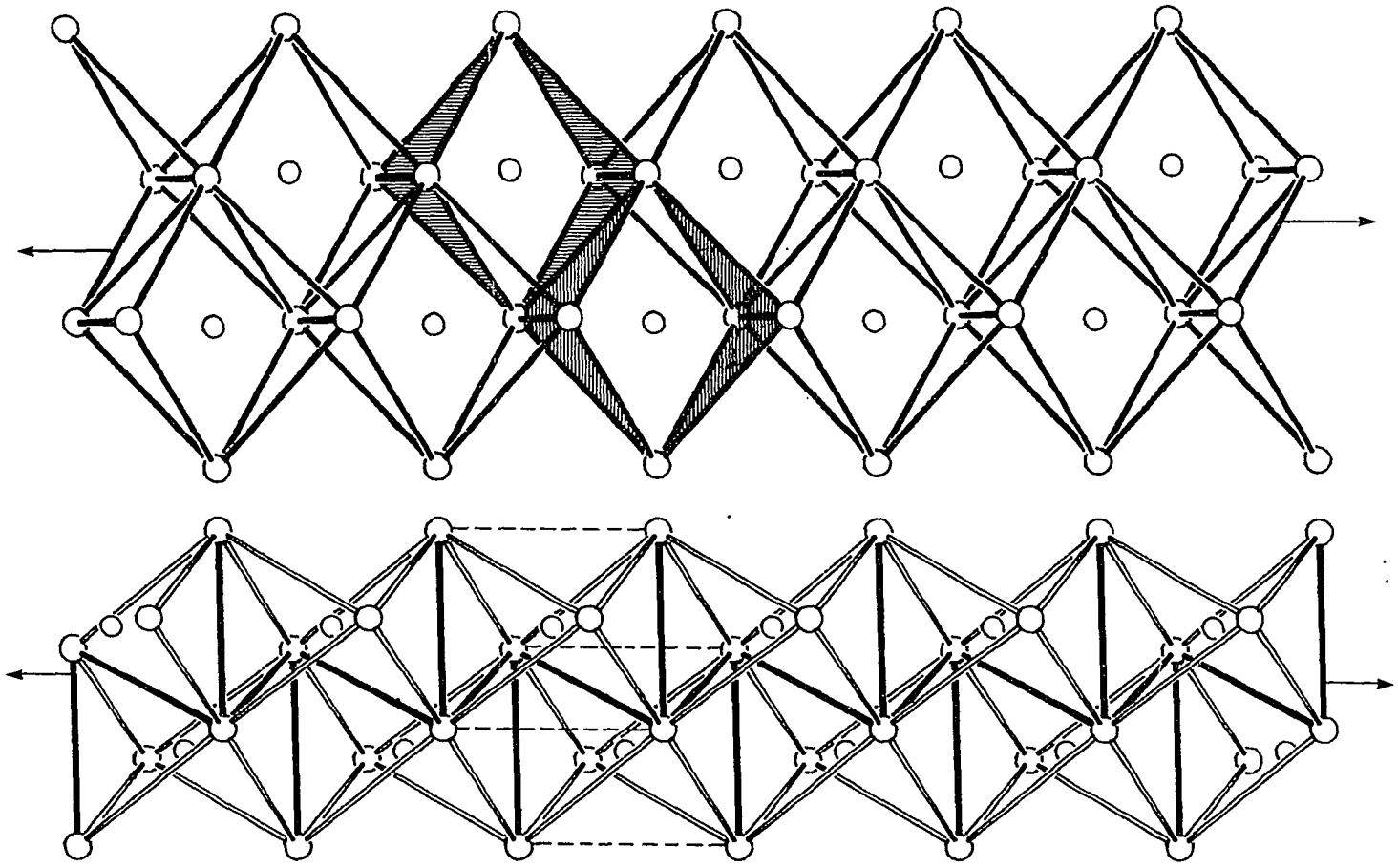

Figure 13. Two approximately normal views of the chain of metal octahedra in $Sc_7Cl_{10}C_2$ together with the centered carbon atoms. The 8% longer repeat along the chain repeat (3.50 A) is ommitted for clarity. Shared edges between octahedra are in heavy outline in the lower view.

scandium(III) are surrounded by chlorine octahedra. Since these have the same period as the metal chain, the chlorine octahedra also share trans edges (Cl5-Cl5) and generate commensurate $Sc1(Cl3)_2(Cl5)_{4/2}$ octahedral chains. These metal and Sc-based chains are not independent, however. All chlorine in the structure are three-coordinate to scandium, achieving this either through bringing pairs of edges of the fused metal octahedra along the chain (Cl1, 2, 4) or by being part of the $ScCl_2Cl_{4/2}$ chains and occupying the remaining, all-important exo positions on the metal chain. Thus, the Cl3 apices of the chlorine octahedra also bridge the side edges of the metal chain (Sc3-Sc3'), while the shared Cl5 atoms are exo to each vertex of the metal chain at Sc2. Partition of the latter according to metal neighbors gives an approximate description as $^1_\infty[(Sc^{III}Cl_2)(Sc_6Cl_8)]$.

Bonding and nearest-neighbor nonbonding distances are given in Table XI together with the corresponding distances in Sc_7Cl_{10}. The metal chains in the two structures are closely comparable, the presence of scandium-carbon bonding generally giving smaller and more regular metal polyhedra. Neglecting the long repeat distances for all atoms along the chain at ca. 3.50 A, the average Sc-Sc distance here is 3.24 A, 0.03 A less than without carbon, with the shared edges still the shortest, as is typical. The Sc3-Sc4 join within the octahedral chains now alternate with carbon atoms

Table XI. Distances (A) in $Sc_7Cl_{10}C_2$ and in Sc_7Cl_{10}[a]

	$Sc_7Cl_{10}C_2$	Sc_7Cl_{10}
Scandium in chain		
Sc2-Sc3	3.245(1)	3.253(2)
Sc2-Sc4	3.290(1)	3.271(2)
Sc3-Sc4	3.072(2)	3.147(3)
Sc3-Sc4[b]	3.302(1)	3.407(3)
Sc4-Sc4[b]	3.131(2)	3.153(3)
Sc1-Sc1[c]	3.4930(4)	3.5366(6)
Chlorine on metal chain		
Sc4-Cl1	2.658(2)	2.695(2)
Sc2-Cl1	2.510(1)	2.443(3)
Sc4[b]-Cl2	2.625(1)	2.627(3)
Sc3-Cl2	2.499(2)	2.570(2)
Sc2-Cl4	2.539(1)	2.487(3)
Sc3-Cl4	2.601(2)	2.631(2)
Bridging chlorine		
Sc3-Cl3	2.666(1)	3.208(4)
Sc1-Cl3	2.560(2)	2.502(2)
Sc2-Cl5	2.799(2)	2.611(3)
Sc1[d]-Cl5	2.539(1)	2.566(3)

[a]Reference 7. [b]1/2-x, 1/2-y, 1-z. [c]All atoms repeat at the b axis length. [d]1/2-x, 1/2-y, z.

Table XI. (Continued)

Carbon in chain		
Sc2-C	2.185(6)	
Sc3-C (x2)	2.284(4)	
Sc4-C (x2)	2.375(4)	
Sc4-C	2.339(6)	
Chlorine-chlorine[c,e]		
C11-C12[b]	3.443(6)	3.460
C11-C15	3.516(6)	3.910
C13-C14	3.520(6)	3.443
C14-C15	3.530(6)	3.698
C12-C13	3.557(6)	3.452
C11-C12[f]	3.560(6)	3.910

[e] $\leq$3.560 A. [f] Interchain distance.

and at 3.07 A is 0.05 A shorter than in Sc_7Cl_{10}. A more striking effect is a 0.105 A decrease in Sc3-Sc4^b. (The actual distances within the octahedra, neglecting the long repeat, still vary over a range of 0.23 A or by 14%.)

The scandium-chlorine distances show nothing unusual although slightly shorter values for bridging chlorine on the chain are to those scandium atoms that are more exposed and have fewer metal neighbors. On the other hand, Cl-Cl repulsions may be responsible for the shortening; clusters and extended arrays are characteristically well-sheathed by the nonmetal,[65] and the longer Sc-Cl distances for Cl1,2,4 correlate quite well with the probable distortions arising from the shorter Cl-Cl separations (Table XI). The exo Sc-Cl distances are characteristically longer and also appear to be limited by Cl-Cl contacts.

The Sc-C distances seem quite reasonable, the 2.31 A average here comparing very well with 2.308(1) A (x6) in Sc_2Cl_2C,[23] and averaged 2.999(5) A in Sc_5Cl_8C (see above). The so-called monocarbide (NaCl type) is carbon-deficient with a composition near Sc_2C and a lattice constant for an apparent NaCl-type subcell that corresponds to 2.36 A for Sc-C; the well-described Sc_4C_3 (anti-Th_3P_4 type) has an average Sc-C distance of 2.24 A.[66]

Structure comparison

Sc_7Cl_{10} As described above, the phase $Sc_7Cl_{10}C_2$ shows a remarkable similarity to Sc_7Cl_{10} in the

double-metal chains. The remainder of the structure is distinctly different, however. Figure 14 compares the Sc_7Cl_{10} (left) and $Sc_7Cl_{10}C_2$ (right) in projection along the short b axes, with dotted atoms differing from open circles by b/2. The chlorine elevations in the two structures are taken to be the same. Their disposition about the scandium chain is such as to cap exposed triangular <u>faces</u> in Sc_7Cl_{10} but to bridge <u>edges</u> in $Sc_7Cl_{10}C_2$, the change also being accompanied by the rotation of the isolated scandium(III) chains by $\sim 70^{\circ}$. The conversion of Sc_7Cl_{10} to $Sc_7Cl_{10}C_2$ (or vice versa) can thus be accomplished by displacement of all metal atoms in the structure by b/2 together with changes in the x and z coordinates of C13 and C15 so as to reestablish reasonable distances within shared chloride octahedra, the displacement of Sc1 serving to interconvert waist and apex functions. The clear change in chlorine placement about the exposed metal vertices of the chain on conversion from face to edge bridging chlorine - Fig. 14 - lengthens the Sc2-C15 interchain link by 0.19 A, but causes a more drastic shortening of the Sc3-C13 bridging by 0.54 A owing to a clearly greater obstruction of the Sc3 vertex in the metal chain by chlorine atoms in Sc_7Cl_{10}. Much of the 6.8% decrease in cell volume accompanying the carbon addition can be associated with a decrease in height of the metal chain from carbon bonding together with tighter Sc3-C13 bridging and thence smaller separations between metal chains.

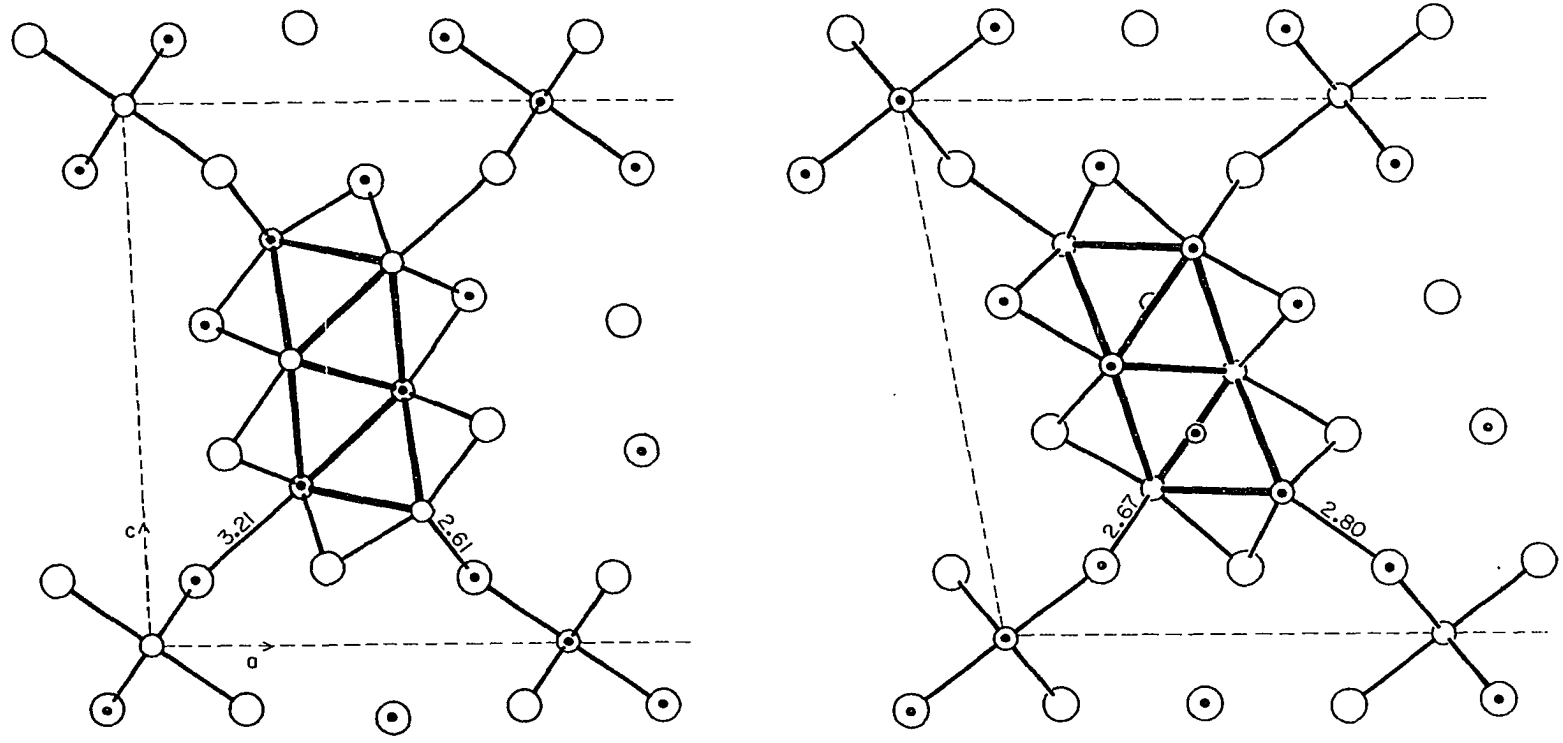

Figure 14. Comparison of the Sc_7Cl_{10} (left, Ref. 7) and $Sc_7Cl_{10}C_2$ (right) structures in projection along the metal chain with dotted atoms separated by b/2 from the remainder. The two structures may be interconverted by displacement of all metal atoms by b/2, changing the chlorine on the metal chain from face-capping to edge-bridging functions.

A fairly simple explanation can be discerned for the change from face- to edge-bridging chlorine around the metal chains on introduction of carbon into the cluster, the reduction of carbon-chlorine interactions. The cluster centers in Sc_7Cl_{10} are only 2.88 and 3.01 A from Cl2 and Cl4, respectively, or 2.86 and 2.89 A in a model with a carbide-like metal chain in the Sc_7Cl_{10} arrangement, while the observed C-Cl separation in $Sc_7Cl_{10}C_2$ is 3.48 A, the same as in Sc_2Cl_2C. The former separations seem to be well less than the sum of reasonable van der Waals radii when it is noted that chlorine is the order of 1.75 A in radius to other chlorines (Table XI). An electrostatic argument can also be used since both chlorine and carbon presumably bear some negative charge. Calculation of the Madelung part of the lattice energy (MAPLE)[67] for several different charge distributions indicate that the observed structure has up to a few percent greater lattice energy as well as a more uniform contribution to that by the three types of scandium atoms in the chain. In general, structures with metal octahedra that are face-capped by nonmetal are more likely to be destabilized by repulsions between the nonmetal and interstitial atoms centered in metal octahedra. The structures of Gd_2Cl_3, Nb_6I_{11}, and ZrX are also of this type, while a much larger number of clusters and chains contain face-capping halide. The transition from 3R-ZrX structures to the 1T-type as in Sc_2Cl_2C on insertion of nonmetal into

the octahedral site (below) is exactly analogous to the transition discussed here in terms of diminished halogen-interstitial interactions.

The new carbide phase also bears a considerable similarity to Sc_7Cl_{10} in that it too exhibits significant variations in cell dimensions. About 16 sets of lattice constants have been refined for different preparations of $Sc_7Cl_{10}C_2$ using 16 to 27 Guinier reflections from each measured relative to powdered silicon (NBS) as an internal standard. Seventy percent of these gave cell volumes within ± 1.1 A^3 of the 757.5 A^3 average for the second and third crystals studied by single crystal means, the extremes in fact occurring for products of high yield reactions. The remaining cell volumes grouped in the range of 761.3 to 763.4 A^3 with the first crystal used to determine the structure providing the upper limit. Since this last group generally were found early in the investigation, some consideration was given to the presence of a different interstitial atom or a mixture, although subsequent attempts to insert boron, nitrogen or oxygen alone in this structure have been unsuccessful. However, a close comparison of the actual structural data from crystal one with that of crystal two (the better) suggests changes in crystal perfection may be responsible instead, the first being the poorer judging from Weissenberg films. In addition, the apparent thermal ellipsoids obtained for metal in the first crystal were

uniformly about twice as large and with standard deviations 15-20% greater than for the second. Likewise, thermal parameters for chlorine were about 10% larger and B_{22} for the isolated Sc1 was 50% greater. In addition, the Sc-Sc distances within the chain were all 0.02 to 0.03 A larger, but with Sc-Cl differences larger by no more than 0.01 A and generally not significantly so. These observations are remarkably similar to those made earlier with respect to two different crystals of Sc_7Cl_{10}[7] even as to the relative sizes of the ellipsoids for Cl3 and Cl5. Since there was no evidence whatsoever for interstitial atoms in the earlier study, we are inclined to prefer the same explanation for the present variations, that is, intrinsic differences in imperfections among crystals with very anisotropic bonding.

Several aspects of the carbon bonding bear comment. At first glance the Sc-C distances (Table XI) seem quite irregular, but these turn out to vary plausibly with the total amount of bonding that can be inferred for each scandium atom based on distances. The metal octahedra are elongated along b and compressed normal to this along the shared edge Sc3-Sc4. The carbon is actually displaced ~0.12 A in c from the waist of the octahedron toward Sc2 and Sc3 to produce the order $2 < 3 < 4^b < 4$ in distances to scandium. As seen in the coordination number summary in Table XII, this follows precisely the change in environment of scandium, that with more chlorine and fewer scandium

neighbors and therefore perhaps with a higher charge having closer carbon contacts. The introduction of carbon is also seen to produce a remarkable uniformity, six nonmetal nearest neighbors for all scandium atoms.

The process of cluster condensation generally involves replacement of some chlorine neighbors about each metal, six in the case of the $ScCl_3$ parent, by a greater number of metal atoms, i.e., five Sc substitute for two Cl on average in the present structure, nine Sc for three Cl in ScCl,[8] and finally 12 for all 6 in the metal. The Sc-Cl separations remain remarkably constant throughout this, the additional electrons generally not screening the Sc-Cl separations significantly, while the added and more numerous metals that replace chlorine occur at relatively long Sc-Sc distances compared with the single bond metal radius (2.92 A). The metal-bonded halides indeed appear to possess just exactly the distance-coordination number intermediacy that one would expect between a salt and a delocalized metal.[68]

Magnetic susceptibility Polycrystalline, black powder of $Sc_7Cl_{10}C_2$ was measured for its magnetic property by DiSalvo et al.[69] The compound possesses a weak temperature-dependent paramagnetism with a Curie tail at the temperature below 50K due to impurities or perhaps defects (Figure 15, curve a). If one fits the susceptibility at Curie tail to the Curie-Weiss equation $\chi = C/(T-\theta) + \chi_o$, one finds $C = 1.25 \times 10^{-2}$ emu k/mole of $Sc_7Cl_{10}C_2$, $\theta = 1.8K$ and

Table XII. Scandium coordination numbers and scandium-carbon distances in $Sc_7Cl_{10}C_2$

Scandium atom	Coordination Number[a,b] To Sc	To Cl	To C	Distance Sc-C, A
1	0	6	0	
2	4	5	1	2.18
3	5	4	2	2.28 (x2)
4	7	3	3	2.34
				2.38 (x2)

[a]To all first neighbors listed in Table XI, all atoms have two additional neighbors of like kind at 3.49 A, the b axis repeat. [b]Sc_7Cl_{10} has the same coordination for Sc and Cl except for four Cl about Sc2, Sc_5Cl_8C is the same lacking Sc4.

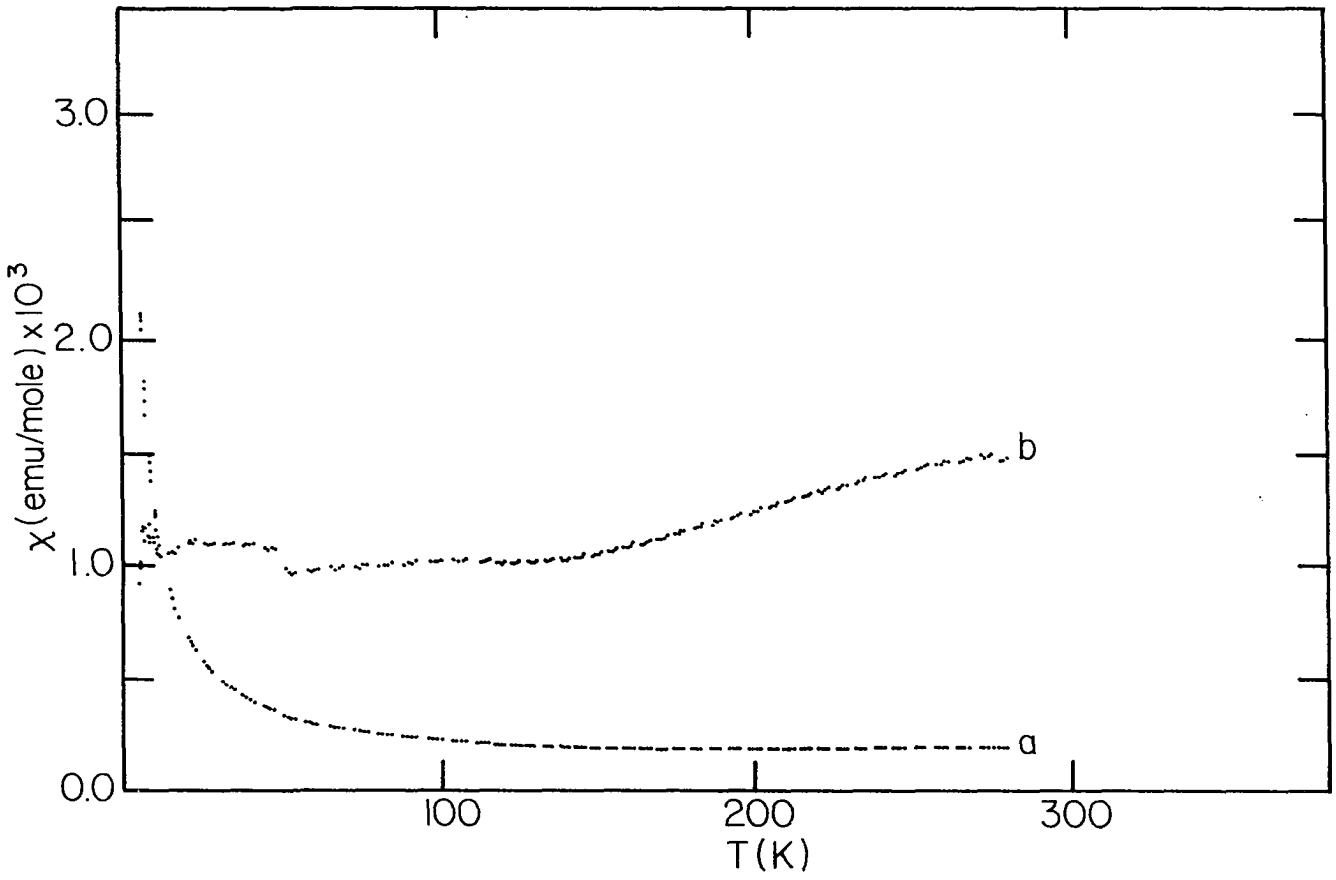

Figure 15. Magnetic susceptibility of $Sc_7Cl_{10}C_2$. a) raw data, b) corrected for Curie tail and plotted for the scale of zero-3.4 x 10^{-4} emu/mole of $Sc_7Cl_{10}C_2$.

χ_o = 1.09 x 10^{-4} emu/mole with standard deviation ca. 0.3%. If one assumes that χ_o is temperature-dependent at T > 50K and produces an increasing χ above ~120K, one can recover the "intrinsic" susceptibility, χ_o, by assuming C is temperature-independent, and substracting C/(T-θ) from χ. This produces the second curve, b, shown on the Fig. 15.

There is a first order phase transition at temperature near 50K that one can also see in the raw data when sighting along the curve. Both the discontinuity in molar susceptibility around 150K and a possible Néel transition at T_N ~275K have been seen in the preliminary measurements above liquid nitrogen temperature performed in Ames Laboratory by Faraday method, i.e., both transitions are reproducible and consequently intrinsic to the sample.

The magnitude of the Curie tail is about eight times smaller than the magnitude for Sc_7Cl_{10}.[70] One calculated an effective moment per formula unit of μ_{eff} = 0.32 μ_B. If these are impurities one would need ~250ppm (atomic) of Fe (μ_{eff} = ~5μ_B) to account for this Curie contribution.

The susceptibilities at the temperatures above 50K have been fitted in the Curie-Weiss equation after they were corrected for the contribution from "impurity", Figure 15b. This relatively weak temperature-dependent paramagnetism suggests a metallic character which is consistent with the UPS data (see following). However, the temperature-independent Pauli paramagnetism should be expected and is contrary

to the experiment results, Figure 15b. This might suggest a possible long range magnetic ordering betwwen 150K and 275K (T_N).

Unsuccessful reactions

Sc_7Cl_{10} According to Poeppelmeier,[11] the quantitative synthesis of polycrystalline Sc_7Cl_{10} requires two steps, i.e., reduction of $ScCl_{1.5}$ (mouse fur)[6] with scandium strips at between 877 and 900°C, followed by reaction for a period of time below 877°C without opening the reaction tube. However, the highest yield of this phase in the present work, ca. 70%, was through the slow cooling of the product of a high temperature (960°C) reaction synthesizing "ScCl" with a stoichiometric amount of powdered metal (chapter IV). Later we learned that the "ScCl" phase is stabilized by various amount of hydrogen left in the dehydrogenated powder metal. The high yields of product of Sc_7Cl_{10} described above does not necessarily suggest the compound has hydrogen in it because earlier preparations[11] gave Sc_7Cl_{10} in nearly 100% yield using scandium metal strips.

The new whisker phase ($ScCl_{1.42}$, see below) was formed quantitatively in the following four reactions attempting to make Sc_7Cl_{10} and $Sc_7Cl_{10}H_{0.5}$ using stoichiometric amount of Sc(strips)/$ScCl_{1.5}$ at 877°/885°C (2 months) or Sc(powder)/$ScCl_3$ at 880°/ 900°C (2 months) and with or without the addition of ScH_2. The reactions had just a

sufficient amount of hydrogen from adding ScH_2 to form the composition "$Sc_7Cl_{10}H_{0.5}$" suggested by later magnetic measurements.[70] The yields of $ScCl_{1.42}$ were nearly 100% in the reaction with no ScH_2 added and ~85% with ScH_2 added. The minor product of the latter was powdered 3R-$ScClH_x$ (ZrBr-type). Here again the $Sc_7Cl_{10}H_{0.5}$ has been proven not to exist within the temperature ranges used to produce Sc_7Cl_{10} in high yields. This new whisker phase has been seen in various systems (binary and ternary systems with KCl or CsCl added) during this course of study. One of the single fiber-like crystals was studied by electron microscopic analysis to give the above composition $ScCl_{1.42}$ and two short axial lengths of 2.9 and 3.9 A, and the intervening angle of 100.9°. This compound has not only the similar composition to $ScCl_{1.43}$ (Sc_7Cl_{10}) but ninety percent of the X-ray scattering occurs at distances calculated for Sc_7Cl_{10} powder pattern, but in addition there are some weak extra lines. Presumably this represents some subtle distortion so that the indexing from a cell of the latter no longer applies. This compound can be reformulated with integers as "$Sc_{12}Cl_{17}$" which is, however, not isomorphous with $Gd_{12}I_{17}C_6$.[71] In fact there is plenty of evidence it can be made with strips, suggesting it might be an interstitial-free compound with 6-8 type condensed clusters.

The observed Guinier powder pattern is listed in Table XIII.

The magnetic susceptibility of this material was measured by DiSalvo et al.[70] to give a weak temperature-dependent paramagnetism. After the correction for impurity shown in a Curie tail ($T < 30K$, $\mu_{eff} = 0.17\mu_B$), the χ_o is equal to 2.1×10^{-5} emu/mole of $ScCl_{1.42}$ (M.W. = 95.30) while $\theta = 26K$ and $C = 7.9 \times 10^{-3}$ emu/mole of $ScCl_{1.4}$. The magnetic data were fit a simple Curie law from 0-300°K with a large mean square error of 5%. This either means, according to DiSalvo,[69] that χ_o is very temperature dependent, or, more likely from the shape of the curve left after subtracting a low temperature fit (from 0~30K), the moment is temperature-dependent and decrease with decreasing temperature.

Layered Compounds Derived from Cluster Condensation and Stabilized by Interstitial Elements. Synthesis and Characterization of Scandium Monochloride Hemicarbide and -nitride, 1T-Sc_2Cl_2Y (Y = C, N) and 3R-Sc_2Cl_2C

Introduction

The monohalides ZrCl,[72] ZrBr,[73] YCl,[74] and ScCl[8] as well as those of many lanthanide elements[75] all provide a novel metal-like array within tightly bound slabs composed of four cubic-close-packed layers sequential X–M–M–X. Two (Sc, Y, etc.) or three (Zr) electrons per metal appear to provide strong bonding of the double-metal layers, and the

Table XIII. Observed Guinier powder pattern of $ScCl_{1.42}$ (≡ $Sc_{12}Cl_{17}$)[a]

#[a,b]	2θ	I	#[a,b]	2θ	I
1	9.88	s	16	31.48	mw
2	11.09	vs	17	32.01	m
3	11.58	vs	18	32.79	vs
4	13.10	mw	19	33.81	mw
5	13.60	mw	20	34.55	mw
6	15.81	vw	21	35.16	mw
7	17.55	w	22	36.20	mw
8	18.43	vw	23	36.55	mw
9	20.55	vw	24	38.39	ms(b)
10	23.26	mw	25	40.62	ms
11	25.25	w	26	42.34	w
12	29.59	m	27	43.53	w
13	30.10	mw	28	51.54	s
14	30.65	mw	29	51.78	s
15	30.93	ms			

[a]See text. [b]Ninety percent of the X-ray scattering occur at distances calculated for Sc_7Cl_{10} powder pattern.

compounds appear to be metallic. These compounds display an extensive interstitial chemistry in which there is insertion of small non-metals within the tetrahedral or trigonal-antiprismatic (TAP) interstices between the double-metal layers. The new 1T-Sc_2Cl_2Y (Y = C, N) phases are isostructural with 1T-Ta_2S_2C[76] which also has a one slab trigonal structure. The latter was found fortuitously during an electrolysis process that used graphite as the anode. Though crystals of 1T-Sc_2Cl_2Y were formed by chance, the purposeful addition graphite or nitrogen into the scandium systems produced high yields of powdered products, as has been found for other similar interstitially stabilized monohalide systems, e.g., 1T-Zr_2Cl_2B,[77] 1T-M_2X_2C (M = Zr,[77] Y,[23,78] and X = Cl or Br), and 1T- or 3R-Zr_2Cl_2N.[77]

Experimental

Synthesis The one-slab scandium monochloride hemicarbide, 1T-Sc_2Cl_2C (1T), was directly synthesized in the range 750–1000°C using a stoichiometric amount of Sc, $ScCl_3$, and graphite powders. The product is a dark-brown black powder material which grinds with a graphitic feel. The quantity ($\leq$18 mg) of graphite used in the synthesis was too small to be measured very accurately, and a variation seems to result in the range of cell parameters (see below). The phase can also be produced by further reducing $Sc_7Cl_{10}C_2$ with stoichiometric amounts of scandium and graphite powder.

In the process of attempting to grow large single crystals of 1T-Sc_2Cl_2C by slow cooling from 1000 to 860°C in sealed Nb tube, the 3R-Sc_2Cl_2C was unexpectedly found. This was first thought of as a "temperature-dependent phase transition". However the so-called transition was clarified by later experiments, which showed it should be greatly dependent on carbon composition.

Use of excess graphite, ca. 5 mol% (equivalent to 1 mg of graphite for every 150 mg of $ScCl_3$), in the same temperature range to make 1T phase results in the different phase, 3R-Sc_2Cl_2C (3R). This has three-slab rhombohedral cell, see below, and is a brown-black powder with a bronze reflectance which is exactly the same appearance as 1T-Y_2Cl_2C.[23,78] So, in the first attempt to prepare single crystals, the 1T-Sc_2Cl_2C accidently picked up moisture on the surface and consequently formed ScOCl (which was seen in the reaction products), leaving excess carbon to make the 3R-type structure.

The 3R compound also smears when ground. Both 1T- and 3R-phases can be synthesized at 950°C within three days in higher than 95% yields based on the Guinier powder patterns. The large excess of scandium strips (5x) are necessary in the reaction with stoichiometric amount of carbon to ensure the product to be 1T, because by experiment, any excess graphite will react with scandium strips to form ScC_x at 1000°C. The products were found equally dispersed along the

long, crimped reaction tubes under a temperature gradient, even if the metal is in only one end, to suggest that carbon is apparently moved through the vapor phase. No large crystals have been found presumably because the rate of the reaction is very large. A suitable transport reagent may be required to grow single crystals for the structure determinations, especially for 3R-Sc_2Cl_2C for which no single crystal structure determination has yet been done.

Only one form of the nitride, 1T-Sc_2Cl_2N, has been synthesized in the temperature range 735–860°C (five weeks) in the system of $Sc/ScCl_3/NaN_3$ when powdered metal was used. The yield is greater than 95% based on either nitrogen available from NaN_3 or the $ScCl_3$ left in the form of the stable salt, Na_3ScCl_6 as approximated from the relative intensities in the Guinier powder pattern of the products. The nitride forms as dark-purple-red flakes. However, the size of these crystals was still too small for a single crystal examination. The identity of the nitride phase from NaN_3 with that for the crystal structure is based on matched Guinier powder patterns and their lattice constants.

Growing large single crystals is a current problem not only for the title compounds but for all the structurally related phases, namely zirconium and yttrium monochloride carbides. The $ScCl_{1.5}$ (mouse fur) is not seen at all in nitride syntheses at 735°C but in carbide at 750°C or below.

The single crystal structures of carbide and nitride phases were determined with crystals serendiptitously synthesized under 1000/980°C (4 weeks) and 830/810°C (5 weeks) temperature gradients in pseudo ternary reactions, $Sc_{strips}/ScCl_3/ScOCl$ and $Sc_{powder}/ScCl_3/CsCl$, respectively. These crystals were transported to the hot end in both reactions. The major products in the first system were ScOCl besides $Sc_7Cl_{10}C_2$ (10% yield) in the hot end while only one crystal of 1T-Sc_2Cl_2C was found. The reaction where nitride crystals were found had mainly $ScCl_{1.42}$ (whiskers, see above) while mostly melts, $Cs_3Sc_2Cl_9$ and $CsSc_{1-x}Cl_3$ presumably, and excess Sc were at cold end.

Single crystal examination The data crystals have identical colors as the known powders, so one can provisionally surmise that the above single crystals are the same impurity-stabilized phases with respect to the specific interstitial atoms, i.e., the black crystal is the carbide and the dark-purple-red one is the nitride phase. The cell parameters and crystallographic data of these phases are collected in Tables I and II, respectively.

These plate-like crystals were mounted such that the plate was parallel to the axis of the capillary tube. This necessitated even larger absorption corrections to account for the difference in intensities arising from variation in the thickness of the crystal in the X-ray beam. The zero and first level Weissenberg photographs for Sc_2Cl_2N crystal

showed an angle of 90° between the c^* and b^* axes and gave $|b^*|/\cos 30^\circ$ approximately equal to $|a^*|$, suggesting a hexagonal cell. There was no extinction condition along any of these axes. The indexing program ALICE confirmed that the cell corresponded to a single slab structure, and the positions of the heavy atoms were chosen according to the corresponding Y and Cl atoms positions in 1T-$K_{0.5}Y_2Cl_2C_{0.8}$[78] and therein the appropriate Sc-Sc and Sc-Cl separations, in the space group of $P\bar{3}m1$. The residual electron densities at (0, 0, 1/2) in the difference Fourier synthsis maps from heavy atoms only were equivalent to ca. 5 e/A^3 and 5.8 e/A^3 for the carbide and nitride, respectively, and <1 e/A^3 for the rest of the map. After the impurity atoms in each structure were assigned, the crystal structures were then solved accordingly (Table II). Simultaneous refinement of interstitial occupancy and isotropic temperature factor in both structures give compositions within 3σ of unity, B = 2.1(4) and 1.7(4), respectively, and R/R_w factors a little bit lower than the former refinements, 0.032/0.050 for the carbide and 0.050/0.060 for the nitride (Table II).

Table A5 provides the calculated and observed powder patterns. The reflections 100, 110, 200, and 210 have very much different intensities than the calculated ones, presumably representing the crystal prefer orientation which was also observed in Y-Cl system.[78] The structure factor tables are in Appendices I (C) and J (N).

Because of a lack of a Guinier powder pattern for the assumed carbide crystal, lattice parameters were determined by applying the program LATT[31] to tuned diffractometer settings on eleven reflections. For comparison, lattice dimensions from both diffractometer and powder data (from the same preparation) are available for the nitrides but they are different. The lattice parameters from the diffractometer data (a = 3.3495(4) A, c = 8.808(1) A) are characteristically smaller than those from the Guinier method (a = 3.3517(7) A and c = 8.813(2) A for known interstitial phase). There are other examples of mismatched lattice constants in Zr-I and currently studied systems. The adventitious $Sc_7Cl_{10}C_2$ (crystal 2)[45] has cell constants from diffractometer data (a = 18.594(2) A, b = 3.4930(4) A, c = 11.796(1) A, and β = 99.81(1)^{o}) different than those of Guinier data (a = 18.620(4) A, b = 3.4975(6) A, c = 11.810(2) A, β = 99.81(2)^{o}). The differences are 0.14, 0.13, and 0.12 percent, respectively. Applying the average percentage error to a and c lattice constants from diffractometer data for 1T-Sc_2Cl_2N results in cell parameters, a = 3.3539(7) A and c = 8.819(2) A, within 3σ of the Guinier data. In fact, the powder data of Sc_2Cl_2N gave the same parameters for evidently the same phase intentionally prepared later, and its cell parameters are very self-consistent throughout this research.

On the contrary, the Guinier lattice parameters for the 1T-Sc_2Cl_2C phases are variable and can be grouped to three different sets as follows:

# set	a(A)	c(A)	V(A^3)	times observed
1	3.4312(4)	9.069(3)	92.37(4)	2
2	3.4330(7)	8.916(4)	90.91(5)	10
3	3.4179(3)	8.874(2)	89.78(3)	2

The varying lattice constants might mean the existence of nonstoichiometry. However, there are always some other ternary carbides, mostly $Sc_7Cl_{10}C_2$, left in the long term substoichiometric reactions of carbon, and the lattice parameters of the 1T phase are invariant, in c particularly. In the examples of the reactions loaded to make 1T-$Sc_2Cl_2C_x$ (x = 0.8 and 0.9) give a mixture of products, namely $Sc_7Cl_{10}C_2$ and the 1T-phase, and the lattice parameters of the latter are in the same range of those in set #2.

The second postulate for the origin of this lattice variation is mixed interstitials, e.g., Y = B+C, or C+N, in which the former should give larger cell and the latter the smaller. However, the 1T-Sc_2Cl_2C formed in these mixed interstitials reactions have lattice dimensions similar with the set #2 above, again suggesting mixed interstitials are very unlikely. The other product in each reaction is Sc_4Cl_6B or ScN at 855°C after 30 days, respectively.

The other possibility is that the residual hydrogen in the powdered scandium metal may go in the scandium

tetrahedral interstices causing the lattice contraction. However, the preliminary examination shows that isostructure compound 1T-Zr_2Cl_2C does not take up hydrogen at 200-300°C and 760 torr.[79]

In searching for the difference in terms of reactants, reaction conditions, products, yields, and so on, it seems no evidence will correlate with these anomalous sets (1 and 3) of cell parameters (as listed above). However, careful examination of the source of the $ScCl_3$ used, shows that these anomalous lattice constants were from the same batch. Therefore, the reasons for all of these observations in terms of variant parameters is ambiguous, unfortunately.

Results

Structure descriptions The atom parameters and selected bond distances are listed in Table XIV. In Figure 16, the one-slab, trigonal scandium monochloride hemicarbide is viewed along the [110] direction, showing that the double-metal layers are sandwiched by chlorine layers. Each layer is topologically a hexagonal net, and these layers are stacked one above the other such that we can use close-packed notation to describe the structure. Specifically, the layers in Sc_2Cl_2C stack as Ab(c)aB (upper case denotes chlorine layers, lower case scandium, and lower case in parentheses, carbon), and the slabs are packed such that the repeat unit along c-axis is one-slab, Figure 17a, or three-slab rhombohedral, Figure 17b. Between slabs is van der

Table XIV. Atom parameters and selected distances for 1T-Sc_2Cl_2Y (Y = C or N)

	1T-Sc_2Cl_2C			1T-Sc_2Cl_2N		
Atom parameters	z	B_{11}[a]	B_{33}	z	B_{11}[a]	B_{33}
Sc:(2d)	0.3629(2)	0.93(8)	1.38(10)	0.3656(2)	0.86(10)	0.82(11)
Cl:(2d)	0.8249(3)	1.25(10)	1.55(11)	0.8242(3)	1.10(10)	0.98(12)
Y:(1b)	0.5	1.3(3)[b]		0.5	1.2(3)[b]	
Distances (A)						
interlayer			ScCl			
Sc-Sc		3.123(3)	3.216(6)		3.057(3)	
Sc-Cl		2.573(2)	2.591(4)		2.556(2)	
Cl-Cl		3.671(5)	3.695(2)		3.651(5)	
Cl-Y		3.484(2)			3.449(2)	
Sc-Y		2.308(1)			2.267(1)	
intralayer						
Sc-Sc		3.3997(8)			3.3495(4)	

[a] $x = y$, $B_{11} = B_{22}$, and $B_{12} = B_{13} = B_{23} = 0$ by symmetry. [b] Isotropic temperature factors, B, based on unit occupancy of interstitial atoms.

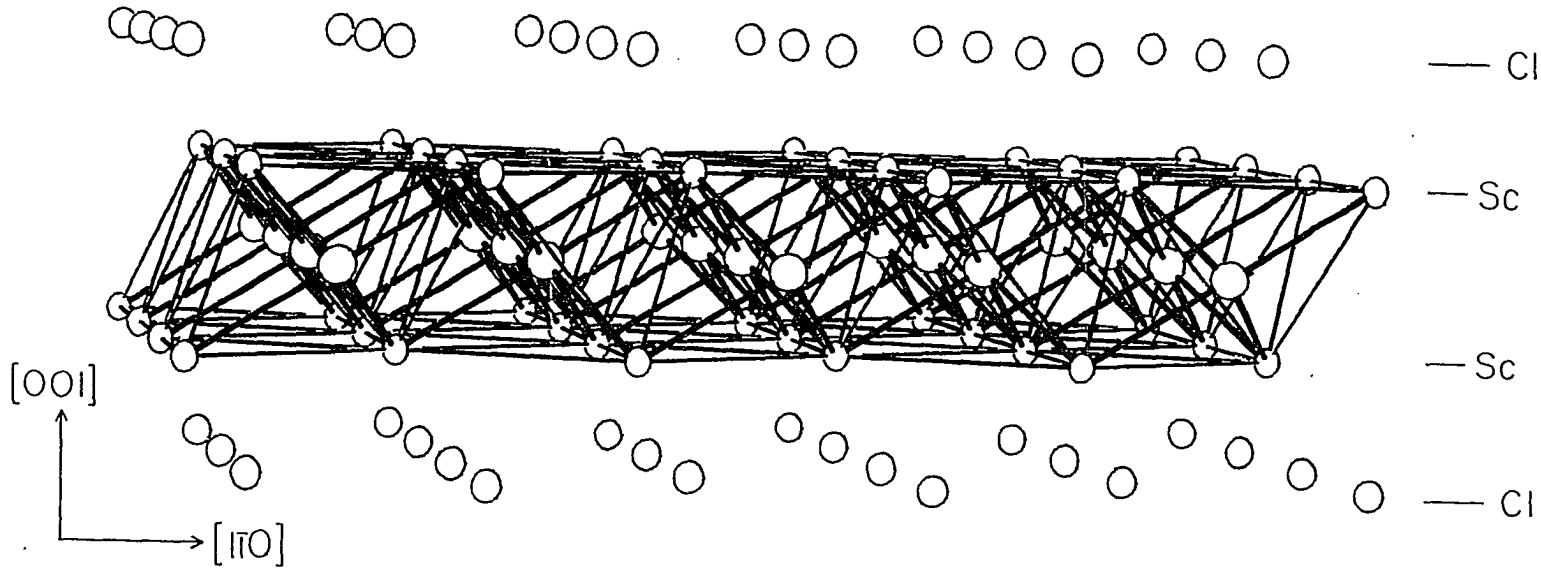

Figure 16. The ORTEP drawing for 1T-Sc_2Cl_2C with spherical atoms. The scandium octahedra are centered by carbon atoms with Sc–C in heavier lines. The scandium to chlorine bonds are omitted for clarity.

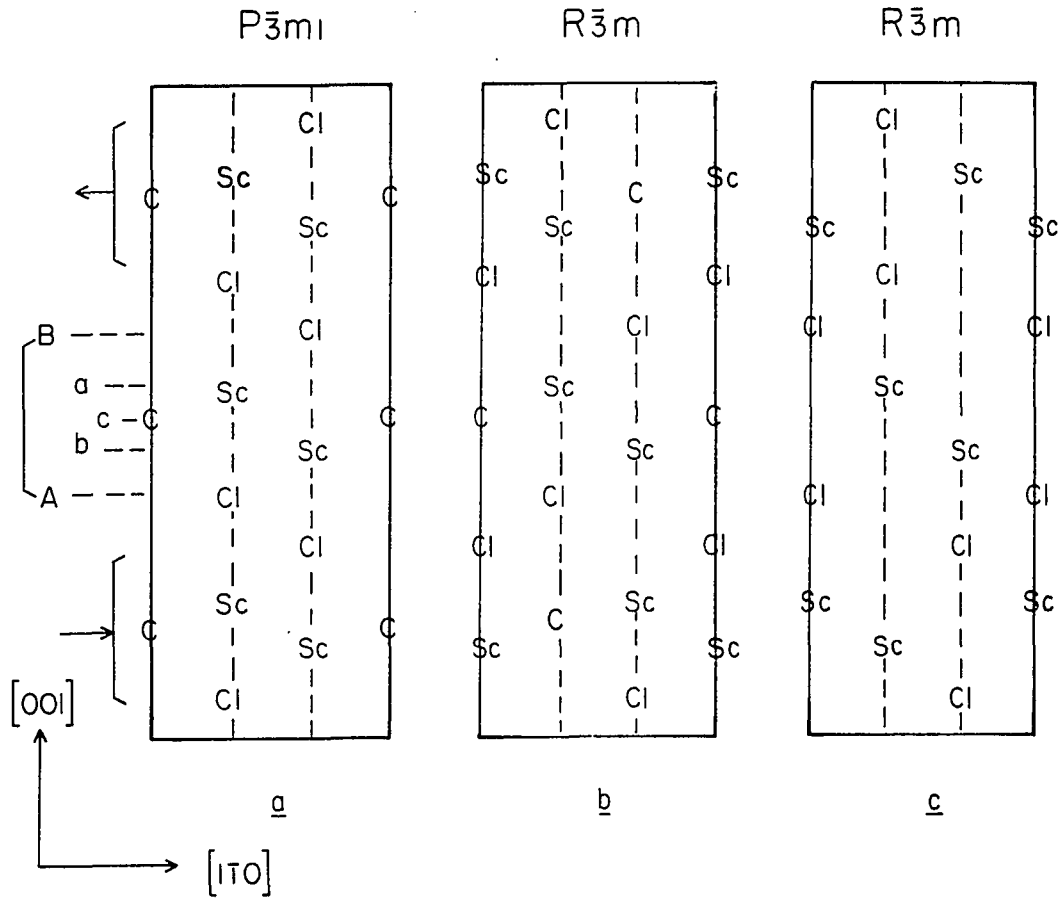

Figure 17. The [110] section of a) three slabs of 1T-Sc_2Cl_2C, b) alternative arrangement of 3R-Sc_2Cl_2C, and c) "3R-ScCl" (ZrBr-type).

Waals gap. The "parent" monochloride in ZrBr type contains similar stacks in which the layers are instead sequenced AcbA, and these are arranged in a three-slab rhombohedral cell, Figure 17c. Formation of either Sc_2Cl_2Y from "ScCl" is thus accompanied by layer displacements within the slabs, there being 0.10 and 0.16 A (~3.1 and 4.8%, respectively) decreases in interlayer scandium distances and 0.07 and 0.12 A (~2.2 and 3.5%, respectively) in intralayer of both carbide and nitride, respectively, Table XIV. Scandium TAP sites are centered by interstitial carbon atoms as shown by heavy lines in Figure 16. All of the exposed edges of each carbon-centered $Sc_6(C)$ unit in the condensed metal array are bridged by chlorine atoms, making the product derived from 6-12 parentage.

The feature of the shortened Sc-Sc bond distance might be misinterpreted in terms of strong metal-metal bonding, but there is only small degree of metal bonding retained according to the overlap populations (see below) from the extended HUckel calculations, 0.04 for intralayer Sc-Sc, 0.01 for interlayer, and 0.38 for Sc-C. Also, the calculated charge on carbon atom is -1.6. The XPS studies give the energy levels of the carbon 1s core as -282 eV (vs. adventitious carbon -285 eV, see p. 132). These data suggest this carbide-like species has covalent bonding with the scandium atoms.

No crystal structure determination for 3R-Sc_2Cl_2C is available but the probable arrangement of these three slab structures, Figure 17b, can be derived by slipping the top and the bottom slabs of 1T-Sc_2Cl_2C, Figure 17a, in opposite directions by one-third of $|\vec{a}\pm\vec{b}|$. The target structure is hexagonally-close-packed within the slab and cubic-close-packed between the slabs, |Sc–Cl—Cl–Sc|, to give a heavy atom packing sequence |BcbC||AbaB||CacA|. This can be achieved by displacing the chlorine close-packed layers of a 6-8 type (Fig. 17c) to a 6-12-type cluster (17a, and b) with respect to the nearest scandium metal array. This may result from nonmetal repulsions between carbon and chlorine. Therefore, one can sketch a one-step structure transformation via a "3R-ScCl" (ZrBr, 6-8 type) structure to 3R-Sc_2Cl_2C (6-12 type) upon inserting carbon in the TAP interstices and with a second step slab displacement to 1T-Sc_2Cl_2C, Figure 17. The calculated Guinier powder patterns of "3R-ScCl" ($R\bar{3}m$), 3R-Sc_2Cl_2C ($R\bar{3}m$), and 1T-Sc_2Cl_2C ($P\bar{3}m1$) are plotted in Figure 18 for comparison.

Discussion In conclusion, this structure transformation has been accomplished at the temperature range described above by either adding excess carbon or, reducing 3R-Sc_2Cl_2C with small amount of $ScCl_3$/Sc (1:2). The scandium tetrahedral holes in the "3R-ScCl" structure, ca. 1.97 A from the center to scandium, are too small for carbon to make composition of "$Sc_2Cl_2C_2$" which is also

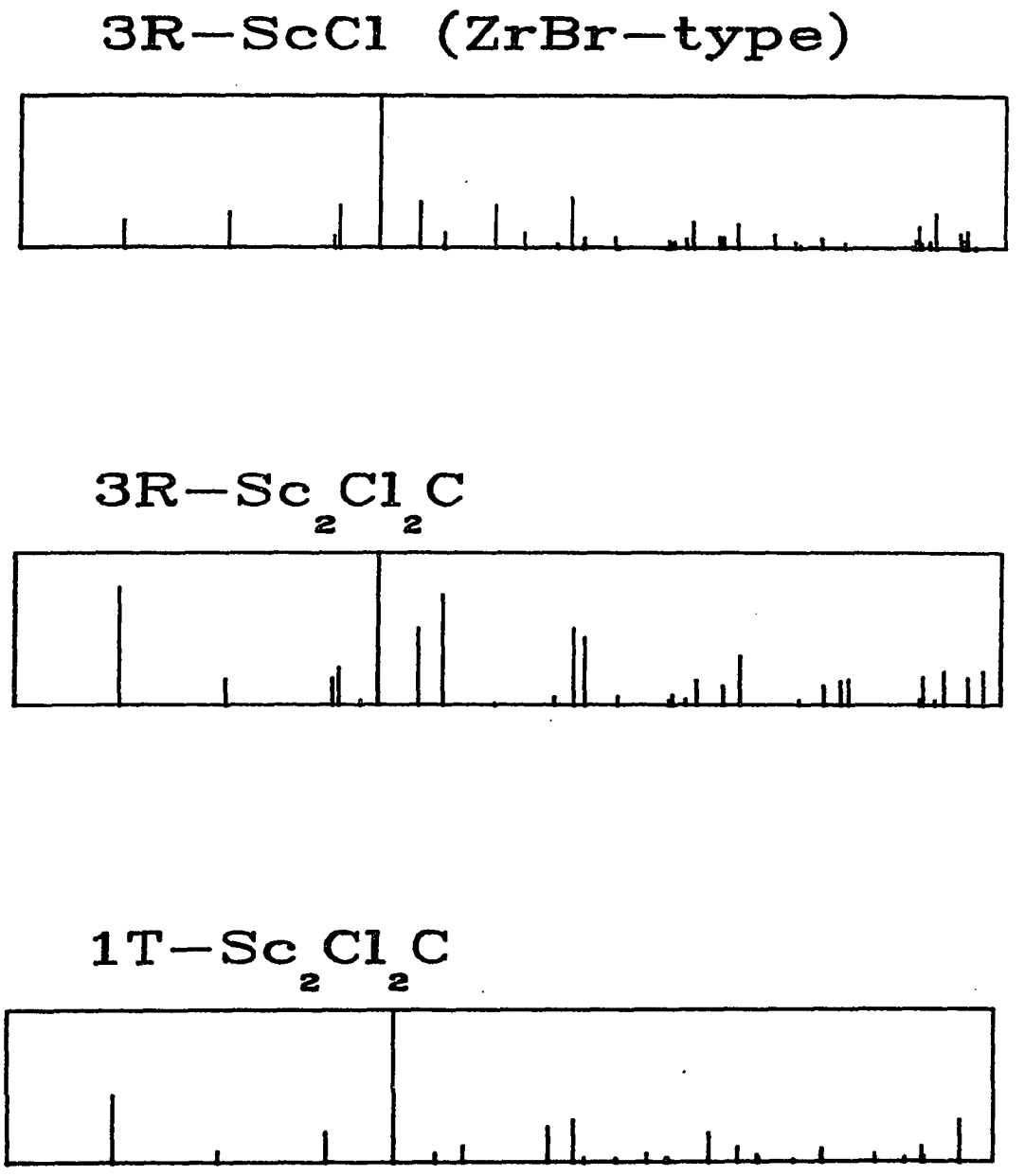

Figure 18. Three calculated Guinier powder patterns. Relative intensities are indicated by line height while 2θ increases from left to right, 0 to 100°.

electron deficient compound. So the amount of carbon per "Sc_2Cl_2" is limited by the numbers of octahedral holes and the number of scandium. Any excess graphite probably forms scandium carbide which however, was not observed with the Guinier powder pattern. However, if the carbon composition were more than 1.0 per "Sc_2Cl_2" unit would cause the lattice expansion which would be detected in the cell parameters.

The powder pattern of the 3R compound (Table XV) can be well-indexed according to the proposed structure (Figure 17b) to give the cell parameters as follows: a = 3.4355(3) A, C = 26.606(3) A and V = 271.67(6) A^3.

Upon inserting interstitial atoms into the scandium metal arrays, all the inter- or intra-scandium bonds are evidently shortened as described above resulting in a large contraction of c. The "3R-ScCl" does not form unless minimum hydrogen is provided, ca. 0.30 mol per formula unit with the interstitial hydrogen atoms in the scandium tetrahedral holes (Chapter IV). The lattice contraction due to the hydrogen atoms is only ca. 0.18 A (0.7%) in c for the composition range from 0.25 to 0.9 mol per formula unit. Therefore, the difference in bond distances quoted with "3R-ScCl" are significant but may be a little smaller than they should be if compared with the interstitial-free compound (if any exists).

As usual, the Cl-Cl separation and Sc-Cl bond distances for the reduced phases reveal little in terms of

Table XV. Observed and calculated Guinier powder patterns for 3R-Sc_2Cl_2C

h	k	l	$2\theta^a_{calc}$	I_{obs}	I^b_{calc}
0	0	3	9.96	50	74
0	0	6	20.01	15	18
1	0	1	30.20	40	18
0	1	2	30.77	55	25
0	1	5	34.51	75	100
1	0	7	38.39	45	50
0	1	8	40.65	55	61
1	1	0	53.28	100	50
1	0	13	54.35	30	38
1	1	6	57.49	10	6
0	2	1	62.47	5	3
0	0	18	62.81	15	4
2	0	5	65.04	40	17
0	2	7	67.56	20	11
1	1	15	77.25	5	13
0	2	13	79.60	10	17
1	1	18	86.86	30	14
1	2	5	88.87	35	22

[a] $2\theta_{obs} = 2\theta_{calc} \pm 0.03^o$. [b] All lines with $I_{calc} \geq 10$ unless otherwise observed.

interstitials, let alone more subtle effects. This is reasonable since involvement of chlorine orbital in the metal-metal or metal-interstitial bonding is quite small.[59] In addition, even in a wide series of scandium chlorides the charge on chlorine might be expected to vary in the extreme from -1 to a value approaching zero as the oxidation state of the metal increases, thereby producing a small decrease in bond distances across the series. However, the actual binding energy change in these particular compounds should be much less since they are all layered and only small charges on and small changes in the adjacent chlorine layers in such structures are to be expected, presumably reflecting appreciable Sc-Cl covalency. The behavior of Sc-Sc bonding described above will be considered later.

Extended Hückel calculations for the 1T-Sc_2Cl_2C shown that the 2s and 2p valence orbitals of the carbon interstitials greatly overlap orbitals from the six neighboring scandiums. Density of states (DOS) curves displayed in Figure 19 were obtained from extended Hückel calculations including 65 k points of the two-dimensional irreducible Brillouin zone and smoothed with Gaussian functions with a half-width of 0.1 eV. The Fermi level is defined as the midpoint between the highest occupied and the lowest unoccupied bands. The band gap is about 1.72 eV in energy, which is an indication of an insulator. The top

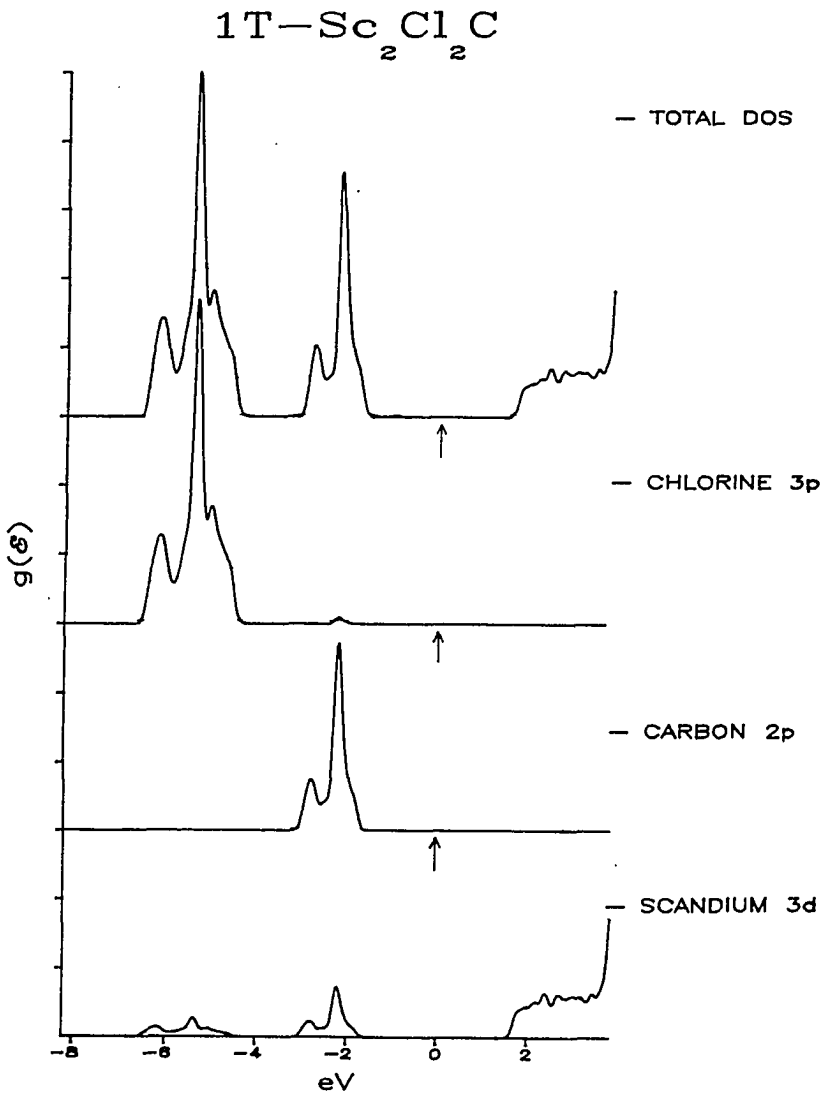

Figure 19. A total density of states (DOS) curve of 1T-Sc_2Cl_2C, calculated by the extended HÜckel method is shown on top and broken down into chlorine (3p), carbon (2p), and scansium (3d). The band near at the Fermi level, E_F, is mainly a carbon band mixed with some scandium band. The conduction band is empty.

filled band is mostly carbon orbitals mixed with some scandium orbitals, mainly $d_{x}2_{-y}2$ orbital. The conduction band above the Fermi level is empty which is consistent with the oxidation state assignment of 3+ for scandium. The chlorine band is ca. 2.7 eV below the Sc and C band both in UPS and the calculated DOS. In fact, it shows a very good match with the UPS data (see next).

Because of the electron deficiency on scandium, it is understandable that compounds such as Sc_2Cl_2B which need 5 electrons for the boron level would not exist.

Unsuccessful reactions Attempts to incorporate other interstitials in the monochloride phases have been tried, especially fluorine from distilled ScF_3. In this system Sc, $ScCl_3$, and ScF_3 powders in the ratio to make Sc_2Cl_2F or $Sc_2Cl_2F_2$ were heated at 1050°C for one month. These produced bluish reflective, black plate crystals along the melts in 10% yield according to Guinier powder pattern (Table XVI). The patterns are clearly different from any of those in Figure 18 in terms of line positions and intensities and can be manually indexed as a three slab structure but with the a-axis doubled. Assuming a similar slab thickness as in the 1T- carbide, the structure is presumably composed of scandium and chlorine layers and fluorine may or may not be in the interstitial sites.

Table XVI. Guinier powder pattern[a] for the plate crystals from $Sc/ScCl_3/ScF_3$ system

h	k	l	2θ(deg.)	I_{obs}
1	0	0	14.91[b]	w
0	1	5	22.15[b]	s
2	0	3	31.51	m
	-		32.01	w(b)
2	1	6	45.12[b]	ms
	-		49.75	w
2	0	12	50.82	ms
3	0	7	51.78[b]	m(b)
1	3	10	65.79	m
3	0	15	70.34[b]	m

[a]Powder pattern was manually indexed based on hexagonal cell from Weissenberg data on single crystal (presumably the same phase) with a = b = 6.8 A, c = 26.8 A.
[b]Five lines in LATT to give a = b = 6.850(6) A, c = 27.23(3) A.

Unfortunately, the single crystals were too small for a crystal structure determination.

Attempted intercalation with potassium, through the high temperature route in the quaternary system $KCl/Sc/ScCl_3/C$ at 950°C for a couple of weeks gives 3R-Sc_2Cl_2C according to the powder pattern. It is not possible for potassium to go in the 3R structure directly because of the Sc-K repulsions as second nearest neighbors. Another route to the intercalated products, Na in $NH_{3(\ell)}$ on 1T-Sc_2Cl_2C at -30°C,[76] gave NaCl. Presumably, a more dilute $Na/NH_{3(\ell)}$ or even lower reaction temperature may be necessary if the intercalation is to succeed.

The Sc_2Cl_2B would be an electron deficient compound, but MSc_2Cl_2B (M = Na, K) is isoelectronic with Sc_2Cl_2C. Attempts to prepare the "KSc_2Cl_2B" at 860°C and 950°C with stoichiometric amount of Sc, $ScCl_3$, B, and KCl powders to give ca. 20% yield of hard, black blocks plus K_2ScCl_5 salt. The Guinier powder pattern of the product was weak, suggesting the material was not very crystalline. The products with NaCl added were powdered and gave an unknown powder pattern.

Photoelectron Spectral Study of Three Reduced Scandium Chloride Carbides

Since X-ray scattering is relatively uniformative as to identity of the interstitial atom, it was considered desirable to establish that interstitial-like carbon was actually present in some new phases. The photoelectron spectra specifically served this purpose during the study of three reduced scandium chloride carbides, namely Sc_5Cl_8C, $Sc_7Cl_{10}C_2$ and 3R-Sc_2Cl_2C. The experimental details are in Chapter II and elsewhere.[11] Figure 20 shows the carbon 1s spectrum (Al Kα) from Sc_5Cl_8C and $Sc_7Cl_{10}C_2$, which have infinite metal chains, relative to that of 3R-Sc_2Cl_2C, which is layered. In all these examples carbon is bound in scandium octahedral interstices. The spectra show these samples are very similar with a carbide-like peak shifted about 3.0 to 3.5 eV to lower binding energy from the inevitable adventitious carbon used for calibration (285.0 eV). (Experience[80] indicates that this source dominates emission from the cellophane tape substrate when good coverage is secured although the two sources generally cannot be distinguished unless sample charging occurs. The XPS results are generally reproducible to ±0.1 eV, ±0.2 eV maximum, even for measurements spread over a period of several years.)

Figure 20. The carbon 1s photoelectron spectra of the following compounds on cellophane tape (Al Kα).
(a) Sc_5Cl_8C (25 scan composite).
(b) $Sc_7Cl_{10}C_2$ (50 scan composite).
(c) 3R-Sc_2Cl_2C (34 scan composite).

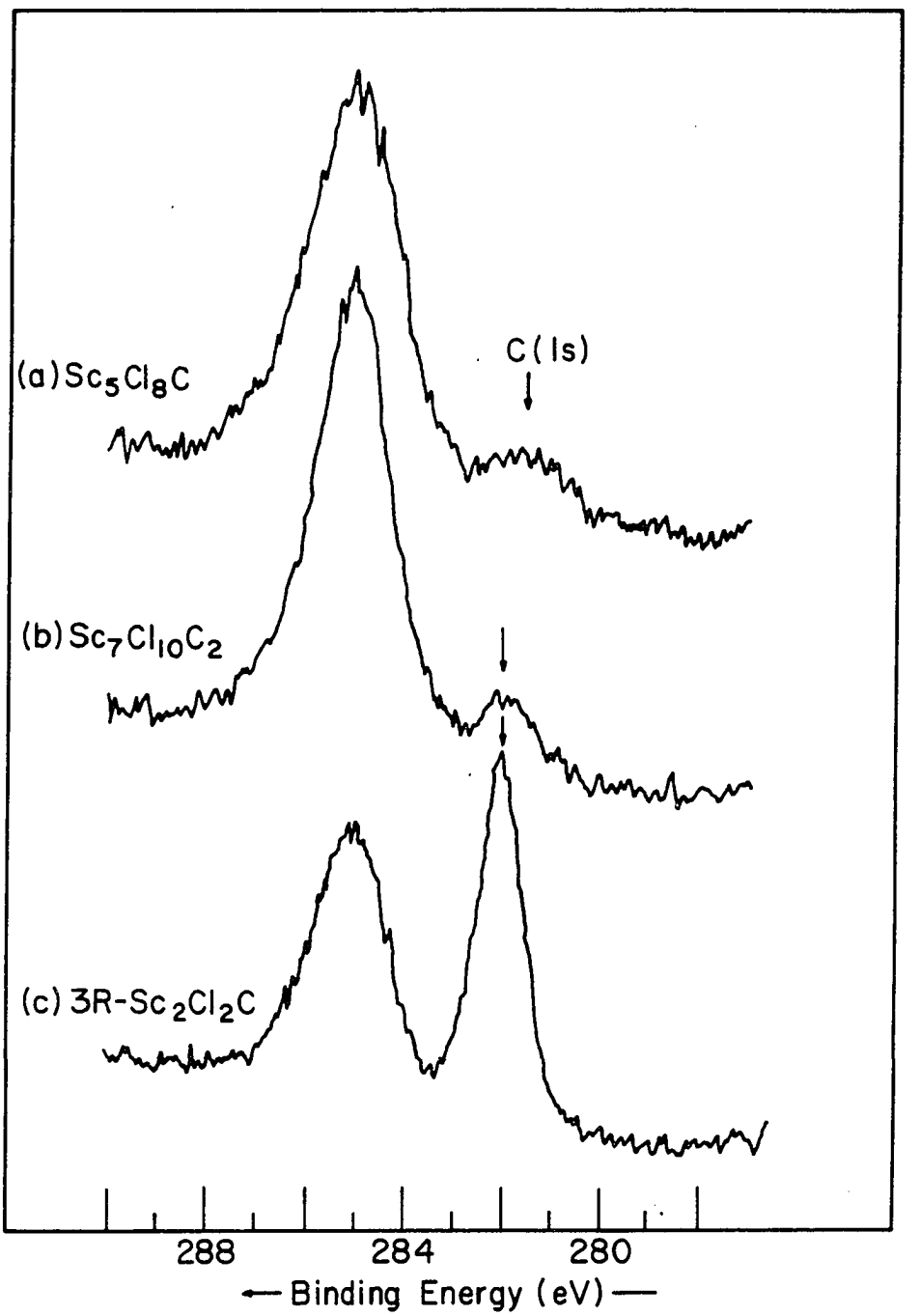
(a) Sc_5Cl_8C
C(1s)
(b) $Sc_7Cl_{10}C_2$
(c) 3R-Sc_2Cl_2C
288
284
280
← Binding Energy (eV) —

Other pertinent XPS data for Sc_7Cl_{10}, $Sc_7Cl_{10}C_2$, Sc_5Cl_8C, 3R-Sc_2Cl_2C, $ScCl_3$ and Sc are summarized in Table XVII. The scandium 2p core peaks for Sc_7Cl_{10}, Sc_5Cl_8C and $Sc_7Cl_{10}C_2$ present an interesting relationship. The core spectra of Sc 2p for latter two compounds and 3R-Sc_2Cl_2C are shown in Figure 21. The earlier Sc2p spectrum for Sc_7Cl_{10} was given a somewhat tentative assignment in terms of the two kinds of scandium known to occur in the compound, a broadened $2p_{3/2}$–$2p_{1/2}$ pair (m) starting at about 399 eV for the collection of metal in the metal chains together with a smaller overlapping pair (n) from the isolated chain at ca. 404 eV.[11,45] Although possible alternatives in terms of shake-up (secondary) process made this assignment seem a little tenuous, quite similar results are obtained for Sc_5Cl_8C and $Sc_7Cl_{10}C_2$, and these encourage the spectral comparison and assignments shown. Some surface oxidation may also contribute to n.

The 3/2-1/2 pairs of Sc 2p transitions so assigned to the metal and scandium(III) chains in Sc_7Cl_{10} agree very well with the energies of these emissions obtained for the metal and the trichloride, respectively (Table XVII). The metal chains in Sc_5Cl_8C and $Sc_7Cl_{10}C_2$ are clearly more oxidized than in Sc_7Cl_{10}, since the Sc 2p binding energies increase 1-2 eV while the other pair, scandium(III), changes at most ca. 0.7 eV. The metal 2p energies in these two

Table XVII. X-ray photoelectron emission data, eV[a]

Compound	Cl 3p	Sc(m)[b] $2p_{3/2}$	Sc(m)[b] $2p_{1/2}$	Sc(n)[b] $2p_{3/2}$	Sc(n)[b] $2p_{1/2}$	Cl $2p_{3/2}$	Sc(m) $2p_{3/2}$ –Cl $2p_{3/2}$	Sc(n) $2p_{3/2}$ –Cl $2p_{3/2}$
Sc		398.7	403.4					
Sc_7Cl_{10}	7.0	398.8	~403.4	~403.9	408.3	200.2	198.6	203.7
$Sc_7Cl_{10}C_2$	6.6	401.0	~405.5	~403.3	~407.7	199.9	201.1	203.4
Sc_5Cl_8C	6.9	400.0	~404.9	~404.0	408.5	199.9	200.1	204.1
3R-Sc_2Cl_2C	6.7	400.5	405.3			199.7	200.8	
$ScCl_3$[c]	6.4			404.0	408.5	200.1		203.9

[a]Referenced to C(1s) = 285.0 eV. [b]The pair of Sc 2p transitions (m) in Sc_7Cl_{10}, $Sc_7Cl_{10}C_2$, and Sc_5Cl_8C with the lower binding energy is assigned to metal chain, while the (n) pair is taken to originate with the isolated scandium(III). [c]Referenced to deposited gold, $4f_{7/2}$ = 84.0 eV.

Figure 21. X-ray photoelectron spectra of the Sc 2p region with Sc $2p_{3/2-1/2}$ assignments for the metal chain (m) and scandium (III) (n) states.
(a) Sc_5Cl_8C (34 scan composite).
(b) $Sc_7Cl_{10}C_2$ (50 scan composite).
(c) 3R-Sc_2Cl_2C (100 scan composite).

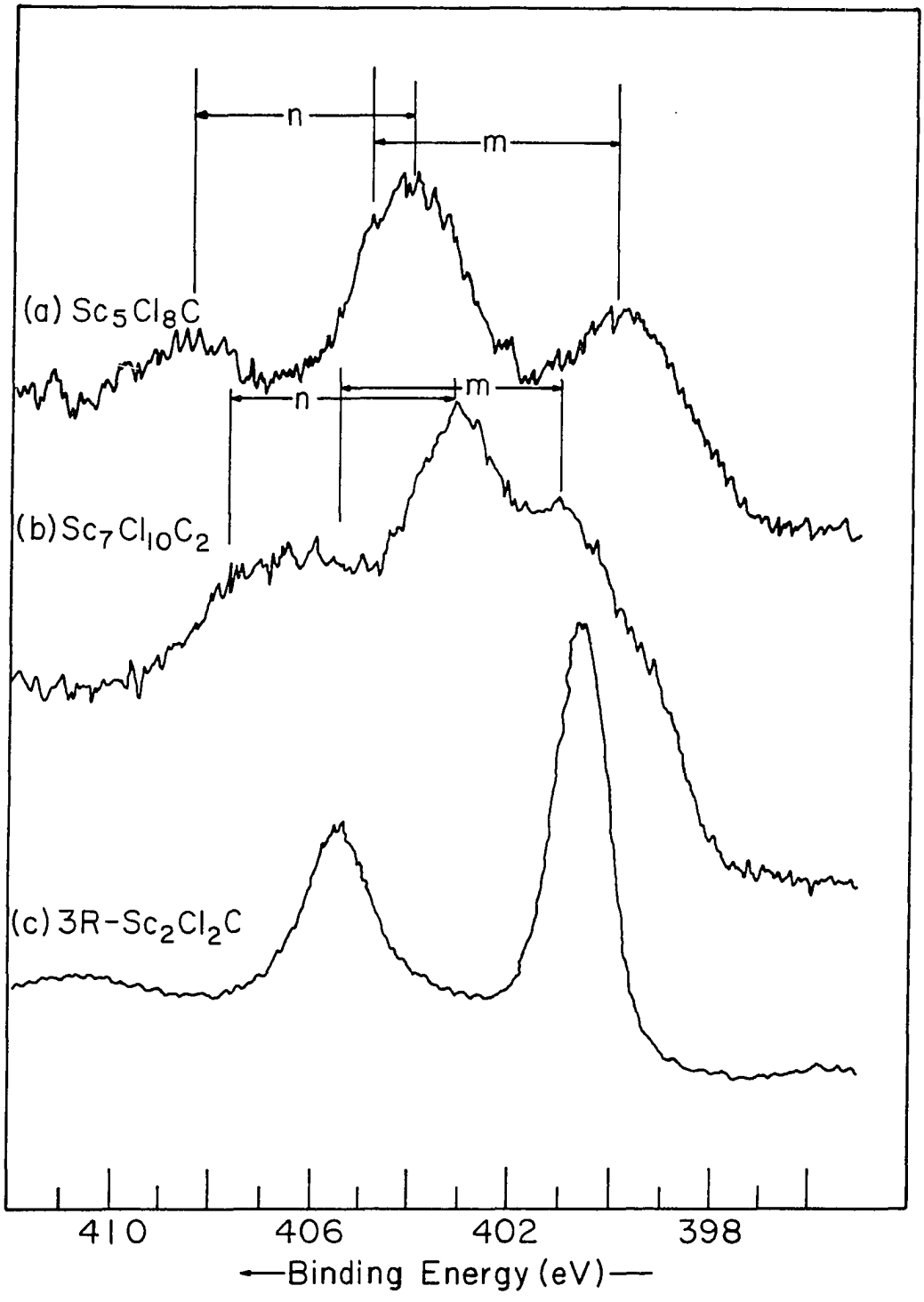
n
m
(a) Sc_5Cl_8C
n
m
(b) $Sc_7Cl_{10}C_2$
(c) 3R-Sc_2Cl_2C
410
406
402
398
Binding Energy (eV)

infinite metal chain compounds are also very comparable to those found for 3R-Sc_2Cl_2C, which is formally a scandium(III) compound. Of course, general comparisons of this sort may be misleading in that the apparent changes in core levels to higher binding energy found on oxidation may actually reflect more of the natural shift of the Fermi level reference to higher values.[80] This ambiguity can be avoided by comparing changes in the scandium $2p_{3/2}$ energies with those for chlorine $2p_{3/2}$ as an internal standard; in the present examples the conclusions are relatively unaffected (Table XVII).

As usual, the chloride data for the reduced phases reveal little in terms of oxidation state, let alone more subtle effects (Figure 22). This is reasonable since involvement of chlorine orbitals in the metal-metal bonding is quite small. In addition, even in a wide series of metal chlorides the charge on chloride might be expected to vary in the extreme from 1- to a value approaching zero as the oxidation state of the metal decreases, thereby producing a small decrease in binding energy across the series. The actual binding energy change of these compounds is very small, presumably reflecting appreciable Sc-Cl covalency. The remarkable $2p_{3/2}$–$2p_{1/2}$ resolution (ca. 1.5 eV) in 3R-Sc_2Cl_2C is evidently in part caused by the equivalence of the chlorine atoms in the adjacent layers. The well

Figure 22. X-ray photoelectron spectra of the Cl 2p region.
(a) Sc_5Cl_8C (25 scan composite).
(b) $Sc_7Cl_{10}C_2$ (50 scan composite).
(c) 3R-Sc_2Cl_2C (100 scan composite).

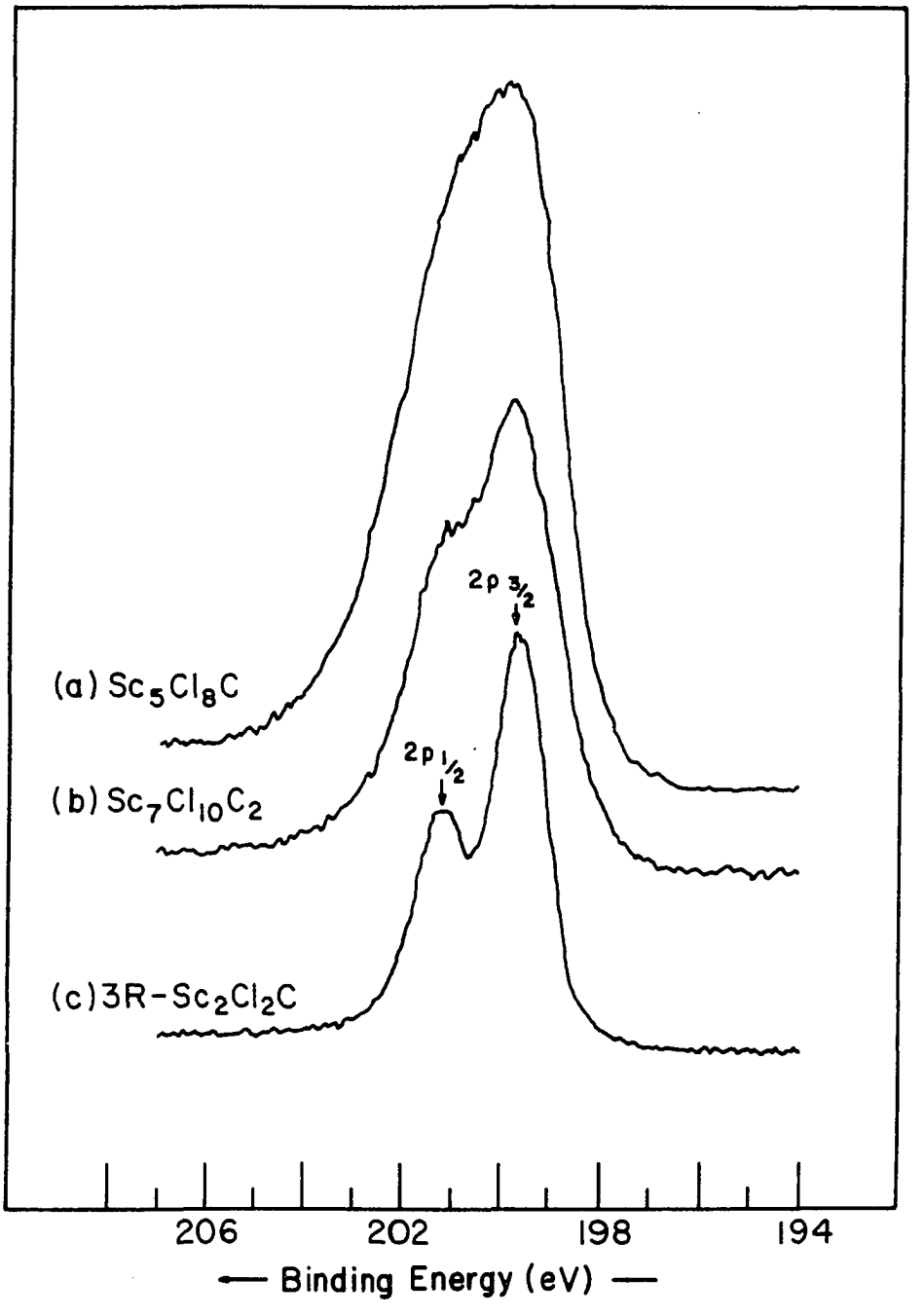
(a) Sc_5Cl_8C
(b) $Sc_7Cl_{10}C_2$
(c) 3R-Sc_2Cl_2C
$2p_{3/2}$
$2p_{1/2}$
206
202
198
194
Binding Energy (eV)

resolved Sc $2p_{3/2}$ and $2p_{1/2}$ are expected for the same reason. By comparison the broadening (in terms of overlap) of 2p spectra of chemically nonequivalent chlorines are shown for both Sc_5Cl_8C and $Sc_7Cl_{10}C_2$ chain compounds (Figure 22, top and middle spectra) where there are four and five symmetry unrelated chlorines, respectively, according to the crystal structure determinations. In fact the top spectrum is 0.5 eV wider than the middle one at one-half of the peak height.

Finally, Figure 23 compares the UPS (He I) spectra for the valence region of Sc_5Cl_8C, $Sc_7Cl_{10}C_2$ and 3R-Sc_2Cl_2C. A metal band in the neighborhood of 0-4 eV with an edge at or near E_F is indicated for $Sc_7Cl_{10}C_2$. However, there is a great contribution from a nominally C 2p band, which causes some broadening in the XPS (Al Kα) spectrum,[45] in the neighborhood of 3 eV. Such a feature clearly appears at 3.6 eV and 4.3 eV in Sc_2Cl_2C and Zr_2Cl_2C,[77] respectively. The DOS of these two compounds show a great deal of consistency in terms of the split carbon band as well as the metal binding energy (bottom spectrum in Figure 23).

The bonding of the interstitial in these appears to exert a strong and stabilizing effect since Sc_7Cl_{12}, edge-bridged Sc_7Cl_{10}, and single slab (1T-) or three slabs (3R-) MCl (M = Sc, Y,[16] etc.) species, for example, are not found without interstitials. The separation of the double-metal-

Figure 23. The UPS valence spectra of $Sc_7Cl_{10}C_2$ (top), Sc_5Cl_8C (middle) and 3R-Sc_2Cl_2C (bottom) on In substrate (He I). The Cl 3p is at around 7eV of the binding energy. The magnified spectrum (x4) of the Sc_5Cl_8C at Fermi edge is shown right on top of it.

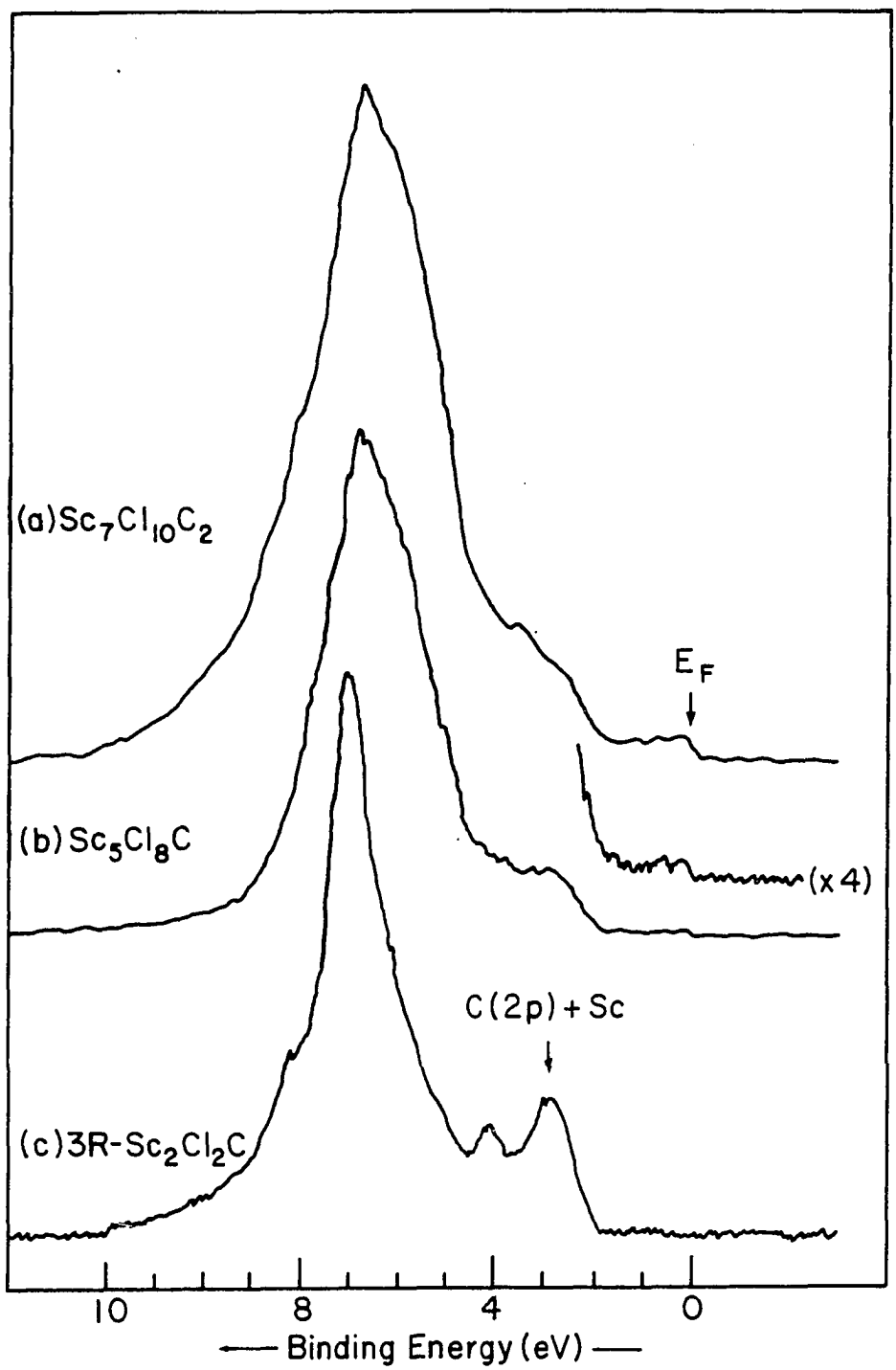
(a)Sc7Cl10C2
(b) Sc5Cl8C
(c)3R-Sc2Cl2C
E_F
(x4)
C(2p) + Sc
10
8
4
0
Binding Energy (eV)

layers is significantly decreased from that in ScClH on formation of Sc_2Cl_2C. Some understanding of the bonding in these carbide compounds can be obtained from extended Hückel calculations on centered clusters and on Sc_2Cl_2C (for details see previous sections A and D). The crystal orbital overlap populations (COOP) suggest the range involves substantial mixing of metal and carbon and are bonding for both metal-metal and metal-carbon, more so for the latter.

It is misleading to think of the interstitial as C^{4-} in character although the familiar process of electron counting for oxidation state assignment or filling of valence bands may be so misconstrued. Extensive band calculations on the rock-salt monocarbides of Ti, Zr, V and Nb emphasize both the metal-carbon covalency and the small negative charge acquired by carbon, estimated values for the latter lying between 0.4 and 1.[81,82] The 3.0 eV difference in Sc 2p binding energy found between Sc_2Cl_2C and $ScCl_3$ for either a Cl 2p or E_F reference (Table XVII) is striking evidence for the Sc-C covalency. In fact, the compounds $Sc_7Cl_{10}C_2$ and Sc_5Cl_8C with average oxidation states of 2.57 and 2.4, respectively are indistinguishable from Sc_2Cl_2C by this means. The covalency and electron redistribution on formation of metal hydrides such as ZrXH and ZrH_2 are conceptually quite similar, the comparable XPS shift being

ca. 1 eV.[62] Qualitative features of the bonding scheme have been described by Lauher for a metal carbonyl carbide cluster,[83] and more pertinent by Smith for a carbon centered metal cluster.[37]

Studies of the ultraviolet photoelectron spectra of Sc_5Cl_8C and $Sc_7Cl_{10}C_2$ show these infinite metal chain carbides are metallic with clear but small density of states at the Fermi level E_F. These polycrystalline materials are black in color consistent with the characteristics of metallic compounds. However, conductivity measurements should be planned to verify this point. On the other hand, the 3R-Sc_2Cl_2C is an insulator with experimental results and theory establishing a sizable band gap ca. 2 eV. For an "isomorphous" compound, namely 1T-Sc_2Cl_2C, the XPS and UPS spectra should be taken, especially the latter which might show the carbon content if the band is changed to partially filled. Conductivity also will clarify the metallic property of this dark-brown black material which is different from brown-black 3R-Sc_2Cl_2C.

CHAPTER IV. RESULTS: M_6X_8-TYPE LAYER COMPOUNDS STABILIZED BY HYDROGEN IN TETRAHEDRAL INTERSTICES

Synthesis and Characterization of Ternary and Quaternary Scandium Monochloride Hydrides

Introduction

The monohalides, MX, where M = Sc-La, Pr, Gd, Tb, Ho, Er, Zr, Hf and X = Cl or Br, have structures which consist of close packed metal and halogen atoms in alternate double layers to form slabs, X-M-M-X.[84] They were reported in two well-known structure types, namely ZrCl[72] (ABCA) or ZrBr[73] (ACBA), in which the slabs stack along c in an R-centered fashion.

The monohalides of group III metals in particular have presented unanswered questions such as reasons for the unreproducible yields and variable lattice parameters. Also, an apparent phase transition has been found for "YCl" structure in which the high temperature form is ZrBr-type and the low temperature form is ZrCl. The lattice constants vary, with the high temperature form having the larger c but the smaller lattice constant a.[44] Another general synthetic feature of these monohalides is that powdered metals and in some cases excess (5x) metal powder is needed to produce high yields. The rationale for this was the powdered metals provide more fresh surface area, especially for those halides that are not volatile, i.e., which form in solid/liquid reactions.

In this section, the synthesis of $ScClH_x$ and the occurrence of the phase transformation (not transition) will be discussed. In addition, intercalation of the monohalides of group III metals (except yttrium) have never been successful. The only example, $Li_{0.1}YCl$, came from a non-reproducible reaction which required a large excess powdered metal to obtain a low (10%) yield product.[85] The preliminary examination of quaternary derivatives, $M^I_zSc_2Cl_2H_x$ (M^I = Li, Na, K, etc.), have very successfully shown the work may be extended to the synthesis of new materials with possibly interesting physical properties.

Experimental

Synthesis

$ScClH_x$ The ZrXH phases, X = Cl, Br, were formed by reacting H_2 with ZrX at 150-450°C. They are metastable and decompose at 630-780°C to give ZrH_2 plus the cluster compound Zr_6X_{12}.[86] In an attempt, reaction of Sc and $ScCl_3$ to synthesize "$Sc_7Cl_{12}H$" at 710°C was carried out with a sealed tantalum tube in a silica jacket, which was open to 700 torr of H_2. The hydrogen diffused through the tantalum wall (at 710°C the diffusion coefficient, D, is 3.6×10^{-6} $cm^2 s^{-1}$).[87] The excess (5x) of scandium strips instead reacted with $ScCl_3$ powder under the hydrogen atmosphere to form $ScClH_x$ ($x \sim 1.0$) and ScH_2. The former, unexpected phase was found to have a ZrCl-type structure based on its Guinier powder pattern.

The monohydride compound can also be obtained from the hydrogenation of 65 mg of "ScCl" (ZrBr-type) crystals (which were synthesized at 950°C in ~10% yield according to the reported method[8] and with stoichiometric amount of scandium, see below) in a Mo boat placed in a silica jacket with a stoichiometric amount of hydrogen. The preliminary experiment showed that the ScCl crystals took up hydrogen quantitatively at 500°C. This is a higher hydrogenation temperature than is possible with the ZrX system presumably because the dissociation pressure of $ScCl_3$ is much lower than that of ZrX_4 at a given temperature. The system was then equilibrated at 500°C overnight. The single phase product is as bluish-black as ScH_2 whereas the reactants have a silver, reflective metallic appearance. Macroscopically, the crystals still retained their smooth faces but were very fragile. Weissenberg photographs of selected crystals showed badly smeared spots along the festoons possibly because the rearrangement from one type of close packed layers to another broke down the crystallinity.

The stoichiometries, products and lattice constants from different routes are listed in Table XVIII. The first method, sealed tantalum tube in silica jacket which opens to the H_2 reservoir, is called route A while direct hydrogenation of the "ScCl" crystals is route B. There is another equivalent route, C. A sealed tantalum container containing stoichiometric amount of Sc and $ScCl_3$ is first brought to

Table XVIII. The stoichiometries, products and lattice constants for reactions[a] in the $ScClH_x$ system

A. Quartz jacket open to the H_2 reservoir.

$$\frac{2}{3}\ Sc^{b} + \frac{1}{3}\ ScCl_3 + \frac{x}{2}\ H_2 \xrightarrow[\text{Temperature (T)}]{\text{3~4 weeks}} ScClH_x$$

x (mole)	Structure type (% yield)	T(°C)	Lattice Constant a(A)	c(A)	V(A^3)
"4.0"[c]	ZrCl (>95)	710	3.493(1)	26.545(8)	280.1(2)
1.0	ZrCl (>95)	755	3.482(3)	26.46(5)	277.8(7)
0.5	ZrBr (>95)	750	3.470(8)	26.51(9)	276(2)

B. Hydrogenation of ScCl (ZrBr)[d] crystals in Mo boat.

$$\text{"ScCl"} + \frac{1}{2}\ H_2 \xrightarrow[\text{over night}]{500^{\circ}C} ScClH$$

Compound (type)	a(A)	c(A)	V(A^3)
ScCl (ZrBr)	3.4755(7)	26.69(2)	279.2(3)
ScClH (ZrCl)	3.4969(8)	26.548(5)	280.8(1)

C. Hydrogen sealed in quartz jacket.

$$\frac{2}{3}\ Sc^{b} + \frac{1}{3}\ ScCl_3 + \frac{x}{2}\ H_2 \xrightarrow[T]{\text{2 weeks}} ScClH_x$$

x (mole)	Structure type (% yield)	T(°C)	Lattice Constant a(A)	c(A)	V(A^3)
1.0[e]	ZrCl (>95)	860	3.4785(2)	26.531(8)	278.02(9)
"0.9"	ZrCl (60)[f]	800	3.4790(5)	26.521(8)	278.0(1)
"0.25"	ZrBr (50)[f]	800	3.469(5)	26.65(8)	278(1)

[a]Reaction container is Ta tube with the hydrogen source on the outside, unless otherwise noted. [b]Powdered metal used (H/Sc = 0.09/1 by vacuum fusion) unless otherwise noted. [c]Excess strips (5x) used. The yield is estimated according to the $ScCl_3$ used; the co-product is ScH_2. [d]Made according to the conditions in Reference 8, see text. [e]Averaged in Figure 25. [f]The major products were $ScCl_3$ and ScH_2, see text.

Table XVIII. (Continued)

D. ScH_2 as the source of hydrogen.

$$(\frac{2}{3} - \frac{x}{2})\ Sc + \frac{x}{2}\ ScH_2 + \frac{1}{3}\ ScCl_3 \xrightarrow[3\ weeks]{860^{\circ}C} ScClH_x$$

x (mole)	Structure type (% yield)	a(A)	c(A)	V(A)
"0"	ZrBr (10)[g]	3.484(1)	26.69(3)	280.5(3)
"0.10"	ZrBr (25)[h]	3.4770(2)	26.736(3)	279.92(5)
"0.25"	ZrBr (70)[h]	3.4745(3)	26.712(7)	279.27(8)
0.33	ZrBr (>95)	3.4760(3)	26.710(4)	279.49(6)
0.5	ZrBr (>95)	3.4760(5)	26.622(7)	278.6(1)
0.67	ZrCl (70) ZrBr (30)	3.4766(1)	26.565(7)	278.1(2)
0.75	ZrCl (>95)[i]	3.4772(3)	26.566(7)	278.18(9)
0.9[e]	ZrCl (>95)[i]	3.4767(6)	26.53(1)	277.7(2)
1.0[e]	ZrCl (>95)[i]	3.4761(6)	26.592(9)	278.3(1)

[g]The major product is Sc_7Cl_{10} (70% yield) plus $ScCl_{1.5}$ (mouse fur) and "Sc_5Cl_8" (trace). [h]The other product is $ScCl_{1.5}$ (mouse fur). [i]Second phase is ZrBr-type in trace amount.

860°C in an opened silica container to take up a measured amount of H_2. The latter is sealed off after the residual hydrogen pressure reached a minimum, normally ca. 0.7 torr (which corresponds to 2.0×10^{-10} mmoles or 0.013% on the reaction scale of 0.74 mmoles of H_2). The reaction tube is then equilibrated at certain temperature (Table XVIII) for three weeks and air quenched. A different feature of this method is that the equilibrium volume for the hydrogen is limited by the sealed silica jacket. The hydrogen compositions are less than the stoichiometries loaded because the tantalum container takes up some hydrogen, as is also true in A (x = 1.0, 0.25) and D (see below) where the same container was used. Two substoichiometric reactions with x = 0.9 and 0.25 run in this method (Table XVIII) gave the by-products $ScCl_3$ and ScH_2 suggesting the reactions were not complete. That might be caused by the furnace cooling down inadvertently in the early stages of the reactions, i.e., the reaction period could be much less than two weeks (Table XVIII). Therefore the hydrogen compositions were very possibly off and consequently the lattice parameters no longer correspond to the particular stoichiometries.

Nevertheless, there were some observations up to this point to show that lattice constant variations (from 26.46 A to 26.69 A with regard to the highest and the lowest hydrogen content) or structure changes were possible with different hydrogen compositions. In addition, a trace

amount of the ZrBr-type phase was coexistent in the product mixture of ScClH (ZrCl-type) suggesting a phase equilibria at x~1.0.

Finally, the fourth method, D, is described in the equation in Table XVIII. This uses ScH_2 powder as the source of the H_2 to react with $ScCl_3$ and Sc powders in sealed tantalum tubes. The $ScH_{2.00}$ powder was prepared by hydrogenation of scandium strips at 700°C; the residual hydrogen pressure is equivalent to at most a 0.1% error in hydrogen composition. The system D reached equilibrium at 860°C after three weeks duration (Table XVIII) and in fact is equivalent to the system C (x = 1.0). A series of reactions with various hydrogen compositions were loaded to study the relationship of the structure or lattice constants to hydrogen composition, x = H/ScCl. The hydrogen partial pressure of $ScClH_x$ phase is not available currently. However, the hydrogen partial pressure of $ScH_{0.1}$ and $ScH_{1.0}$ is 0.04 and 16 mm at 860°C.[88] These partial pressures would lead the errors in x for $ScClH_x$ of 0.75% and 3.0%, respectively. There was less than 5% of α-ScH_x left in the reaction products based on its absence from the Guinier powder patterns. Therefore, the hydrogen compositions are nearly the same as the loaded stoichiometries.

The first reaction (D) was set up to make "ScCl" by using the reported conditions.[8] The products were Sc_7Cl_{10} (70% yield), "ScCl" (ZrBr-type, 10% yield), $ScCl_{1.5}$ (mouse

fur) and "Sc_5Cl_8" (trace amount). The next two reactions, x = 0.1 and 0.25 as loaded, gave as products $ScCl_{1.5}$ in 75% and 30% yield, respectively, besides the powders which were identified as ZrBr-type monochloride hydride phases. The same structure type compound was also observed in the reactions with x = 0.33 and 0.5 (>95% yield) and partly in x = 0.67. The 0.67 value of x gave a two-phase mixture, 30% of ZrBr and 70% of ZrCl-type monochloride hydrides. The last three reactions with x = 0.75, 0.90, and 1.00 gave a two-phase product, but the yield of the bromide structure type was only about 5%, again based on Guinier powder patterns.

The single crystals of $ScClH_{1.0}$ were formed at 860°C in a 8-cm Ta tube which was long enough to establish a natural temperature gradient for the crystal growth through the vapor phase (normally for the isothermal reaction, a 6-cm length of tubing was used and the products were always powders). Evidently the crystals of $ScClH_{1.0}$ can be grown as large as 2.0 x 1.5 x 0.2 mm. They look like single phase. The one mounted for single crystal study was 0.25 x 0.20 x 0.02 mm in size (Table II).

$M^I_zScClH_x$ Six preliminary intercalation reactions of scandium monochloride monohydride have been performed at 860°C (three days, tantalum container) using vacuum dried alkali metal chloride, $ScCl_3$, Sc, and ScH_2 powders. The stoichiometries, products and lattice

constants for these reactions are in Table XIX. The first reaction used a stoichiometric amount of LiCl to saturate the possible "octahedral" chlorine interstices in the van der Waals gaps at the proposed stoichiometry, $Li_{0.5}ScClH_x$ (x = 0.33 in this case). However, there was in fact some LiCl, besides Sc, left from the reaction according to the Guinier powder pattern indicating the real content of lithium is less than 0.5. In addition, in the equivalent reaction to intercalate $ScClH_{0.33}$, a single phase product $Li_{0.1}ScClH_{0.33}$ formed. These suggest a midpoint z for the saturation of the alkali metal ion in the octahedral holes between the chlorine layers. The c lattice constant of the latter compound (z = 0.1) is within 2σ of that for the nominal z = 0.5, suggesting the composition of lithium in the reaction product from the first reaction is probably 0.1. Nevertheless, the lattice does expand 0.23 A in c upon inserting lithium cations into the van der Waals gaps judging from 26.710(4) A for $ScClH_{0.3}$ and 26.94(2) A for $Li_{0.1}ScClH_{0.33}$. Similar expansions in c have been seen in other systems, 0.24 A in Li_xYClO.[89] A larger expansion in Li_zYClH_x is found, 0.43 A, however.[79] Because of these data as well as the crystal data obtained from $Li_{0.1}YCl$ phase,[85] a z value of 0.1 was chosen for the composition of the alkali metal in the rest of the reactions. This was to ensure all of the MCl was taken up to give a set of cell parameters for comparison.

Table XIX. The stoichiometries, products and lattice constants for reactions in the $M^I_zScClH_x$ system

$$z\ M^ICl + \frac{1-z}{3}\ ScCl_3 + \frac{4-3x+2z}{6}\ Sc + \frac{x}{2}\ ScH_2 \xrightarrow[\text{Ta tube}]{860^oC,\ 3\ days} M^I_zScClH_x$$

Stoichiometry			Lattice constant		
z	x	Products[a]	a(A)	c(A)	V(A^3)
0.5	0.33	$Li_yScClH^b_{0.33}$ + LiCl + Sc	3.474(8)	26.90(2)	281.2(2)
0.1	0.33	$Li_{0.1}ScClH_{0.33}$	3.4709(6)	26.94(2)	281.1(3)
0.1	0.60	$Li_{0.1}ScClH_{0.6}$	3.4726(4)	26.934(7)	281.3(1)
0.1	0.90	$Li_{0.1}ScClH_{0.9}$	3.4745(5)	26.880(9)	281.0(1)
0.1	0.60	$Na_{0.1}ScClH_{0.6}$	3.4740(4)	29.01(2)	303.2(2)
0.1	0.60	$K_{0.1}ScClH_{0.6}$	3.480(3)	32.8(5)	344.0(9)

[a] ZrBr-type. [b] $0.1 < y < 0.5$; see text.

As in the ternary hydride system, the c lattice constant decreases in the $Li_{0.1}ScClH_x$ phases as the hydrogen composition x increases from 0.33 to 0.9. Interestingly, the intercalated phase, Li_zScClH_x, with x = 0.9 has the ZrBr-type structure while the ternary hydride phases otherwise are the ZrCl-type.

The intercalations with Na or K were successful but those with the larger cations Rb and Cs were not. The lattice parameters of each intercalated phase revealed a relatively large expansion in c with only a negligible change in a. This indicates the chlorine octahedral holes are too small for the other cations unless there is expansion of the layer along the c direction.[89] The c lattice constants can be linearly related with the Shannon[52] crystal radii of the corresponding six-coordinate metal cations (0.90 A for Li, 1.16 A for Na, and 1.51 A for K).

Powder diffraction The ScClH powder patterns of both ZrCl and ZrBr type structures are similar. Approximately ten (out of twenty) of the lines from the ZrCl type overlap those (out of twenty-five) of the ZrBr type at high 2θ angles. The strongest reflections in the powder patterns, (104) in the ZrCl-type and (105) in the ZrBr-type, are the main distinguishing features for these structures.

The Guinier powder patterns of the single phase products gave rather sharp lines. On the contrary, the powder patterns of the products in the region $0.67 \leq x <$

1.0 show the diffuse lines between (104) from ZrCl and (105) from ZrBr-type phase plus the other two reflections, (101) and (012) that are only seen in ZrBr-type pattern. The product is again a mixture of two polytypes. From the relative intensities of the powder pattern, 70% of $ScClH_x$ is in ZrCl-type for x = 0.67 vs. 95% for x = 0.75-1.0 (Table XVIII). There was no grinding damage to cause broadened lines. A couple of lines at higher 2θ angles were broad because of the overlap of two different patterns from these mixed phases. Otherwise the lines looked sharp suggesting the mixed phases have identical lattice constants probably resulting from the same hydrogen compositions in each phase.

Single crystal examination Weissenberg photographs of a plate crystal of nominal composition $ScClH_{1.0}$ showed R-centering (-h + k + l = 3n) as in "3R-ScCl". The reflections with lower 2θ angles were somewhat broadened and slightly streaked, reflecting the rather poor crystal quality. This streaking was presumably due to displacement of the slabs and to the shape of the crystal. To avoid the streaking problems (or elongated peaks) which usually give high backgrounds in the peak profile, the 2θ/θ-scan mode was chosen to scan across the peak (default is ω-scan). Consequently, this resulted in a low background data set which gave a better refinement (Chapter II). An absorption correction, using ψ-scan at 2θ = 27.88°, was applied to the data from this plate-like crystal.

The cell parameters and crystallographic data are in Tables I and II, respectively. The crystal structure refinement started with the atomic parameters from the ZrCl model and proceeded uneventfully. A final difference-Fourier synthesis was flat, $<1\ e/A^3$, at both atom sites and elsewhere. The atomic parameter for hydrogen atom was not refined as the scattering of this atom is too small to be settled.

The final atomic parameters for the heavy atoms and selected bonding and nonbonding distances are in Table XX for 3R-ScClH as well as for "3R-ScCl"[8,11] for comparison. The most striking feature is the B_{33}/B_{11} ratio which is smaller for the hydride. The smaller values imply "better" crystallinity.

Results

Both structure types, ZrCl[72] and ZrBr,[73] have been well described in terms of the layer packing sequence. The former structure has a |CabC||AbcA||BcaB| sequence with |BcaB||AbcA||CabC| for the latter. In Figure 24, two [110] projections of the structure types in $ScClH_x$ compounds are presented with the arrangements of the heavy atoms. The slab stacking sequence on the outside of the bracket is |CAB| and |BAC|, respectively. Comparison of these two stacking sequences reveals one notable difference. There is a second nearest neighbor chlorine-scandium interaction in the ZrBr type structure which has a stabilizing effect. The

Table XX. Atom parameters and selected distances for 3R-ScClH (ZrCl) and "3R-ScCl"[a], $R\bar{3}m$

	3R-ScClH (ZrCl)			"3R-ScCl" (ZrBr)		
Atom parameters	z	B_{11}[b]	B_{33}	z	B_{11}[b]	B_{33}
Sc: (6c)	0.1192(1)	0.99(9)	1.8(1)	0.2137(1)	0.9(1)	3.8(2)
Cl: (6c)	0.3912(1)	1.4(1)	1.7(1)	0.3914(1)	1.0(1)	3.8(2)
Distance (A)						
interlayer						
Sc-Sc		3.222(5)			3.216(6)	
Sc-Cl		2.584(3)			2.591(4)	
Cl-Cl		3.670(6)			3.695(8)	
Sc-H[c,d]		2.06			2.06	
H-H[d]		2.57			2.57	
H-Cl		2.89			2.90	
intralayer						
Sc-Sc		3.4785(2)			3.473(2)	

[a]References 8 and 11. [b]$B_{11} = B_{22} = 2B_{12}$, $B_{23} = B_{13} = 0$ by symmetry. [c]The distance in ScH_2 is 2.07 A; see text. [d]Calculated for protons centered in Sc_4 tetrahedra.

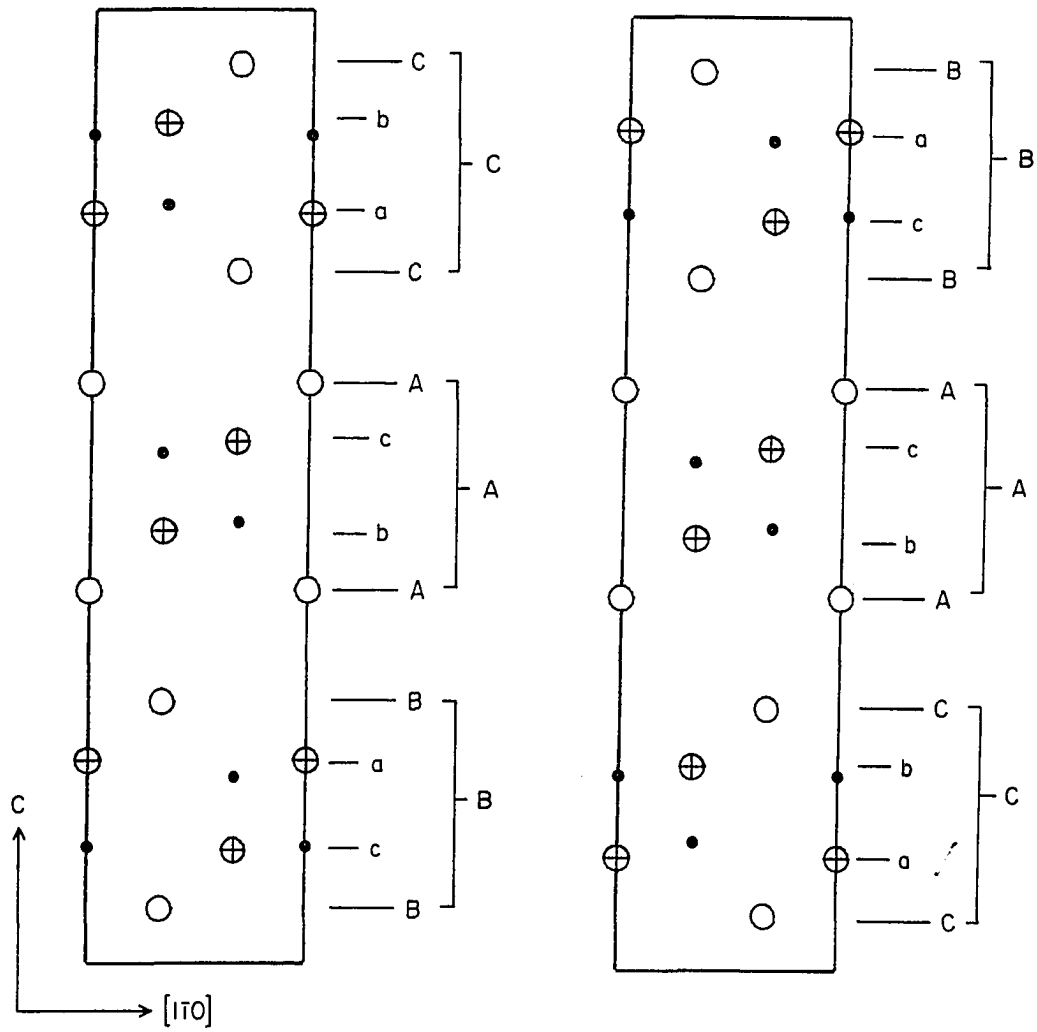

Figure 24. The [110] sections of $ScClH_x$ in ZrBr-type (left) and ScClH in ZrCl-type (right) structures with the layer packing sequence labeled inside the bracket and the slab packing sequence on the outside of the brackets. The upper case letters correspond to the Cl layers and the lower case the Sc layers. The hydrogen atoms in each projection are sitting in the Sc_4 tetrahedral interstices (●).

hydrogen atoms are presumably in the Sc_4 tetrahedral interstices (crosses).

These two structures are 6-8 type condensed metal octahedra which are face-capped by chlorines in the nearest layers. The distances from center of the metal octahedra to the nearest chlorine are 2.90 A for "ScCl" and 2.88 A for $ScClH_{1.0}$, very close to the distances from the center of Sc_4 tetrahedra, 2.90 and 2.89 A, respectively (Table XX). Nevertheless, the hole size of Sc_6 octahedral is too big, ca. 2.38 A, for the single hydrogen. Tetrahedral site occupation has been confirmed in YClH[16] (single crystal X-ray diffraction) and more evidently in $TbClD_{0.8}$[90] (powder neutron diffraction).

The calculations for protons centered in the tetrahedra give Sc-H bond and H-H distances of 2.06 A and 2.57 A, respectively, for $ScClH_{1.0}$ and "ScCl" (Table XX). The Sc-H distance in ScH_2 (fluorite structure, a = 4.783 A) is 2.07 A,[92] (Table XX). This again suggests the tetrahedral sites are more suitable for single hydrogen than the octahedral interstices.

The c lattice constants ($\pm 3\sigma$) from Table XVIII-D are plotted vs x in Figure 25. The $ScClH_x$ phase retains ZrBr-type structures up to x = 0.67 at which a 30 to 70% mixture of that and ZrCl type results. At the left side of the Figure with x = "0.1" and "0.25" (open circles), a second phase ($ScCl_{1.5}$, mouse fur) was seen. If the lattice

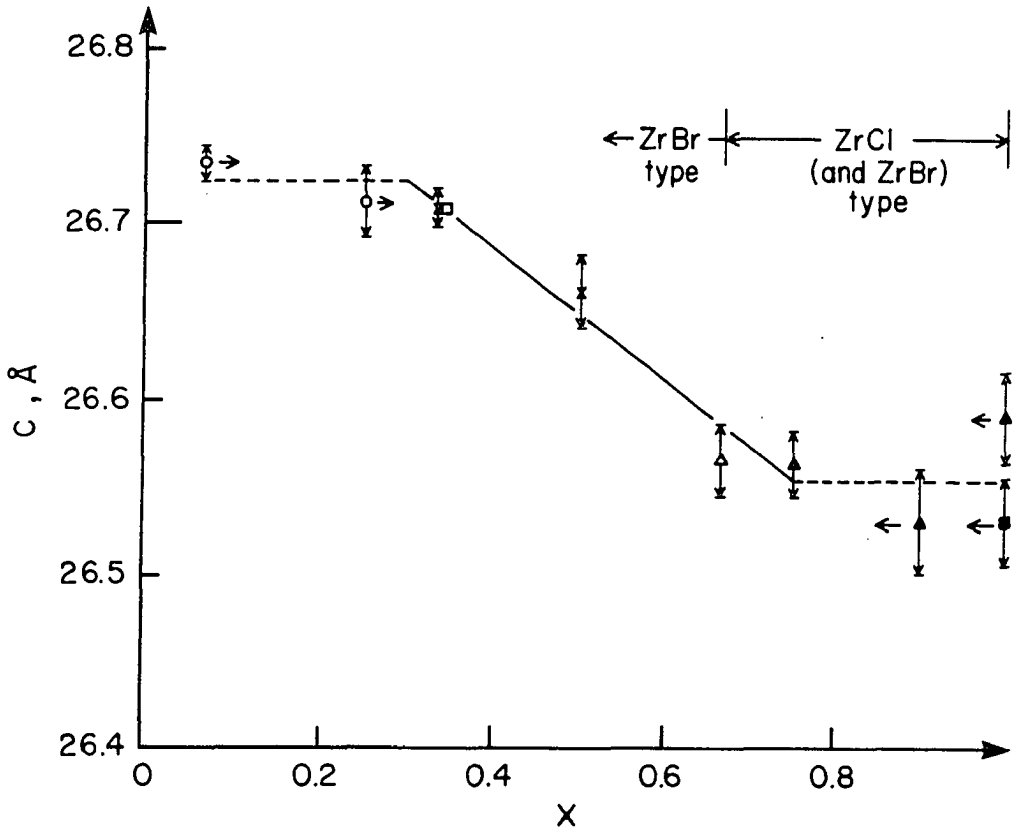

Figure 25. A plot of c (±3σ) versus x (H/ScCl) for $ScClH_x$. (o) Coexistence of $ScCl_{1.5}$. (x) Single phase region, ZrBr-type. (Δ) Two phase region, 70% in ZrCl-type, 30% in ZrBr-type. (▲) Two phase region, x = 0.75, 0.9, 0.1; 95% in ZrCl-type and 5% in ZrBr-type. (□) Reference 8, "ScCl". (■) $ScClH_{1.0}$, single crystal.

parameters of these hydride phases are plotted with the others, those with $x < 0.33$ give a horizontal line and the line through the other points ($0.33 < x \leq 0.75$) which intersects the first at $x = 0.30$. This point presumably represents the lower limit of the hydrogen composition necessary to stabilize the "ScCl" mother structure. If $ScCl_{1.5}$ is assumed not to take up any hydrogen, the corrected x in compounds with "0.1" and "0.25" loaded compositions should be 0.33 and 0.31 (±0.05), respectively, according to the estimated products distributions. These estimations are consistent with their corresponding lattice constants (Table XVIII and Fig. 25). The single phase region in Figure (crosses), $0.30 < x < 0.67$, shows a decrease in c as the hydrogen content increases. The decreasing continues until x reaches the next two-phase region (open and solid triangles), $0.67 \leq x < 1.0$. Both dashed lines in the Fig. 25 represents the averaged values of c lattice from the phase in the regions, $x < 0.3$ and $0.75 \leq x < 1.0$. Notably, the reaction with excess hydrogen did not give any of ZrBr-type phase (Table XVIII, method A) but ScH_2 instead, and the latter phase is very possibly from the reaction of hydrogen and the excess scandium strips.

The interpolation of the c lattice constant from the previously found "ScCl",[8,11] gives a hydrogen coefficient of ca. 0.35.

There is no evidence of forming $ScClH_2$ on adding one mole of hydrogen to $ScClH_{1.0}$ at 200-300°C.[79] This temperature range might be thought too low to displace the slabs as the latter structure (1T) would be expected in $ScClH_{2.0}$ such as from ccp to hcp in 3(1T) structure. But in early experiments with excess hydrogen there was no evidence for this dihydride formation at 710°C either (Table XVIII).

These monochloride hydrides contain metal layers with strong Sc-Sc bonding between and within these (d(Sc-Sc) = 3.21-3.22 A and 3.47-3.48 A, respectively). Hydrogen presumably fills tetrahedral interstices between the metal layers, withdrawing electrons from the conduction band to form a hydride "anion" with appreciable covalent bonding to scandium according to theory. In pure YCl a high DOS develops at the Fermi level E_F.[79] This serves to explain why this pure binary compound is not stable and thus does not exist without the additional hydrogen. The pure ScCl probably does not exist for the same reason.

There are some notable changes in lattice dimensions upon varying the hydrogen composition. There is an expansion in (a) but a contraction in (c) as the x increases in the range of $0.30 < x \leq 0.75$. The increase in Sc-H overlap consequently decreases the Sc-Sc overlap for intralayer scandium where the bond distances (also the a or b) increase. Since ZrCl and ZrBr structure types are quite similar, small variations in the factors affecting bonding

or nonbonding interactions could cause the structure change. Metal cations intercalate into the octahedral interstices, causing the retention of the ZrBr-type structure even up to the hydrogen composition 0.9. This is understandable because of the M^I-Sc interaction in the ZrCl-type structure is presumably much larger (Figure 26). Therefore, the alternate "$M^I_zScClH_x$" structure is derived from the ZrBr type structure of the phase $ScClH_x$ ($0.33 \leq x \leq 0.9$; $z < 0.5$) with M^I in octahedral interstices between chlorine layers, Figure 26. The calculated and observed Guinier powder patterns of Na_zScClH_x are in Table XXI. The preferred orientation is evident here and other intercalated layer compounds as well.[78,89]

In theory, there may remain a density of occupied states at the Fermi level, E_F, meaning the intercalated $M^I_zScClH_x$ is possibly still metallic as the experiments have shown for the some of the monohalides. One also could surmise the conductivity of the two dimensional conductor, $ScClH_x$, along ab plane becomes stronger and even possibly in the third dimension as the number metal cations in $M^I_zScClH_x$ increases. The intercalated compounds are air and moisture sensitive and dark bluish-black in color. This suggests they are reduced and/or possibly metallic.

In conclusion, the low yield, pseudo binary "ScCl" is actually an interstitially-stabilized ternary hydride phase, $ScClH_x$. The excess powdered metal used does provide more

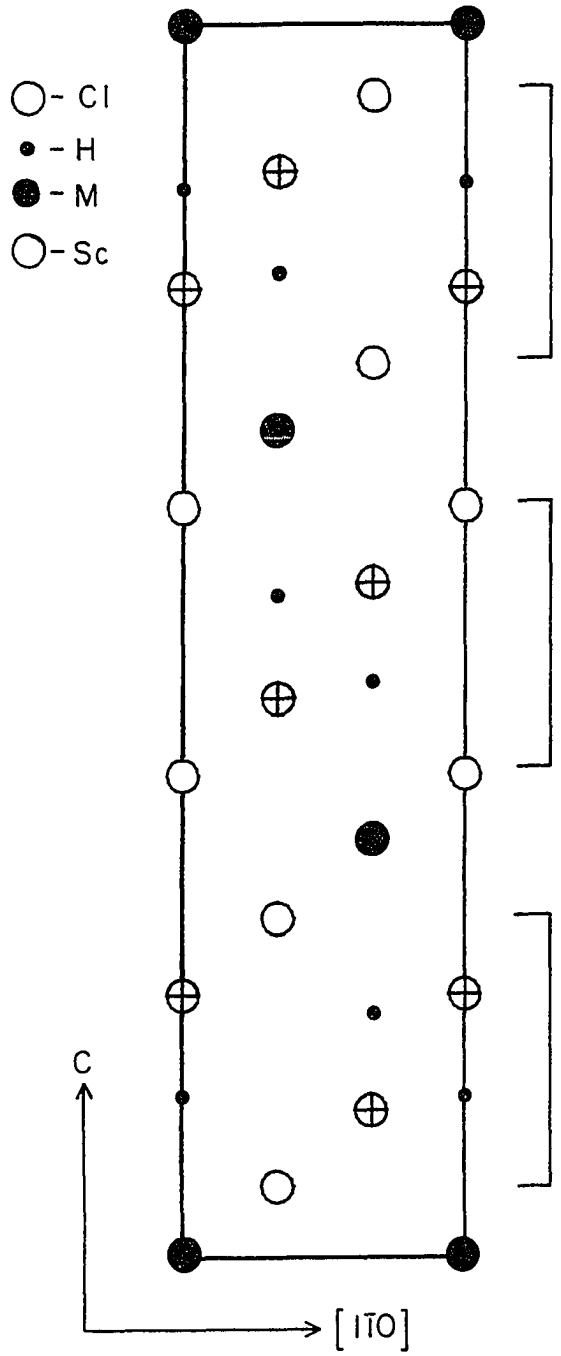

Figure 26. The [110] section of alternate structure of 3R-$M^{I}_{Z}ScClH_{X}$ structure.

Table XXI. Calculated and observed Guinier powder patterns for 3R-Na_zScClH_x

h	k	l	$2\theta^{a}_{calc}$	I^{b}_{obs}	I^{c}_{calc}
0	0	3	9.14	10	6
0	0	6	18.33	5	23
1	0	1	29.83	20	6
0	1	2	30.31	30	26
0	1	5	33.52	90	100
1	0	7	36.89	5	34
0	0	12	37.16	–	13
1	0	10	43.29	20	23
0	1	11	45.71	5	8
1	0	13	50.90	–	13
1	1	0	52.65	100	32
1	1	6	56.22	–	6
0	0	18	57.10	–	6
0	1	17	62.52	–	7
2	0	5	63.87	30	15
0	2	7	66.01	–	7
1	1	12	66.19	–	15
0	2	10	70.45	10	6
1	1	18	81.38	–	17
0	1	23	82.93	–	10
1	2	5	87.30	40	19
2	1	7	89.24	10	9

[a] $2\theta_{obs} = 2\theta_{calc} \pm 0.04^{o}$. $2\theta < 90^{o}$. [b] Substantial preferred orientation. $I_{obs} > I_{calc}$ for $h + k \geq 1$. [c] All lines with $I_{calc} \geq 6$ reported.

fresh surface area but, more importantly, the residual hydrogen in the powdered metal provides enough hydrogen to make the product in moderate to high yield. The similar lattice variation and "phase transition" observed in the Y-Cl system have also been shown to result from variations of the hydrogen content.[16]

The scandium monobromide monohydride (according to loaded composition) retains the ZrBr-type structure. This is probably because the second nearest neighbor interaction is more important for the monobromide since the ratio of halogen to metal radii is larger than in the chlorides.

CHAPTER V. FUTURE WORK

The importance of the interstitial-containing halide clusters that have been found in the course of this investigation and other recent studies, replacing what use to be low-yield materials, is the gain in knowledge of the synthesis and chemistry of these compounds. Most of these phases are now available in large quantities to allow for more complete characterization and evalution in terms of physical property measurements. Of course, a large class of new materials of this kind have been found not only in the scandium chloride system, but in the other early transition and rare earth metal halides. There are, however, several areas where unanswered questions remain and new questions have been raised. In this section, several suggestions for further investigation are made as guide for what might be possibly done.

There is still some work remaining in the quantitative synthesis of nitride phases which have been studied during this course of work. Alternative preparative schemes which increase the yields need to be developed. As noted previously, both Sc_2Cl_2C and Sc_2Cl_2N phases have not been made in recognizable single crystals in the reactions where interstitials are purposely added. Electronically, the latter phase has one more electron per formula unit than the former which is an insulator as predicted. The conductivity measurements on single crystals of both phases would be very

helpful in an further understanding of their physical properties. Therefore, other synthetic routes, electrolysis of molten salt using graphite electrode or with bubbling nitrogen gas, for example, are necessary.

Besides the missing members of chains containing second period interstitials in some of the structure types as mentioned earlier, the second and third most reduced phases in the Sc-Cl system would be compositions "Sc_6Cl_7" and "Sc_4Cl_5" isostructural with Er_6I_7 and Er_4I_5,[13] respectively. Evidently, these are 6-12 type condensed halide clusters. According to the structure model developed in Chapter I, these 6-12 type structures might be isolated with a certain interstitial. Different conditions which help the synthesis of these phases would necessarily need to be studied.

The analogous compounds in bromide and iodide systems ought to be interesting. Of course the different anions, which evidently have larger matrix effects than chloride, might give unexpected structural solutions.

It is noteworthy that Y_2Cl_3 structure (Gd_2Cl_3-type) has never been found for scandium while the structure types reported here have not been seen for either yttrium and lanthanum (except $YClZ_x$ where Z = H or C). The yttrium and lanthanum metal atoms have a larger extension of their outermost d orbitals than for scandium. Therefore, more or maybe different structure types of halide clusters may be expected. Further, larger interstitials, the third period

nonmetals, for example, may be possible in the metal clusters, stabilizing the compound formation. The new structure types in Gd–X–C systems[93] containing dicarbon unit have not been seen in any of the currently studied systems M–X–C (where M = Sc or Zr, X = Cl, Br, or I) in which the metal atoms might have been either too few in valence electrons (3 for Sc) or too small an extension of their outermost d orbitals to allow for the larger metal cluster expansion. Therefore, with larger yttrium or lanthanum metal cations, these structure types may be expected.

The crystals $ScCl_{1.5}$ (mouse fur) and $ScCl_{1.42}$ (whisker) have a cross section too small to do single crystal structure determinations. It might be worthwhile to do XAFS analysis to determine the relative atom positions, especially as these two compounds can be synthesized in quantitative yield and apparently interstitial-free. Quantitative analysis for any interstitials, e.g., vacuum fusion for H, N, O, etc., should be done.

Because of the thermal stability of ScOCl, the search for any possible interstitial oxides with any structure type has been unsuccessful. However, the less studied scandium chloride fluorides have several times given in a small amount of a plate-like phase (Chapter III). This possible fluoride-containing phase is very interesting for further investigation in terms of synthesis and structure determination.

Preliminary studies of the intercalated phases $M_xSc_2Cl_2H_z$ (where M = Li, Na, K) have indicated the existence of these materials which may be two-dimensional conductors. In addition, the similar compositions for yttrium have been identified with M = Li and Na.[79] The lack of large cations, Rb and Cs, in these intercalated compounds is very possible due to the misplaced reaction conditions, and alternative preparative schemes which lead the intercalation of larger cations are needed. According to DOS band calculations of the monochloride phases,[79] both Sc—Cl and Y—Cl systems are capable for further reduction. Therefore, the intercalation of alkaline earth metal cations should be very interesting.

The only structure determined pure binary phase, in the metal-rich region ($1 < X:M < 2$) of the $Sc-ScCl_3$ phase diagram, is Sc_7Cl_{10}. Evidently, there are four structurally uninvestigated phases, namely $ScCl_{1.50}$, $ScCl_{1.45}$, $ScCl_{1.42}$, and $ScCl_{1.40}$. Besides, any of additional pure binary phase and the ternary system M—Sc—Cl need to be studied.

REFERENCES

1. McCollum, B. C., Ph.D. Dissertation, Iowa State University, Ames, IA, 1970.

2. Poeppelmeier, K. R.; Corbett, J. D. J. Am. Chem. Soc. 1978, 100, 5039.

3. Poeppelmeier, K. R.; Corbett, J. D.; McMullen, T. P.; Torgeson, D. R.; Barnes, R. G. Inorg. Chem. 1980, 19, 129.

4. Meyer, G.; Corbett, J. D. Inorg. Chem. 1981, 20, 2627.

5. Corbett, J. D.; Poeppelmeier, K. R.; Daake, R. L. Z. Anorg. Allg. Chem. 1982, 491, 51.

6. McCollum, B. C.; Camp, M. J.; Corbett, J. D. Inorg. Chem. 1973, 12, 778.

7. Poeppelmeier, K. R.; Corbett, J. D. Inorg. Chem. 1977, 16, 1107.

8. Poeppelmeier, K. R.; Corbett, J. D. Inorg. Chem. 1977, 16, 294.

9. Corbett, J. D. J. Solid State Chem. 1981, 37, 335.

10. Simon, A. Z. Anorg. Allg. Chem. 1967, 355, 311.

11. Poeppelmeier, K. R., Ph.D. Dissertation, Iowa State University, Ames, IA, 1978.

12. Berroth K.; Simon A. J. Less-Common Met. 1981, 76, 41.

13. Berroth, K, Ph.D. Dissertation, der Universität, Stuttgart, West Germany, 1980.

14. Corbett, J. D.; Daake, R. L.; Poeppelmeier, K. R.; Guthrie, D. H. J. Am. Chem. Soc. 1978, 100, 652.

15. Guthrie, D. H.; Corbett, J. D. Inorg. Chem. 1982, 21, 3290.

16. Wijeyesekera, S. D.; Corbett, J. D., Ames Laboratory, Iowa State University, Ames, IA, unpublished research, 1984.

17. Struss, A. W.; Corbett, J. D. Inorg. Chem. 1970, 9, 1373.

18. Marek, H. S.; Corbett, J. D.; Daake, R. L. J. Less-Common Met. 1983, 89, 243.

19. Imoto, H.; Corbett, J. D. Inorg. Chem. 1980, 10, 1241.

20. Seaverson, L. M.; Corbett, J. D. Inorg. Chem. 1983, 22, 3202.

21. Warkentin, E.; Masse, R.; Simon, A. Z. Anorg. Allg. Chem. 1982, 491, 323.

22. Warkentin, E.; Simon, A. Rev. Chem. Minerale 1983, 20, 488.

23. Ford, J. E., Corbett, J. D.; Hwu, S.-J. Inorg. Chem. 1983, 22, 2789.

24. Smith, J. D.; Corbett, J. D. J. Am. Chem. Soc. 1985, accepted.

25. Ziebarth, R. P.; Corbett, J. D. J. Am. Chem. Soc. 1985, in press.

26. Ziebarth R. P., Ames Laboratory, Iowa State University, Ames, IA, private communication.

27. Löchner, U.; Diplomarbeit, Universität Karlsruhe, Karlsruhe, West Germany, 1973.

28. Rustad, D. S.; Gregory, N. W. Inorg. Chem. 1982, 21, 2929.

29. Cisar, A. Ph.D. Dissertation, Iowa State University, Ames, IA, 1978.

30. Imoto, H., Ames Laboratory, Iowa State University, Ames, IA, unpublished research, 1978.

31. Takusagawa, F., Ames Laboratory, Iowa State University, Ames IA, unpublished research, 1981.

32. Clark, C. M.; Smith, D. K.; Johnson, G. J. "A Fortran IV Program for Calculating X-Ray Powder Diffractions Patterns-Version 5", Department of Geosciences, Pennsylvania State University, University Park, PA, 1973.

33. Powder Diffraction File, JCPDS International Centre for Diffaction DATA, 1601 Park Lane, Swathmore, PA, 1982.

34. Kim, S. S.; Shin, W. C. "GEOMK, a computer program for geometry calculation", Seoul N. University, South Korea, 1982.

35. Schroeder, D. R.; Jacobson, R. A. Inorg. Chem. 1973, 21 210.

36. Jacobson, R. A. Applied Crystallogr. 1976, 9, 115.

37. Smith, J. D., Ph.D. Dissertation, Ames Laboratory, Iowa State University, Ames, IA, 1984.

38. Jacobson, R. A., Ames Laboratory, Iowa State University, Ames, IA, unpublished research, 1982.

39. Karcher, B., Ph.D. Dissertation, Iowa State University, Ames, IA, 1981.

40. Rodgers, J.; Jacobson, R. A., AEC Report IS-2155, Iowa State University, Ames, IA, 1967.

41. Lawton, S. A.; Jacobson, R. A. Inorg. Chem. 1968, 7, 2124.

42. Lapp, R. L.; Jacobson, R. A., U.S. Department of Energy Report IS-4708, Iowa State University, Ames, IA, 1979.

43. Powell, D. R.; Jacobson, R. A., U.S. Department of Energy Report IS-4737, Iowa State University, Ames, IA, 1980.

44. Simon, A., Max-Planck-Institut FKF, Stuttgart, West Germany, unpublished research.

45. Hwu, S.-J.; Corbett, J. D.; Poeppelmeier, K. R. J. Solid State Chem. 1985, 57, 43.

46. Johnson, C. K., "ORTEP: A Fortran Thermal-Ellipsoid Plot Program for Crystal Structure Illustrations", ORNL Report 3794, Oak Ridge National Laboratory, Oak Ridge, TN, 1970.

47. Schaffer, A. M.; Gouterman, M.; Davidson, E. R. Theoret. Chim. Acta (Berl.) 1973, 30, 9.

48. Hoffmann, R. J. Chem. Phys. 1963, 39, 1397.

49. Hinze, J.; Jaffé, H. H. J. Phys. Chem. 1963, 67, 1501.

50. Smith, J. D., Ames Laboratory, Iowa State University, Ames, IA, unpublished research, 1983.

51. Jacobson, R. A., "DAPT, A computer program for distances, angles, L. S. planes and tort angles calculation", Ames Laboratory, Iowa State University, Ames, IA.

52. Shannon, R. D. Acta Cryst., Sect. A., 1976, A32, 751.

53. Dudis, D. S., Ames Laboratory, Iowas State University, Ames, IA, private communication, 1985.

54. Van-Uitert, L. G., J. Appli Phys. 1981, 52, 5547.

55. Mattausch, Hj.; Simon, A.; Eges, R. Z. Anorg. Allg. Chem 1980, 17, 516.

56. Araujo, R. E.; Corbett, J. D. Inorg. Chem. 1981, 20, 3082.

57. Lokken, D. A.; Corbett, J. D. Inorg. Chem. 1973, 12, 556.

58. Torardi, C. C.; McCarley, R. E. J. Am. Chem. Soc. 1979, 101, 3963.

59. "New Transition Metal Halides and Oxides with Extended Metal-Metal Bonding" Corbett, J. D. and McCarley, R. E., Chapter in "Crystal Chemistry and properties of Materials with Quasi-One-Dimensional Structures", (J. Rouxel, ed.) D. Reidel Publishing Co., Dordrecht, Holland, accepted, 1984.

60. Hwu, S.-J.; Corbett, J. D., Iowa State University, Ames IA, unpublished research.

61. Fromm, E. and Gebhardt, E., "Gase und Kohlenstoff in Metallen", Springer-Verlag, Heidelberg, West Germany, 1976.

62. Corbett, J. D.; Marek, H. S. Inorg. Chem. 1983, 22, 3194.

63. Wijeyesekera, S.; Hoffmann, R. Organometallics 1984, 3, 949.

64. DiSalvo, E. J.; Safran, S. A.; Haddon, R. C.; Waszczak, J. V. Phys. Rev. 1979, B20, 4883.

65. Corbett, J. D. Adv. Chem. Ser. 1980, 186, 329.

66. Krikorian, N. H.; Bowman, A. L.; Krupka, M. C. High Temp. Sci. 1969, 1, 360.

67. Hoppe, R. Angew. Chem. 1981, 20, 70.

68. Corbett J. D., Pure Appl. Chem. 1984, 56, 1527.

69. DiSalvo, E. J., AT&T Bell Laboratories, private communication, 1985.

70. DiSalvo, F. J.; Waszczak, J. V.; Walsh, W. M. Jr.; Rupp, L. W. Jr.; Corbett, J. D., submitted for publication.

71. Simon, A.; Warkentin, E. Z. Anorg. Allg. Chem. 1983, 497, 79.

72. Adolphson, D. G.; Corbett, J. D. Inorg. Chem. 1976, 15, 1820.

73. Daake, R. L.; Corbett, J. D. Inorg. Chem. 1977, 16, 2029.

74. Mattausch, Hj.; Hendricks, J. B.; Eger, R.; Corbett, J. D.; Simon, A., Inorg. Chem. 1980, 19, 2128.

75. Mattausch, Hj.; Simon, A.; Holzer, N.; Eger, R. Z. Z. Anorg. Allg. Chem. 1980, 466, 7.

76. Beckmann, O.; Boller, H.; Nowotny, H., Monatsh. Chem. 1970, 101, 955.

77. Ziebarth, R. P.; Corbett, J. D., Ames Laboratory, Ames IA, unpublished research, 1985.

78. Ford, J. E., Ph.D. Dissertation, Iowa State University, Ames, IA, 1983.

79. Wijeyesekera, S. D., Ames Laboratory, Iowa State University, Ames, IA, private communication, 1985.

80. Corbett, J. D., Meyer, G.; Anderegg, J. W. Inorg. Chem. 1984, 23, 2625.

81. Neckel, A. Int. J. Quant. Chem. 1983, 23, 1317.

82. Klein, B. M.; Papaconstantopoulos D. A.; Boyer, L. L., Phys. Rev. 1980, B22, 1946.

83. Lauher, J. W. J. Am. Chem. Soc. 1978, 100, 5305.

84. Simon, A. Angew. Chem. Intl. Eng. Ed. 1981, 20, 1.

85. Ford, J. E.; Gerd, M.; Corbett, J. D. Inorg. Chem. 1984, 23, 2094.

86. Imoto, H.; Corbett, J. D. Inorg. Chem. 1981, 20, 145.

87. Hört, G.; Speck, H.; Fromm, E.; Jehn, H. "Physik Daten", Max-Planck-Institut für Metallforschung, Stuttgart, West Germany, No.5~9, 1981.

88. Franzen, H. F.; Khan, A. S.; Peterson, D. T. J. Less-Common Metals 1977, 55, 143.

89. Ford, J. E.; Corbett, J. D. Inorg. Chem. 1985, accepted.

90. Wijeyesekera, S. D.; Corbett, J. D. Solid State Commun. 1985, 54, 657.

91. Ueno, F; Ziebeck, K.; Mattausch, Hj.; Simon, A. Rev. Chim. Miner., in press.

92. McGuire, J. C.; Kemptn, C. P. J. Chem. Phys. 1960, 33, 1584.

93. Hwu, S.-J.; Corbett, J. D. Ames Laboratory and Department of Chemistry, Iowa State University, Ames IA, unpublished research.

94. Simon, A. J. Solid State Chem. 1985, 57, 2.

ACKNOWLEDGEMENTS

For since the creation of the world His invisible attributes, His eternal power and divine nature, have been clearly seen, being understood through what has been made, so that they are without excuse.

Romans 1:20

These works reported herein is only a miniscule part of our understanding of the universe. However, to the author, it represents another manifestation of God. Of course, the greatest help and assistance have been given through the professors, family, friends, and colleagues of the author.

Therefore, I would like to thank Professor John D. Corbett for his patience, guidance, and constructive criticism throughout this research.

This dissertation is dedicated as a memorial to my father, Tze-Chung (16 October 1905 – 31 December 1978). I also thank my mother and sister without whose support and encouragement I would not be able to finish this study.

Special thanks are due Dr. R. A. Jacobson and the members of his group for their assistance with diffractometers and Dr. R. N. Shelton and the members of his group for the magnetic susceptibility measurements.

I am indebted to B. Beaudry and co-workers for providing scandium metal, to F. Laabs for electron microprobe analysis, to E. Dekalb and N. Beymer for

elemental analysis, to G. Meyer for MAPLE calculations, and to S. Wijeyesekera and R. P. Ziebarth for the extended Hückel calculations.

I also wish to thank all group members, past and present, for their help and friendship.

Last, I would like to give the most thanks to my precious wife, Yuan-Lee, for her patience, understanding, and encouragement.

APPENDIX A. CALCULATED AND/OR OBSERVED GUINIER POWDER PATTERNS

Table A1. Calculated Guinier powder pattern[a] for $Sc_7Cl_{12}B$

h	k	l	I^b_{calc}	h	k	l	I^b_{calc}
1	0	1	7	3	2	-2	2
1	1	0	24	0	5	1	4
0	2	1	11	1	0	4	3
0	1	2	2	2	4	1	5
2	1	1	8	5	0	2	2
3	0	0	3	1	3	4[c]	32
2	0	2	2	5	2	0	32
2	2	0	3	1	3	-5	1
1	2	2	3	0	0	6[c]	6
1	3	1	5	2	6	2	17
1	1	3	5	7	1	3	2
1	3	-2	100	2	6	-4	12
3	2	1	5	5	2	-6	10
1	4	0	2	9	1	2	10
0	4	2	2				

[a]Cu $K\alpha_1$ radiation, Guinier geometry. [b]The minimum intensity is 10 unless otherwise observed. [c]The distance of the next reflection is too closed to be resolved in observed powder pattern for $Sc_7Cl_{12}N$.

Table A2. Calculated Guinier powder pattern for Sc_4Cl_6B[a]

h	k	l	I^b_{calc}	h	k	l	I^b_{calc}
1	1	0	100	2	3	1	17
0	2	0	4	3	2	1	42
2	0	0	4	3	4	0	19
2	2	0	4	5	1	0	4
1	3	0	3	2	5	0	4
3	1	0	5	3	3	1	3
0	0	1	3	4	4	0	6
2	3	0	6	1	5	1	3
0	2	1	5	5	2	1	9
2	0	1	5	5	4	0	5
2	1	1	10	0	0	2	11
1	4	0	2	0	6	1	17
3	3	0	6	1	1	2	3
2	2	1	25	1	6	1	3
2	4	0	4	6	1	1	8
1	3	1	5	6	2	1	6

[a]Cu $K\alpha_1$ radiation, Guinier geometry. [b]The minimum intensity is 10 unless otherwise observed.

Table A3. Calculated Guinier powder pattern[a] for Sc_5Cl_8C

h	k	l	I^b_{calc}	h	k	l	I^b_{calc}
0	0	-1	15	1	-1	-3	5
2	0	1	16	-3	-1	-1	25
-2	0	0	19	5	-1	-1	37
2	0	-2	42	-6	0	0	33
-2	0	-1	10	5	-1	-4	46
4	0	-1	18	2	0	-5	10
2	0	-3	14	6	0	-6	11
4	0	-3	8	-1	-1	-4	51
1	-1	-1	3	0	-2	0	29
3	-1	-1	25	9	-1	-3	27
-3	-1	0	13	9	-1	-5	4
3	-1	-3	100	9	-1	-7	2
-1	-1	-2	6	12	0	-6	12

[a]Cu $K\alpha_1$ radiation, Guinier geometry. [b]The minimum intensity is 10 unless otherwise observed.

Table A4. Calculated Guinier powder pattern for $Sc_7Cl_{10}C_2$

h	k	l	I^b_{calc}	h	k	l	I^b_{calc}
0	0	1	15	-5	1	2	29
2	0	0	29	-6	0	4	37
-2	0	1	10	3	1	3	47
2	0	1	32	-3	1	4	14
4	0	1	14	8	0	1	13
-1	1	2	31	2	0	5	10
-2	0	4[c]	8	-9	1	1	50
3	1	1	5	0	2	0	30
-6	0	3	32	6	0	5	13
3	1	2[c]	100	-3	1	6	34
6	0	2	7	-6	2	3	10
-3	1	3	23	0	0	8	12

[a]Cu $K\alpha_1$ radiation, Guinier geometry. [b]The minimum intensity is 10 unless otherwise observed. [c]The observed intensities are between 40 and 50.

Table A5. Calculated[a] and observed[b] Guinier powder patterns of 1T-Sc_2Cl_2Y (Y = C, N)

			1T-Sc_2Cl_2C		1T-Sc_2Cl_2N
h	k	l	I^c_{calc}	I_{obs}	I_{obs}
0	0	1	55	70	60
0	0	2	10	20	20
1	0	0	25	50[d]	70[d]
1	0	2	100	100	100
0	0	4	10	15	10
1	0	3	11	20	25
0	1	4	28	30	35
1	1	0	35	90[d]	80[d]
1	1	1	4	–	5
0	1	5	10	–	–
2	0	0	4	30[d]	20[d]
0	2	2	18	20	25
1	1	4	12	5	–
2	0	4	11	–	5
1	1	6	13	–	20
2	1	0	5	20[d]	20[d]
2	1	2	26	20	30

[a]Cu $K\alpha_1$, Guinier geometry. [b]From interstitial reactions. [c]The minimum intensity is 10 unless otherwise observed. [d]Preferred orientation evident; $I_{obs} > I_{calc.}$ for hk0.

Table A6. Calculated[a] and observed Guinier powder pattern for $ScClH_{1.0}$ (ZrCl-type)

h	k	l	I^{b}_{calc}	I^{c}_{obs}
0	0	3	13	10
0	0	6	19	10
1	0	1	1	5
0	1	2	2	5
1	0	4	100	90
0	1	8	41	5
1	0	10	13	–
1	1	0	27	100
1	1	6	6	5
0	1	14	10	–
0	2	4	16	20
2	0	8	10	–
1	1	12	13	–
2	1	4	20	–
1	1	18	12	40

[a]Cu $K\alpha_1$ radiation, Guinier geometry. [b]$I_{calc} \geq 10$, unless otherwise observed. [c]Preferred orientation problem, ref. 78, 89.

APPENDIX B. CALCULATED AND OBSERVED STRUCTURE FACTOR AMPLITUDES FOR $Sc_7Cl_{12}B$

L = -9

H	K	FO	FC
0	9	12	12

L = -8

H	K	FO	FC
-1	10	73	72
0	8	9	9

L = -7

H	K	FO	FC
-2	11	16	16
-1	12	8	7
0	7	7	7
0	10	10	10

L = -6

H	K	FO	FC
-4	14	70	68
-3	12	13	14
-2	10	12	12
-1	8	19	19
-1	11	38	38
0	6	17	17
0	9	11	11
0	12	10	11
1	10	17	17
2	11	18	18

L = -5

H	K	FO	FC
-3	11	13	13
-3	14	5	4
-2	9	11	11
-2	12	28	28
-1	7	7	7
-1	10	33	34
-1	13	8	7
0	5	35	35
0	8	4	4
0	11	36	36
1	9	6	5
1	12	8	8
2	10	15	15

L = -4

H	K	FO	FC
-4	12	24	24
-4	15	29	29
-3	10	8	8
-3	13	3	3
-2	8	44	44
-2	14	9	9
-1	6	25	24
-1	9	9	9
0	4	5	4
0	7	9	8
0	13	77	75
1	8	29	29

1	11	7	7
2	9	4	5
2	12	10	10
3	10	33	34
4	11	11	11

L = -3

H	K	FO	FC
-6	15	14	14
-5	13	6	6
-4	14	30	31
-3	9	47	46
-3	15	32	32
-2	7	35	34
-2	10	4	5
-1	5	17	16
-1	8	48	48
-1	11	18	18
0	3	16	15
0	6	23	23
0	9	12	12
0	12	4	4
1	7	13	13
1	10	7	7
2	8	5	5
2	11	26	27
3	9	31	32
3	12	10	10
4	10	43	42

L = -2

H	K	FO	FC
-7	16	22	22
-5	12	29	30
-5	15	10	10
-4	10	12	12
-4	13	8	7
-4	16	8	8
-3	8	16	15
-2	6	13	13
-2	12	31	31
-2	15	9	9
-1	4	11	13
-1	7	10	10
-1	10	122	119
0	2	21	23
0	5	40	41
0	8	5	5
0	11	32	34
0	14	25	25
1	9	18	18
2	7	37	38
2	10	3	4
2	13	12	12
3	8	11	11
3	11	8	8
4	9	7	7

4	12	71	69

L = -1

H	K	FO	FC
-6	13	45	46
-6	16	4	4
-5	11	32	32
-5	14	12	13
-4	9	4	3
-4	12	37	38
-4	15	9	10
-3	10	10	10
-3	13	6	6
-2	5	56	56
-2	8	18	18
-2	11	4	5
-2	14	9	9
-1	3	41	43
-1	6	15	15
-1	9	3	2
-1	15	30	30
0	1	22	21
0	7	23	24
0	10	7	6
0	13	30	30
1	5	15	16
1	8	42	43
1	11	3	1
1	14	37	37
2	6	34	33
2	9	8	9
2	12	9	9
3	7	53	54
3	10	7	8
4	8	8	8
4	11	6	6
6	10	20	19

L = 0

H	K	FO	FC
-8	16	15	15
-7	14	7	7
-6	12	23	23
-6	15	5	5
-5	10	8	8
-5	13	13	13
-5	16	29	28
-4	8	21	21
-4	11	7	7
-4	14	92	90
-3	9	41	41
-3	12	9	9
-3	15	28	29
-2	4	29	29
-2	7	169	174
-2	13	8	8
-1	2	45	44
-1	5	3	5
-1	8	42	43

-1	11	24	25
-1	14	10	10
0	3	26	27
0	6	25	26
0	9	7	7
0	12	9	9
1	4	36	36
1	7	17	17
1	10	5	3
1	13	7	7
2	5	18	17
2	8	12	13
2	11	21	21
3	6	24	23
3	9	109	108
3	12	5	4
4	10	36	36
5	8	23	24
5	11	5	5

L = 1

H	K	FO	FC
-8	15	30	30
-7	16	23	23
-6	11	12	12
-5	9	37	36
-5	12	6	6
-4	7	19	19
-4	10	7	7
-4	16	4	5
-3	5	10	10
-3	8	9	8
-3	11	21	21
-3	14	8	8
-2	3	7	6
-2	6	6	5
-2	9	5	4
-2	12	42	42
-2	15	4	4
-1	4	44	47
-1	7	19	19
-1	10	32	32
-1	13	14	15
0	2	37	40
0	5	57	58
0	8	5	5
0	11	42	43
1	3	53	47
1	6	7	7
1	9	21	22
2	4	61	62
2	7	3	3
2	10	5	5
2	13	4	4
3	5	8	8
3	8	6	6
3	11	5	4
4	6	11	12
4	9	13	13

4	12	29	29
5	7	28	29
5	10	5	5
6	8	7	7

L = 2

H	K	FO	FC
-9	16	24	24
-7	12	18	18
-6	10	14	14
-6	13	31	32
-6	16	8	8
-5	8	20	19
-5	11	124	119
-5	14	5	5
-4	6	41	40
-4	9	3	3
-4	12	32	32
-4	15	11	11
-3	4	163	208
-3	7	8	7
-3	10	9	10
-3	13	3	3
-2	5	42	43
-2	8	17	17
-2	11	24	24
-1	0	20	22
-1	3	18	19
-1	6	12	12
-1	9	12	12
-1	12	20	21
0	4	39	40
0	7	12	12
0	10	19	19
0	13	84	81
1	2	35	35
1	5	13	11
1	8	24	24
1	11	5	5
2	3	45	44
2	6	162	149
2	12	14	14
3	4	11	12
3	7	42	43
3	10	14	15
4	5	31	30
4	11	6	6
5	6	11	11
5	9	5	4
6	7	17	17
6	10	9	8
7	8	85	82

L = 3

H	K	FO	FC
-9	15	15	15
-8	13	16	17
-7	11	6	6
-7	14	6	6

-6	12	11	11
-6	15	13	13
-5	13	4	4
-4	5	26	26
-4	8	33	34
-4	11	17	17
-4	14	30	31
-3	6	15	15
-3	9	50	50
-3	15	27	27
-2	1	49	49
-2	4	28	28
-2	7	35	34
-2	10	15	15
-2	13	10	10
-1	5	16	17
-1	8	42	42
-1	11	3	3
-1	-1	52	51
0	0	58	50
0	3	9	9
0	6	30	31
0	9	7	6
1	4	6	6
1	7	7	6
1	10	12	12
1	13	13	14
2	5	12	12
2	8	3	3
2	11	31	30
3	3	24	24
3	6	25	25
3	9	33	33
3	12	11	11

L = 4

H	K	FO	FC
-9	14	20	21
-8	12	8	8
-8	15	78	75
-7	10	28	29
-7	13	3	3
-6	8	140	131
-5	6	9	8
-5	9	28	28
-5	15	25	25
-4	7	3	2
-4	10	7	7
-4	13	5	5
-3	2	26	26
-3	5	5	4
-3	8	40	40

-3	11	12	12
-3	14	10	11
-2	0	5	2
-2	6	23	23
-2	9	23	23
-2	12	20	20
-1	4	27	28
-1	7	32	32
-1	10	108	106
-1	13	6	6
-1	-2	8	8
0	5	18	18
0	11	33	33
0	-1	48	48
1	3	185	170
1	9	15	15
2	4	42	41
2	7	7	6
2	10	18	18
3	2	24	24
3	5	3	0
3	8	9	9
3	11	22	23
4	3	27	26
4	6	6	6
4	9	26	26
5	4	17	16
5	7	5	5
5	10	5	4
6	5	112	106
7	6	32	33
8	7	7	7

L = 5

H	K	FO	FC
-9	13	6	6
-8	11	3	4
-8	14	6	5
-7	9	22	23
-7	12	19	19
-7	15	11	12
-6	7	5	5
-6	13	38	38
-5	8	22	22
-5	11	33	34
-5	14	17	16
-4	3	25	25
-4	6	44	43
-4	9	5	4
-4	12	21	21
-3	1	23	22
-3	7	17	17
-3	10	13	14
-2	5	28	28
-2	8	11	11
-2	11	9	10
-2	14	8	8
-2	-1	27	26
-1	0	13	13

-1	6	3	2	0	6	8	9	4	9	22	22	-5	4	4	4	-1	-3	35	36
-1	9	5	4	0	-3	33	33	5	7	16	16	-4	2	13	14	0	-2	4	5
-1	12	8	8	1	4	3	3	6	2	27	27	-4	8	11	12				
-1	-3	39	37	1	7	30	30	6	5	33	34	-3	0	15	16				
0	4	21	21	1	10	8	8	7	3	4	4	-3	9	21	21				
0	7	19	20	2	5	18	18	7	6	23	22	-2	1	11	11				
0	10	22	22	2	8	24	24	8	4	25	25	-2	7	36	36				
0	13	29	31	2	11	7	7					-2	10	15	14				
0	-2	24	24	3	3	16	15		L =	8		-2	-5	4	5				
1	5	3	3	3	6	36	36	H	K	FO	FC	-2	-2	22	22				
1	8	32	32	3	9	83	79	-9	10	9	8	-1	8	9	9				
1	11	6	6	4	10	27	27	-8	11	8	7	-1	-7	18	18				
2	3	33	32	5	2	125	115	-7	6	9	9	-1	-4	23	23				
2	6	36	36	5	5	4	4	-7	9	39	39	-1	-1	15	15				
2	9	12	12	5	8	14	14	-7	12	14	14	0	0	38	40				
2	12	14	14	6	3	30	30	-6	10	23	23	0	6	14	14				
3	4	6	6	7	4	7	7	-5	2	38	38	0	9	4	4				
3	7	34	34	7	7	4	3	-5	8	20	20	0	-3	14	14				
3	10	10	10	8	5	5	5	-5	11	75	71	1	7	12	12				
4	2	7	7					-4	0	35	36	2	5	10	10				
4	5	32	31		L =	7		-4	3	10	10	2	8	7	6				
5	3	15	15	H	K	FO	FC	-4	9	7	6	3	6	25	24				
5	9	7	7	-8	9	19	20	-4	12	18	18	4	4	11	11				
6	4	11	11	-8	12	14	14	-3	1	26	27	5	5	6	6				
6	7	5	5	-7	10	33	32	-3	7	5	5	5	-4	4	3				
7	5	23	23	-6	5	18	18	-3	-2	20	20	6	3	13	14				
7	8	30	30	-6	8	36	36	-2	8	9	9								
8	6	8	8	-6	11	18	17	-2	11	28	29		L =	10					
				-5	3	27	27	-2	-4	7	6	H	K	FO	FC				
	L =	6		-5	9	10	10	-2	-1	3	3	-8	6	35	34				
H	K	FO	FC	-5	12	13	12	-1	0	7	7	-7	4	22	22				
-10	14	19	19	-4	1	39	38	-1	9	8	9	-6	2	17	18				
-9	12	84	80	-4	7	11	11	-1	-6	17	17	-6	5	17	16				
-8	10	5	4	-3	2	12	12	-1	-3	106	101	-5	0	5	4				
-8	13	16	16	-3	8	18	19	0	7	15	15	-4	1	75	75				
-7	8	3	3	-3	11	12	12	0	10	24	24	-4	-2	16	15				
-7	14	7	8	-3	-1	20	20	0	-5	22	23	-3	2	12	12				
-6	9	5	5	-2	0	12	12	0	-2	17	17	-3	8	32	32				
-6	12	35	35	-2	6	10	10	1	5	20	20	-3	-4	4	4				
-5	4	10	10	-2	9	5	5	1	8	4	1	-3	-1	16	16				
-5	7	5	5	-2	12	27	27	2	6	87	84	-2	0	13	13				
-5	10	10	10	-2	-3	15	15	3	4	7	8	-2	-6	65	64				
-5	13	26	27	-1	7	25	26	3	7	24	24	-2	-3	12	12				
-4	2	3	2	-1	10	33	34	4	5	9	9	-1	7	25	25				
-4	8	22	21	-1	-5	10	10	5	3	7	7	-1	-5	11	12				
-4	11	18	18	-1	-2	10	11	5	6	18	18	-1	-2	5	5				
-4	14	69	67	0	5	25	26	6	4	9	9	0	-7	16	16				
-3	6	18	18	0	11	19	19	7	2	10	11	0	-4	8	9				
-3	9	15	15	0	-4	18	19	7	5	34	33	0	-1	30	30				
-2	1	30	29	0	-1	26	26	8	3	11	11	3	5	8	8				
-2	7	123	115	1	6	13	13												
-2	10	4	4	1	9	17	17		L =	9			L =	11					
-2	13	8	7	2	4	23	23	H	K	FO	FC	H	K	FO	FC				
-2	-2	36	36	2	7	16	16	-8	7	22	22	-5	2	21	21				
-1	5	11	11	2	10	4	5	-8	10	6	6	-4	0	15	15				
-1	8	29	29	3	5	8	7	-7	5	36	36	-4	3	4	5				
-1	-4	47	46	3	8	5	5	-6	3	10	10	-3	1	13	13				
-1	-1	5	5	4	3	10	10	-6	9	15	15	-2	-1	7	7				
0	0	165	144	4	6	11	11	-5	1	19	20	-1	0	16	17				

APPENDIX C. CALCULATED AND OBSERVED STRUCTURE FACTOR AMPLITUDES FOR $Sc_7Cl_{12}N$

L =-12

H	K	FO	FC
0	0	44	45
0	3	19	17
2	2	18	17

L =-11

H	K	FO	FC
-6	-1	11	13
-5	-3	17	18
-2	-6	30	29
-2	-3	21	19
-1	-2	14	12
0	-7	6	7
1	0	16	17
1	3	33	32
2	4	9	11
3	5	13	13
4	0	15	14
4	3	13	15
6	2	16	18

L =-10

H	K	FO	FC
-6	-2	32	31
-5	-4	13	14
-5	-1	13	14
-4	-6	9	12
-4	-3	21	20
-2	-7	11	12
-2	-4	13	13
-2	-1	8	9
-1	-3	66	64
0	1	30	28
0	4	8	10
0	7	15	15
1	5	10	11
2	0	13	12
2	3	12	13
2	6	52	54
3	1	12	13
4	2	13	13
5	3	31	29
6	1	23	22
7	2	22	21

L = -9

H	K	FO	FC
-10	-1	19	20
-7	-4	7	9
-7	-1	17	19
-6	-6	15	16
-6	-3	12	13
-5	-2	35	34
-4	-7	8	8
-4	-4	7	10
-3	-9	29	28
-3	-6	25	24
-3	-3	9	11

-2	-8	10	9
-2	-5	8	8
-2	-2	12	13
-1	-7	12	11
-1	-4	20	19
-1	-1	9	10
0	0	40	38
0	3	15	14
0	9	9	9
1	1	12	12
1	4	24	24
1	7	17	18
2	2	22	21
3	0	15	15
3	6	14	15
3	9	24	26
4	4	10	11
5	2	35	34
6	0	12	12
6	3	19	19
6	6	14	15
7	1	8	9
7	4	16	16
8	2	13	14
10	1	15	16

L = -8

H	K	FO	FC
-10	-2	15	15
-9	-4	8	8
-9	-1	64	64
-8	-3	9	10
-7	-5	32	31
-7	-2	11	11
-6	-7	18	18
-6	-4	6	7
-6	-1	9	10
-5	-6	16	17
-4	-5	7	8
-3	-10	6	6
-3	-7	20	19
-3	-1	10	10
-2	-6	73	74
-2	-3	39	36
-1	-5	20	19
-1	-2	26	25
0	2	15	15
0	5	20	19
0	8	7	8
0	11	9	10
1	0	8	8
1	3	94	90
1	6	15	16
2	7	37	37
3	2	16	16
3	5	18	18
3	8	8	9

4	0	37	34
4	3	6	5
4	6	22	22
4	9	9	10
5	4	6	7
5	7	9	11
6	2	10	11
6	5	64	63
7	0	13	13
7	6	7	8
8	1	6	7
8	4	12	13
9	2	28	27
10	0	22	21
11	1	26	25

L = -7

H	K	FO	FC
-11	-1	6	8
-9	-2	16	15
-8	-4	24	23
-7	-6	22	22
-6	-8	5	5
-6	-5	33	33
-6	-2	29	28
-5	-7	16	16
-5	-1	17	17
-4	-9	22	21
-4	-6	11	11
-4	-3	9	10
-3	-11	13	12
-3	-5	8	7
-3	-2	23	24
-2	-7	16	16
-2	-4	21	22
-2	-1	11	10
-1	-9	13	16
-1	-6	13	13
-1	-3	35	38
0	1	29	28
0	4	20	19
0	10	9	9
0	13	24	25
1	2	10	10
1	5	9	10
1	8	18	19
2	0	8	8
2	3	16	15
2	6	35	35
2	9	7	8
3	7	31	31
3	10	16	17
4	2	9	9
4	5	8	9
4	8	11	12
5	0	25	24
5	3	20	20
5	6	18	17

5	9	6	6
6	1	25	26
6	4	8	8
6	7	11	12
6	10	25	26
7	3	11	11
7	6	31	33
7	9	19	18
8	2	27	26
8	5	14	14
8	8	12	13
9	1	10	10
9	4	22	21
10	2	16	16
10	5	6	7
11	3	13	13

L = -6

H	K	FO	FC
-12	-3	13	14
-10	-4	63	61
-10	-1	37	36
-9	-3	12	12
-8	-5	7	6
-8	-2	10	11
-7	-4	9	8
-7	-1	17	17
-6	-9	8	8
-6	-3	26	27
-5	-8	13	13
-5	-5	5	4
-5	-2	101	105
-4	-10	25	24
-4	-1	9	10
-3	-9	75	71
-3	-6	33	35
-3	-3	16	15
-2	-11	7	7
-2	-8	25	24
-2	-5	16	16
-1	-13	15	15
-1	-10	8	7
-1	-7	28	29
-1	-4	5	5
-1	-1	28	27
0	0	138	131
0	3	33	32
0	6	14	13
0	9	8	9
0	12	12	13
1	1	5	5
1	4	44	46
1	10	16	16
1	13	6	7
2	2	33	34
2	8	6	6
2	11	15	15
3	3	18	18
3	6	7	7
3	9	74	73
4	1	10	10
4	4	18	19
4	10	17	17

5	2	101	104
5	5	8	8
5	8	12	12
6	0	9	9
6	3	15	14
6	6	35	34
7	1	25	26
7	4	13	15
7	7	9	10
8	5	27	26
9	6	7	6
10	4	57	60
11	2	8	8
12	3	18	18
13	1	18	18

L = -5

H	K	FO	FC
-12	-1	9	10
-11	-3	6	5
-10	-5	10	10
-10	-2	30	29
-9	-7	21	21
-9	-4	34	33
-8	-6	11	11
-8	-3	12	13
-7	-8	30	29
-7	-5	25	24
-7	-2	11	11
-6	-10	17	18
-6	-7	9	8
-6	-4	7	8
-6	-1	7	7
-5	-9	9	7
-4	-8	32	30
-4	-2	7	6
-3	-10	9	10
-3	-7	37	34
-3	-1	23	21
-2	-12	13	13
-2	-9	14	13
-2	-6	36	36
-2	-3	34	34
-1	-11	8	7
-1	-8	34	32
-1	-2	23	23
0	2	23	22
0	5	37	34
0	11	37	36
0	14	14	14
1	0	14	12
1	3	37	38
2	1	24	23
2	4	40	42
2	7	25	24
2	10	15	15
3	2	28	27
3	5	21	21

3	8	4	5
4	0	23	23
4	3	18	17
4	9	7	5
4	12	25	24
5	7	19	19
6	2	11	11
6	5	34	33
6	8	7	7
7	0	20	19
7	3	12	13
7	6	39	38
7	9	10	10
8	4	21	20
8	7	7	9
9	2	9	10
9	5	18	18
10	0	22	21
11	1	11	12
11	4	6	7
13	0	32	30

L = -4

H	K	FO	FC
-14	-1	18	19
-13	-3	10	10
-12	-2	7	8
-11	-4	27	26
-10	-6	12	12
-8	-7	9	9
-8	-4	24	23
-8	-1	10	10
-7	-6	34	31
-7	-3	7	5
-6	-11	13	12
-6	-5	105	98
-6	-2	44	43
-5	-10	7	5
-5	-7	6	6
-4	-9	25	23
-4	-6	5	6
-4	-3	25	24
-3	-11	22	22
-3	-8	6	8
-3	-2	23	24
-2	-10	17	17
-2	-4	41	40
-2	-1	24	25
-1	-9	15	15
-1	-3	151	155
0	1	46	47
0	7	7	8
0	10	5	4
0	13	71	69
1	2	6	6
1	5	9	9

1	8	29	28
1	14	20	21
2	6	118	121
2	12	6	7
3	1	27	28
3	7	29	29
3	10	32	32
4	2	20	21
4	5	25	25
4	8	5	5
4	11	13	13
5	0	19	19
5	3	40	40
5	9	19	20
6	1	30	30
6	4	7	8
6	10	9	10
7	2	23	23
7	8	69	69
8	3	11	11
8	9	20	21
9	1	99	97
9	7	16	18
10	2	20	20
10	5	23	23
11	0	32	31
11	3	8	7
12	1	7	7
12	4	22	23

L = -3

H	K	FO	FC
-13	-1	8	9
-12	-3	33	32
-11	-5	35	33
-10	-4	31	30
-10	-1	20	19
-9	-6	14	15
-8	-8	15	14
-8	-5	6	6
-8	-2	8	7
-7	-10	7	7
-7	-7	5	3
-7	-1	50	48
-6	-9	8	9
-6	-6	7	7
-6	-3	50	47
-5	-8	26	24
-5	-5	8	7
-5	-2	34	35
-4	-10	41	39
-4	-7	6	3
-4	-4	33	32
-4	-1	12	11
-3	-12	15	15
-3	-9	34	33
-3	-6	26	26
-3	-3	22	22
-2	-14	7	8

H	K	FO	FC
-2	-11	33	32
-2	-8	5	6
-2	-5	11	12
-1	-13	12	12
-1	-10	12	12
-1	-7	7	7
-1	-4	5	5
-1	-1	47	47
0	0	50	51
0	3	15	16
0	6	21	20
0	9	10	10
1	1	47	48
1	4	28	30
1	7	13	14
2	2	28	30
2	11	27	28
3	0	11	9
3	3	11	11
3	9	31	32
3	12	11	13
4	1	14	14
4	4	34	34
4	10	43	43
5	2	33	33
5	8	15	15
6	0	30	29
6	3	51	51
6	6	11	12
6	9	15	16
7	1	42	42
7	4	14	15
8	2	17	18
8	5	5	6
9	6	11	13
10	4	30	31
10	7	7	7
11	2	7	9
11	5	35	37
12	3	27	27
15	0	11	10

L = -2

H	K	FO	FC
-13	-2	7	7
-10	-5	9	10
-10	-2	33	31
-9	-7	21	20
-9	-4	7	7
-9	-1	120	111
-8	-9	31	29
-7	-8	82	75
-7	-5	29	27
-6	-10	8	9
-6	-7	16	15
-6	-4	10	10
-6	-1	6	6
-5	-12	10	11
-5	-6	8	9
-5	-3	14	13
-4	-8	5	3
-4	-5	30	30
-4	-2	12	11
-3	-10	12	12
-3	-7	44	43
-3	-4	11	11
-3	-1	13	15
-2	-12	12	12
-2	-6	140	138
-2	-3	42	42
-1	-14	30	29
-1	-8	26	25
-1	-5	12	11
-1	-2	33	33
0	2	23	25
0	5	41	43
0	11	34	33
0	14	23	23
1	0	19	18
1	3	171	186
1	6	13	13
1	9	16	16
1	15	8	11
2	1	19	21
2	4	41	42
2	7	37	37
2	13	9	11
3	2	41	43
3	5	17	16
3	8	12	12
4	0	39	38
4	3	5	4
4	6	13	13
4	12	65	64
5	1	10	10
5	7	17	18
6	2	14	14
6	5	111	110
6	11	13	13
7	0	12	13
7	3	9	10
7	6	32	32
7	9	22	22
8	1	10	11
8	4	30	30
9	2	23	23
9	8	18	18
10	0	16	16
11	1	20	20
11	4	9	9
13	0	79	75
14	1	19	19

L = -1

H	K	FO	FC
-14	-1	31	32
-12	-5	5	5
-12	-2	9	9
-11	-7	26	26
-11	-4	8	9
-9	-5	16	16
-8	-4	40	38
-7	-6	51	48
-7	-3	7	7
-6	-11	14	14
-6	-8	9	10
-6	-5	34	33
-6	-2	20	20
-5	-10	6	6
-5	-7	31	30
-5	-1	15	15
-4	-12	30	28
-4	-9	13	12
-4	-6	10	10
-3	-14	22	23
-3	-11	7	6
-3	-8	4	5
-3	-5	6	7
-2	-10	5	6
-2	-4	63	63
-2	-1	40	39
-1	-9	20	20
-1	-6	10	10
-1	-3	50	49
0	1	24	24
0	7	22	22
0	13	30	30
1	2	7	8
1	5	13	12
1	8	45	45
1	14	36	38
2	0	36	36
2	3	10	11
2	6	31	34
2	9	12	12
3	1	45	46
3	4	16	16
3	7	56	56
3	10	8	7
3	13	9	11
4	2	4	4
4	5	35	36
5	0	58	58
5	3	9	10
5	6	14	15
6	1	18	19
6	10	19	20
7	8	29	30
7	11	11	12
8	3	20	21
8	9	41	41
9	1	32	33
9	7	22	23
10	2	44	45
10	8	16	18
11	0	46	45
11	3	6	6
12	1	18	19
14	3	25	26

L = 0

H	K	FO	FC
-11	7	4	3
-4	-1	4	6
0	-9	4	5
1	1	44	46
1	4	34	34
1	7	16	16
2	2	26	26
2	5	17	16
2	8	11	11
2	11	21	21
3	0	25	24
3	6	20	20
3	9	105	101
3	12	7	7
4	4	22	23
4	10	36	35
4	13	14	15
5	2	155	159
5	5	5	6
5	8	22	22
5	11	7	8
6	0	25	26
6	3	42	43
6	6	21	21
6	-15	5	5
7	1	43	44
7	7	6	7
7	10	8	10
8	5	12	12
8	8	11	12
9	3	7	8
10	1	23	22
10	4	86	83
11	2	7	7
11	5	28	28
12	0	9	9
12	3	27	27
13	1	9	10
13	4	10	12
15	0	12	13

L = 1

H	K	FO	FC
-12	14	5	7
-5	12	5	6
0	-10	5	5
10	-6	5	6
16	-12	6	5

L = 2

H	K	FO	FC
-5	14	5	7
1	-13	5	5

L = 3

H	K	FO	FC
14	-7	5	6

L = 4

H	K	FO	FC
17	-11	5	5

L = 6

H	K	FO	FC
8	-16	20	23

L = 7

H	K	FO	FC
0	-7	6	5

L = 8

H	K	FO	FC
6	-2	4	5

L = 10

H	K	FO	FC
-8	3	7	8
3	-1	4	4
5	-5	5	4
9	-4	5	7
9	-1	10	11

L = 11

H	K	FO	FC
2	-6	5	8
6	-5	6	7

L = 12

H	K	FO	FC
1	-2	8	9
2	-4	10	10
2	-1	8	7
3	-3	6	7

APPENDIX D. CALCULATED AND OBSERVED STRUCTURE FACTOR AMPLITUDES (x10) FOR Sc_4Cl_6B

L = 0

H	K	FO	FC
-13	-4	85	114
-12	-7	118	118
-6	-14	123	134
-2	-11	77	89
0	2	367	383
0	4	450	465
0	6	473	474
0	8	298	299
0	10	324	327
0	12	718	694
0	14	218	210
1	1	950	928
1	2	102	111
1	3	337	349
1	4	419	415
1	5	424	432
1	6	261	274
1	7	166	180
1	8	286	293
1	9	243	243
1	10	178	177
1	11	241	246
1	12	517	492
1	13	165	177
1	15	160	156
1	16	162	158
1	17	325	294
2	0	353	360
2	1	229	237
2	2	387	396
2	3	559	566
2	4	609	605
2	5	705	719
2	6	410	412
2	7	155	164
2	8	782	790
2	9	815	800
2	10	139	153
2	13	193	191
3	1	458	466
3	2	107	126
3	3	730	715
3	4	1489	1481
3	6	250	258
3	8	827	805
3	10	235	245
3	11	119	128
3	12	182	189
3	13	248	246
3	14	135	160
3	15	110	110
3	16	157	162
4	0	280	255
4	1	332	325
4	2	429	431
4	3	457	448
4	4	942	929
4	6	206	212
4	7	77	91
4	8	207	207
4	9	122	128
4	14	352	330
4	15	154	180
4	16	440	413
5	1	716	714
5	2	284	288
5	3	205	214
5	4	978	962
5	5	586	578
5	6	142	148
5	7	251	247
5	8	377	381
5	10	162	175
5	11	101	109
5	13	524	498
5	16	103	134
6	0	679	681
6	1	211	219
6	2	430	428
6	3	85	107
6	4	527	525
6	5	784	772
6	6	141	137
6	7	549	542
6	8	711	704
6	9	155	164
6	10	199	189
6	12	208	207
6	13	222	225
7	1	211	225
7	5	254	254
7	7	278	280
7	8	211	216
7	9	115	119
7	10	294	291
7	11	125	157
7	12	447	431
7	13	172	185
7	15	117	142
8	0	1275	1268
8	1	700	696
8	3	153	155
8	4	323	322
8	5	359	359
8	7	141	141
8	8	108	136
8	9	231	249
8	10	248	253
8	11	263	267
8	12	370	370
8	13	157	181
8	14	196	191
9	1	423	414
9	2	376	374
9	3	390	397
9	4	357	361
9	6	156	161
9	10	153	164
9	11	240	254
9	12	195	196
10	1	176	174
10	3	275	285
10	5	128	136
10	6	229	230
10	7	245	244
10	8	139	147
10	9	610	588
10	10	125	124
10	11	144	142
10	12	102	111
11	2	83	122
11	3	432	421
11	4	479	474
11	5	320	311
11	6	218	220
11	7	340	319
11	8	476	467
12	1	262	273
12	2	127	142
12	3	351	360
12	4	155	171
12	6	183	188
12	8	178	170
12	9	112	128
13	1	247	251
13	2	244	245
13	5	355	342
14	0	332	321
14	1	214	207
14	2	117	119
14	3	333	313
14	5	274	269
14	6	296	287
14	7	254	258
14	8	162	160
14	9	135	134
15	2	101	111
15	7	131	147
16	0	114	104
16	1	320	325
16	3	142	134
16	4	149	151

L = 1

H	K	FO	FC
-6	-9	80	109
-5	-16	181	174
-3	-11	80	66
-2	-7	82	96
-1	-13	112	118
0	0	474	481
0	2	578	592
0	4	546	551
0	6	1827	1818
0	8	120	115
0	12	381	372
1	3	460	464
1	4	67	71
1	5	506	506
1	6	549	543
1	7	466	461
1	10	315	308
1	11	422	408
1	12	184	196
1	14	231	233
1	16	124	146
2	0	588	589
2	1	617	612
2	2	1092	1055
2	3	987	961
2	4	292	291
2	5	267	269
2	6	101	116
2	8	170	177
2	11	324	323
2	12	149	163
2	14	392	380
2	15	431	412
3	1	94	105
3	2	1563	1534
3	3	464	454
3	4	198	194
3	5	66	71
3	6	145	157
3	7	425	417
3	8	113	124
3	9	330	325
3	10	582	572
3	12	202	215
3	13	92	96
3	14	215	225
3	15	121	138
3	16	206	190
4	0	424	421
4	2	299	299
4	3	285	280
4	5	170	175
4	6	100	116
4	7	124	153
4	8	470	460
4	9	292	307
4	10	739	718
4	14	225	224
5	1	465	469
5	2	923	908
5	3	130	154
5	5	150	153
5	7	750	726
5	8	205	217
5	9	103	113
5	10	440	436
5	11	355	356
5	13	114	139
6	0	155	168
6	1	916	911
6	2	802	800
6	4	348	342
6	5	214	209
6	6	445	445
6	8	246	258
6	10	107	137
6	11	280	276
6	13	121	143
6	14	385	380
6	15	134	141
7	2	202	203
7	3	104	106
7	4	162	177
7	6	400	391
7	7	295	303
7	9	130	135
7	11	259	263
7	13	220	234
8	1	243	252
8	2	293	295
8	3	253	257
8	4	291	284
8	5	540	530
8	6	884	858
8	7	441	435
8	8	158	160
8	10	110	122
8	11	314	302
8	12	106	128
9	2	106	119
9	3	347	345
9	4	327	329
9	5	375	375
9	6	182	191
9	7	221	234
9	8	149	152
9	9	158	166
9	10	413	397
9	11	132	139
9	12	160	167
10	0	242	248
10	2	111	126
10	3	585	584
10	5	204	215
10	11	125	144
10	12	154	164
10	13	234	226
11	1	428	413
11	2	591	573
11	3	326	325
11	4	121	136
11	9	224	235
11	10	220	218
11	12	232	229
12	0	301	293
12	3	229	230
12	4	191	188
12	5	207	212
12	7	155	175
12	9	331	342
12	10	188	190
13	1	241	244
13	7	329	322
13	8	278	279
14	0	354	351
14	1	346	346
14	2	131	146
14	3	248	250
14	5	209	217
14	6	285	281
14	8	96	107
15	5	161	166
16	0	207	194
16	1	112	117

L = 2

H	K	FO	FC
-12	-2	97	121
-10	-11	96	122
-4	0	89	117
-4	-9	89	102
0	0	2083	2116
0	2	211	217
0	4	335	337
0	6	344	342
0	8	239	237
0	10	270	263
0	12	597	583
0	14	177	183
1	1	559	542
1	3	240	241
1	4	235	245
1	5	309	306
1	6	193	199
1	7	118	135
1	8	231	220
1	9	202	192
1	10	132	143
1	11	207	206
1	12	410	415
1	13	132	153
1	15	136	133
2	0	206	210
2	1	130	146
2	2	235	234
2	3	380	373
2	4	400	390
2	5	529	510
2	6	298	302
2	7	99	121
2	8	645	628
2	9	671	635
2	10	110	126
2	13	154	165
3	1	319	317
3	3	491	474
3	4	1064	1024
3	6	173	188
3	8	652	631
3	10	189	198
3	11	107	106
3	12	153	160
3	13	204	209
3	14	143	138
4	1	190	205
4	2	297	293
4	3	313	313
4	4	695	661
4	6	136	159
4	8	153	168
4	14	282	286
4	15	147	156
5	1	527	508
5	2	210	205
5	3	140	151
5	4	741	714
5	5	454	439
5	6	96	111
5	7	191	198
5	8	296	305
5	10	132	144
5	13	436	428
6	0	499	500
6	1	146	160
6	2	324	315
6	4	409	402
6	5	618	592
6	6	101	104
6	7	446	437
6	8	599	579
6	9	116	131
6	10	143	158
6	12	171	178
6	13	170	193
7	1	165	169
7	5	192	205
7	7	220	227
7	8	171	174
7	10	257	247
7	11	121	134
7	12	384	368
7	13	138	160
8	0	1025	995
8	1	564	550
8	3	109	118
8	4	251	253
8	5	287	291
8	9	196	212
8	10	214	214
8	11	213	227
8	12	297	318
8	13	123	156
9	1	328	331
9	2	296	298
9	3	333	322
9	4	301	300

9	6	125	133
9	9	94	99
9	10	130	139
9	11	210	219
9	12	151	170
10	1	141	139
10	3	236	237
10	5	117	112
10	6	182	193
10	7	199	206
10	8	105	123
10	9	509	502
11	3	353	354
11	4	397	401
11	5	266	263
11	6	171	186
11	7	285	272
11	8	404	401
12	1	217	230
12	3	300	306
12	4	119	146
12	6	181	161
12	8	120	146
12	9	137	113
13	1	216	215
13	2	211	212
13	4	97	95
13	5	300	294
13	6	113	93
14	0	275	277
14	1	176	180
14	3	275	267
14	5	221	232
14	6	258	250

L = 3

H	K	FO	FC
-12	-5	131	148
-9	-6	125	137
-9	-2	88	87
-8	-8	85	117
-4	-6	104	98
-3	-6	93	108
-3	-4	84	110
-2	-6	80	79
0	0	221	231
0	2	302	311
0	4	297	300
0	6	1143	1104
0	12	277	269
1	3	235	248
1	5	303	294
1	6	329	332
1	7	288	284
1	10	217	219
1	11	294	290
1	12	148	145
2	0	299	300
2	1	326	320
2	2	556	544
2	3	541	524
2	4	158	164
2	5	143	152
2	8	105	115
2	11	221	232
3	2	872	836
3	3	257	252
3	7	270	261
3	9	226	225
3	10	418	406
3	12	148	155
4	0	221	226
4	2	165	163
4	3	146	160
4	5	118	113
4	8	312	310
4	9	208	214
4	10	523	509
5	1	291	278
5	2	559	540
5	5	88	89
5	7	496	483
5	8	126	148
5	10	316	312
5	11	257	264
6	1	568	556
6	2	525	503
6	4	229	217
6	5	110	133
6	6	307	300
6	8	175	177
6	11	202	203
7	2	108	115
7	4	113	118
7	6	272	269
7	7	199	212
7	11	190	192
8	1	155	164
8	2	190	196
8	3	156	173
8	4	193	190
8	5	375	368
8	6	635	604
8	7	313	309
8	11	207	221
9	3	238	238
9	4	226	228
9	5	275	268
9	7	155	173
9	8	111	113
9	9	106	121
9	10	289	289
10	0	158	174
10	3	430	413
10	5	126	152
11	1	308	298
11	2	421	415
11	3	241	237
12	0	224	213
12	3	188	172
12	4	145	140
13	1	166	180

L = 4

H	K	FO	FC
-5	-8	184	190
-5	-2	119	113
-3	-6	133	106
-2	0	129	117
-1	-6	120	112
0	0	1085	1072
0	4	151	172
0	6	192	192
0	8	135	145
0	10	144	158
0	-2	104	113
1	1	272	272
1	3	128	120
1	4	148	147
1	5	148	165
1	8	118	132
1	9	97	115
2	3	203	198
2	4	206	218
2	5	287	278
2	6	156	173
2	8	371	377
2	9	404	394
3	1	153	161
3	3	260	257
3	4	584	570
3	8	404	385
3	10	110	128
4	1	91	115
4	2	134	160
4	3	157	172
4	4	376	368
4	8	90	101
5	1	276	275
5	4	426	412
5	5	240	261
5	7	104	122
6	0	284	289
6	2	164	177
6	4	236	238
6	5	373	352
6	7	260	268
6	8	368	358
7	7	116	144
8	0	614	600
8	1	335	329
8	4	154	157
8	5	172	177
9	1	189	210
9	2	167	185
9	3	190	199
9	4	165	183

L = 5

H	K	FO	FC
0	0	105	113
0	2	125	165
2	0	124	152
2	1	129	169

APPENDIX E. CALCULATED AND OBSERVED STRUCTURE FACTOR AMPLITUDES (x10) FOR Sc_4Cl_6N (1)

L = -4

H	K	FO	FC
-4	2	97	118
-2	2	88	99
0	-2	44	73

L = -3

H	K	FO	FC
-8	2	119	129
-7	4	76	97
-4	5	82	90
-3	6	56	80
-2	0	234	227
-2	1	303	291
-2	10	64	101
4	-7	71	86

L = -2

H	K	FO	FC
-11	1	93	108
-10	2	44	25
-9	6	107	94
-8	6	61	73
-8	7	82	91
-8	8	59	95
-4	0	214	199
-4	1	158	161
-2	0	126	139
-2	1	149	146
-2	12	72	17

L = -1

H	K	FO	FC
-11	4	70	106
-7	12	92	121
-2	7	56	54
3	-1	75	60
4	-12	61	46
6	-12	69	101
10	-8	43	69
11	-8	40	75

L = 0

H	K	FO	FC
-12	2	55	63
-7	4	59	47
-5	9	59	64
0	2	285	287
0	4	423	438
0	6	436	421
0	8	309	300
0	10	396	386
0	12	967	814
0	14	290	297
1	1	879	931
1	2	103	112
1	3	302	293
1	4	397	395
1	5	422	406
1	6	284	292
1	7	175	192
1	8	186	176
1	9	299	296
1	10	216	194
1	11	227	205
1	12	394	457
1	13	205	215
2	0	224	268
2	1	222	241
2	2	448	332
2	3	548	552
2	4	744	727
2	5	781	780
2	6	392	366
2	7	147	150
2	8	808	817
2	9	780	780
2	10	174	156
2	13	152	163
2	-14	58	57
3	1	393	418
3	2	96	78
3	3	678	662
3	4	1413	1474
3	5	77	14
3	6	305	314
3	8	836	851
3	10	300	302
3	11	169	169
3	12	195	203
3	13	285	275
3	14	118	117
4	0	361	367
4	1	255	263
4	2	405	421
4	3	384	352
4	4	916	902
4	5	128	24
4	6	248	189
4	7	56	45
4	8	223	132
4	9	147	155
4	10	184	84
4	11	55	45
4	12	217	198
5	1	711	733
5	2	259	258
5	3	250	273
5	4	898	943
5	5	534	530
5	6	175	137
5	7	298	304
5	8	426	460
5	10	146	144
5	11	146	148
5	13	647	530
5	-12	39	57
6	0	625	668
6	1	214	221
6	2	410	411
6	3	88	97
6	4	616	651
6	5	722	742
6	6	195	112
6	7	437	439
6	8	811	771
6	9	214	211
6	10	128	139
6	12	222	227
6	13	197	177
7	1	216	219
7	5	222	221
7	6	161	152
7	7	244	240
7	8	180	174
7	9	125	111
7	10	329	305
7	12	375	395
7	-11	86	57
8	0	1325	1355
8	1	567	562
8	2	122	105
8	3	199	203
8	4	280	254
8	5	388	391
8	6	224	90
8	7	125	116
8	8	243	123
8	9	274	279
8	10	275	255
8	11	297	331
9	1	411	411
9	2	304	309
9	3	356	333
9	4	406	415
9	6	128	121
9	7	154	163
9	8	95	20
9	9	163	187
9	10	190	172
9	11	191	197
9	-5	55	66
10	0	165	153
10	1	166	165
10	2	155	39
10	3	293	292
10	4	124	109
10	5	166	148
10	6	278	250
10	7	214	184
10	8	306	245
10	9	552	553
10	10	92	15
11	1	128	132
11	3	404	377
11	4	520	538
11	5	293	313
11	6	236	214
11	7	294	297
11	8	485	474
12	0	152	128
12	1	292	274
12	3	307	289
12	4	250	227
12	6	192	196
12	-7	42	50
13	1	296	275
13	2	262	222
13	4	128	143
13	5	337	317

L = 1

H	K	FO	FC
-7	-5	215	34
-5	-4	86	42
0	0	464	412
0	2	513	509
0	4	556	538
0	6	1838	1823
0	8	203	203
0	10	62	74
0	12	373	351
0	14	114	143
1	2	67	46
1	3	481	462
1	4	78	81
1	5	482	474
1	6	460	449
1	7	507	500
1	9	64	72
1	10	341	344
1	11	410	386
1	12	212	221
1	13	116	128
1	14	137	134
2	0	474	505
2	1	625	639
2	2	1117	1060
2	3	944	897
2	4	267	267
2	5	214	215
2	6	100	113
2	8	137	133
2	9	67	71
2	10	141	145
2	11	352	366
2	12	172	150
2	13	99	111
3	2	1468	1486
3	3	408	428
3	4	198	211
3	6	123	126
3	7	415	420
3	8	63	65
3	9	305	319
3	10	577	647
3	12	238	276
3	13	91	81
4	0	349	371
4	2	369	384
4	3	245	272
4	5	134	144
4	6	200	223
4	7	125	135
4	8	470	478
4	9	229	216
4	10	646	652
5	1	417	452
5	2	820	890
5	3	204	234
5	5	153	150
5	6	91	16
5	7	723	733
5	8	214	180
5	9	73	78
5	10	448	475
5	11	291	330
5	12	90	115
5	13	215	211
6	0	84	103
6	1	760	779
6	2	796	878
6	3	98	124
6	4	254	277
6	5	204	214
6	6	431	442
6	7	134	35
6	8	294	303
6	9	130	151
6	10	199	196
6	11	286	312
7	2	183	181
7	3	106	100
7	4	179	186
7	6	330	343
7	7	250	226
7	8	155	45
7	9	152	143
7	11	250	266
8	1	273	283
8	2	216	229
8	3	294	290
8	4	298	293
8	5	447	472
8	6	902	938
8	7	349	366
8	8	137	137
8	9	71	62
8	10	74	83
8	11	300	303
9	1	109	111
9	2	177	201
9	3	349	349
9	4	254	275
9	5	299	308
9	6	182	200
9	7	246	261
9	8	119	150
9	9	100	92
9	10	408	413
10	0	280	269
10	2	205	220
10	3	515	526
10	5	164	182
10	6	106	114
10	9	172	34
11	1	388	367
11	2	590	609
11	3	259	239
11	5	137	143
11	7	89	107
12	0	286	275
12	3	217	237
12	4	133	139
12	5	231	217
12	6	111	132
13	1	229	236
13	2	99	115

L = 2

H	K	FO	FC
-9	-8	72	16
-6	-3	79	79
-3	-2	126	49
0	0	2224	1952
0	2	152	151
0	4	337	289
0	6	294	293
0	8	252	219
0	10	313	298
0	12	754	652
1	1	556	519
1	2	63	73
1	3	209	190
1	4	233	230
1	5	291	269
1	6	197	197
1	7	141	142
1	8	125	115
1	9	222	221
1	10	157	140
1	11	171	164
1	12	355	365
2	2	210	194
2	3	350	338
2	4	440	456
2	5	524	519
2	6	305	254
2	7	96	100
2	8	613	623
2	9	589	580
2	10	147	123
3	1	265	264
3	3	418	417
3	4	950	979
3	6	233	219
3	8	620	631
3	10	201	231
3	11	136	138
3	12	152	164
4	2	318	269
4	3	247	229
4	4	671	609
4	5	265	11
4	6	265	150
4	8	103	104
4	9	108	115
4	12	156	167
5	1	486	489
5	2	186	170
5	3	168	183
5	4	640	667
5	5	381	371
5	6	117	98
5	7	212	229
5	8	322	350
5	10	110	116
5	11	128	124
6	0	442	460
6	1	158	151
6	2	282	292
6	4	603	474
6	5	521	537
6	6	108	77
6	7	326	335
6	8	575	606
6	9	144	154
6	10	75	109
7	1	157	157
7	5	177	170
7	6	84	109
7	7	192	183
7	8	125	125
7	9	76	86
7	10	253	238
8	0	1009	1016
8	1	423	422
8	2	73	81
8	3	134	143
8	4	203	182
8	5	287	300
8	9	208	219
9	1	297	302
9	2	230	233
9	3	250	253
9	4	303	327
9	7	117	137
10	0	83	111
10	1	127	128
10	3	222	234
10	4	199	94
10	5	120	113
10	6	213	191

10	7	165	149
11	3	316	302
11	4	428	427
11	5	243	247
12	0	65	109
12	1	236	223
12	2	148	54

L = 3

H	K	FO	FC
-9	-1	84	83
-7	-5	104	29
-7	-3	50	51
-7	-2	43	76
-2	-6	49	69
-1	-9	43	52
0	0	192	187
0	2	238	229
0	4	284	274
0	6	1018	1019
0	8	79	108
1	2	108	26
1	3	228	221
1	5	237	240
1	6	245	247
1	7	250	265
1	10	215	227
2	2	517	508
2	3	497	430
2	4	137	147
2	5	116	113
2	8	79	90
3	2	752	735
3	3	213	208
3	4	86	107
3	7	210	232
3	9	174	204
4	0	200	206
4	2	185	187
4	3	124	136
4	6	152	172
4	8	272	279
4	9	127	131
5	1	227	233
5	2	496	479
5	3	110	118
5	7	425	429
5	8	124	107
6	1	435	423
6	2	505	504
6	4	161	162
6	5	91	122
6	6	260	257
6	7	60	22
6	8	221	189
7	6	214	214
7	7	145	145
8	1	152	169
8	3	157	165
8	4	200	176
8	5	312	296
8	6	584	599
9	2	101	129
9	3	220	209
9	4	166	174

L = 4

H	K	FO	FC
-4	0	113	138
-4	-1	64	82
-3	-4	542	461
-2	-1	72	64
0	0	1011	872
0	4	87	108
1	1	228	213
1	3	64	73
1	4	91	129
2	3	128	144
2	4	212	230
3	1	109	104
3	3	215	194

APPENDIX F. CALCULATED AND OBSERVED STRUCTURE FACTOR AMPLITUDES (x10) FOR Sc_4Cl_6N (2)

L = -3

H	K	FO	FC
-5	5	66	77
7	-5	44	46

L = -2

H	K	FO	FC
-11	2	45	28
-4	11	44	25
2	-12	58	36

L = -1

H	K	FO	FC
-3	11	50	42

L = 0

H	K	FO	FC
-9	11	146	148
0	2	253	251
0	4	376	394
0	6	413	419
0	8	251	255
0	10	357	368
0	12	722	695
0	14	272	264
1	1	964	913
1	2	121	113
1	3	340	341
1	4	429	416
1	5	454	449
1	6	277	287
1	7	147	146
1	8	216	214
1	9	274	279
1	10	215	212
1	11	187	171
1	12	452	436
1	13	166	174
2	0	233	229
2	1	238	230
2	2	312	311
2	3	528	523
2	4	702	689
2	5	742	754
2	6	365	366
2	7	94	101
2	8	803	799
2	9	782	768
2	10	104	123
2	12	43	48
2	13	186	171
3	1	435	440
3	2	118	82
3	3	631	631
3	4	1442	1461
3	6	318	331
3	8	777	773
3	10	291	287
3	11	135	133
3	12	206	197
3	13	242	236
3	14	124	114
4	0	379	363
4	1	283	278
4	2	385	372
4	3	448	392
4	4	920	920
4	5	93	25
4	6	159	149
4	7	54	76
4	8	137	142
4	9	150	151
4	12	172	165
5	1	702	714
5	2	270	278
5	3	186	193
5	4	851	847
5	5	494	507
5	6	178	150
5	7	242	228
5	8	353	348
5	10	146	138
5	11	138	131
5	13	457	467
5	-12	55	39
6	0	585	610
6	1	211	227
6	2	362	366
6	3	115	115
6	4	560	587
6	5	666	677
6	6	128	128
6	7	413	405
6	8	709	699
6	9	180	171
6	10	92	103
6	12	165	171
6	13	178	176
7	1	139	136
7	5	216	211
7	6	119	111
7	7	221	225
7	8	176	168
7	9	84	83
7	10	301	279
7	11	117	131
7	12	342	334
7	-4	54	57
8	0	1088	1135
8	1	501	518
8	2	53	60
8	3	157	161
8	4	197	198
8	5	334	337
8	6	53	38
8	7	80	87
8	8	38	52
8	9	240	239
8	10	230	223
8	11	263	251
9	1	304	327
9	2	268	286
9	3	315	328
9	4	333	346
9	6	96	98
9	7	104	97
9	8	65	12
9	9	96	136
9	10	156	135
9	-5	39	47
10	0	138	152
10	1	144	138
10	3	179	177
10	4	60	73
10	5	111	95
10	6	174	174
10	7	211	191
10	8	169	161
10	9	448	411
10	10	51	43
11	1	74	85
11	3	282	282
11	4	370	355
11	5	240	243
11	6	181	177
11	7	249	243
11	8	339	325
12	0	47	78
12	1	184	205
12	2	66	91
12	3	212	221
12	4	152	161
12	6	134	140
12	-7	54	63
13	1	161	163
13	2	163	157
13	4	72	57
13	5	202	194

L = 1

H	K	FO	FC
-10	-4	44	40
-8	-10	47	50
-8	-9	40	31
-7	-12	75	80
-6	-12	59	74
-6	-7	68	47
-5	-4	47	39
-4	-1	64	81
-3	-8	61	68
-3	-5	42	41
-1	-14	158	154
-1	-13	65	76
-1	-9	40	56
-1	-4	84	89
-1	-1	41	48
0	0	450	400
0	2	528	506
0	4	540	549
0	6	1822	1850
0	8	219	229
0	12	348	350
0	14	87	97
1	2	131	32
1	3	486	496
1	5	421	435
1	6	493	494
1	7	449	474
1	10	326	324
1	11	409	401
1	12	211	200
2	0	521	504
2	1	639	614
2	2	1137	1088
2	3	895	929
2	4	230	231
2	5	223	214
2	6	46	60
2	7	66	84
2	8	122	125
2	9	47	49
2	10	78	102
2	11	331	325
2	12	162	166
2	13	100	121
3	1	139	123
3	2	1441	1507
3	3	402	403
3	4	211	220
3	6	136	141
3	7	414	410
3	9	263	262
3	10	572	566
3	12	254	263
3	13	66	77
4	0	361	357
4	2	363	359
4	3	273	283
4	5	152	143
4	6	205	214
4	7	132	137
4	8	452	454
4	9	252	248
4	10	673	641
4	12	74	84
5	1	390	405
5	2	793	811
5	3	176	178
5	5	137	138
5	7	726	710
5	8	205	197
5	10	377	375
5	11	305	303
5	12	71	102
5	13	158	151
6	0	144	149
6	1	731	757
6	2	803	827
6	3	80	89
6	4	242	235
6	5	211	207
6	6	387	391
6	8	272	270
6	9	139	128
6	10	170	165
6	11	255	243
7	2	184	181
7	3	93	86
7	4	165	160
7	5	76	71
7	6	331	324
7	7	197	182
7	8	41	25
7	9	127	118
7	11	238	228
8	1	238	232
8	2	183	168
8	3	256	256
8	4	257	259
8	5	423	421
8	6	749	751
8	7	325	322
8	8	151	141
8	11	270	263
9	1	71	90
9	2	144	158
9	3	309	317
9	4	242	254
9	5	245	247
9	6	169	167
9	7	197	200
9	8	81	112
9	9	93	106
9	10	339	340
10	0	197	181
10	2	145	152
10	3	401	402
10	5	151	160
10	6	97	122
10	9	58	31
11	1	311	312
11	2	448	430
11	3	177	188
11	4	65	72
11	5	57	81
11	7	70	86
12	0	206	215
12	3	162	167
12	4	126	130
12	5	148	158
12	6	82	91
13	1	111	123
13	2	48	53

L = 2

H	K	FO	FC
-10	-4	62	61
-8	-7	70	69
-8	-2	60	53
-4	-12	139	139
-4	-10	46	37
-4	-8	116	122
-4	-7	41	57
-4	-6	137	122
-1	-7	113	107
-1	-2	72	70
0	0	2259	2132
0	2	125	139
0	4	273	284
0	6	294	304
0	8	191	205
0	10	284	299
0	12	596	576
1	1	524	520
1	3	238	235
1	4	241	252
1	5	307	315
1	6	202	203
1	8	160	152
1	9	212	220
1	10	165	167
1	11	144	141
1	12	374	365
2	0	134	130
2	1	146	142
2	2	186	185
2	3	326	335
2	4	432	439
2	5	519	523
2	6	255	272
2	7	72	70
2	8	629	627
2	9	597	598
2	10	79	105
3	1	320	297
3	2	62	51
3	3	392	406
3	4	922	997
3	6	228	240
3	8	594	597
3	10	219	228
3	11	101	110
3	12	165	166
4	0	198	194
4	1	181	176
4	2	262	254
4	3	296	268
4	4	616	637
4	5	125	15
4	9	103	117
5	1	500	501
5	2	206	194
5	3	135	128
5	4	601	622
5	5	366	370
5	6	123	111
5	7	193	177
5	8	283	277
5	10	115	113
5	11	96	111
6	0	431	447
6	1	178	164
6	2	283	273
6	3	83	90
6	4	423	437
6	5	499	511
6	6	71	88
6	7	312	324
6	8	545	567
6	9	125	133
6	10	73	87
7	1	105	97
7	4	38	28
7	5	184	172
7	6	85	84
7	7	184	177
7	8	131	130
7	9	81	67
7	10	239	232
8	0	844	874
8	1	407	405
8	3	123	119
8	4	147	155
8	5	273	269
8	6	50	36
8	9	198	199
9	1	248	252
9	2	244	224
9	3	273	264
9	4	290	284
9	6	85	79
9	7	68	82
10	0	114	113
10	1	108	109
10	2	47	31
10	3	158	147
10	5	71	76
10	6	146	145
10	7	161	161
11	1	77	70
11	3	264	235
11	4	304	295
11	5	208	202
12	1	190	172
12	2	63	75

L = 3

H	K	FO	FC
-9	-4	192	173
-9	-1	55	67
-7	-7	142	126
-7	-3	44	49

-6	0	93	70
-6	-8	191	187
-4	-5	109	95
-3	-1	69	75
0	0	192	196
0	2	270	267
0	4	304	308
0	6	1071	1088
0	8	125	126
1	2	37	20
1	3	253	265
1	5	243	237
1	6	294	297
1	7	262	274
1	10	228	231
2	0	263	261
2	1	323	306
2	2	578	547
2	3	513	485
2	4	136	142
2	5	128	120
2	8	69	92
3	2	777	799
3	3	224	210
3	4	101	118
3	6	84	98
3	7	240	252
3	8	41	43
3	9	178	178
4	0	224	208
4	2	172	178
4	3	149	155
4	6	158	161
4	7	77	94
4	8	305	302
4	9	165	167
5	1	253	225
5	2	471	476
5	3	89	90
5	7	435	459
5	8	120	131
6	1	455	450
6	2	503	503
6	4	161	155
6	5	128	131
6	6	267	262
7	2	83	91
7	4	90	99
7	6	235	220
8	1	149	147
8	2	99	115
8	3	165	163
8	4	189	177
8	5	324	287
9	2	117	111
9	3	222	214

L = 4

H	K	FO	FC
-4	-2	140	143
-2	-1	76	68
0	0	1116	1038
0	4	121	142
0	-2	74	87
1	1	272	242
1	3	89	116
1	4	155	157
2	0	71	90
2	2	83	108
2	3	151	166
2	4	252	234
3	1	141	146
3	3	228	211
4	0	123	131
4	1	102	100

APPENDIX G. CALCULATED AND OBSERVED STRUCTURE FACTOR AMPLITUDES FOR Sc_5Cl_8C

-12	15	49	54	-2	5	495	509	12	0	123	124	9	6	57	69	12	2	55	69	10	1	302	294
-12	16	95	104	-2	7	602	611	12	2	84	85	11	2	217	218	12	3	158	151				
-10	1	316	310	-2	8	316	289	12	3	182	174	11	3	155	160	14	2	285	284				
-10	2	345	336	-2	10	64	66	12	6	124	116	11	5	239	245	16	1	81	88				
-10	3	109	111	-2	11	194	194	14	2	337	328	11	6	87	92								
-10	4	58	64	-2	13	109	114	14	4	100	100	13	0	80	83		K =	3					
-10	5	187	199	0	1	144	137	14	-1	42	55	13	2	195	212	H	L	FO	FC				
-10	7	83	89	0	2	66	81	16	1	94	99	13	3	91	94	-13	0	66	65				
-10	8	53	65	0	3	86	98	16	2	99	100	15	0	198	203	-9	-4	57	66				
-10	9	45	50	0	4	221	237	16	3	59	40	15	1	191	179	-1	-3	47	66				
-10	10	105	103	0	5	146	148									1	1	85	79				
-10	11	82	94	0	7	83	115		K =	1			K =	2		1	2	147	133				
-10	12	197	174	0	8	59	73	H	L	FO	FC	H	L	FO	FC	1	4	633	634				
-10	13	250	229	0	9	110	113	-13	-4	53	48	0	0	1311	1111	1	5	116	115				
-10	14	367	353	0	10	54	74	-11	-1	44	42	0	1	95	83	1	6	64	65				
-10	15	118	109	0	12	161	156	1	0	60	57	0	2	53	56	1	8	133	142				
-10	16	82	73	2	0	224	213	1	1	167	161	0	3	77	79	1	9	96	99				
-8	1	197	201	2	1	239	241	1	2	233	227	0	4	174	174	3	0	193	184				
-8	2	137	142	2	2	244	248	1	3	110	109	0	5	101	105	3	1	312	290				
-8	3	342	340	2	3	133	138	1	4	924	1018	0	7	74	95	3	2	57	65				
-8	4	304	314	2	4	72	92	1	5	183	182	0	9	91	97	3	3	122	118				
-8	5	461	451	2	5	90	96	1	6	107	106	0	10	46	62	3	4	101	98				
-8	7	692	678	2	6	147	156	1	8	180	188	2	0	135	121	3	6	109	115				
-8	8	429	409	2	7	155	161	1	9	141	141	2	1	172	161	3	7	86	95				
-8	9	111	113	2	8	480	482	1	12	71	72	2	2	179	167	5	1	45	62				
-8	10	325	323	2	9	109	106	3	0	368	346	2	3	98	95	5	3	110	127				
-8	11	190	193	2	10	140	137	3	1	531	525	2	4	41	67	5	5	213	225				
-8	12	53	45	2	11	111	112	3	2	115	117	2	5	56	65	5	6	126	132				
-6	1	44	48	2	12	104	103	3	3	186	183	2	6	120	128	7	1	142	148				
-6	2	257	264	4	0	225	230	3	4	189	179	2	7	121	134	7	2	176	174				
-6	3	263	242	4	1	814	837	3	5	48	47	2	8	398	412	7	3	61	69				
-6	4	125	132	4	2	326	336	3	6	140	146	2	9	92	92	7	4	318	331				
-6	5	192	160	4	3	103	108	3	7	121	133	2	10	121	120	7	5	53	48				
-6	6	653	624	4	4	294	301	3	8	53	70	4	0	152	142	7	6	101	97				
-6	7	121	6	4	5	410	419	3	10	60	56	4	1	609	572	9	0	116	118				
-6	8	77	73	4	7	96	100	3	11	111	98	4	2	245	239	9	1	245	251				
-6	9	210	207	4	8	129	111	5	0	50	59	4	3	68	78	9	3	75	84				
-6	12	47	49	4	11	111	103	5	1	121	118	4	4	243	249	11	2	172	169				
-6	13	238	221	6	0	861	881	5	3	182	194	4	5	325	337	11	3	108	118				
-6	14	72	69	6	1	78	78	5	4	53	55	4	7	77	89	13	2	165	165				
-6	15	89	87	6	2	45	60	5	5	291	304	4	8	92	93	15	0	153	158				
-4	1	342	348	6	3	399	402	5	6	172	182	6	0	636	626								
-4	2	81	87	6	4	145	148	5	8	251	244	6	1	46	52		K =	4					
-4	3	239	247	6	5	97	92	5	9	221	216	6	3	320	320	H	L	FO	FC				
-4	4	83	84	6	7	75	88	5	10	66	71	6	4	120	124	-10	0	64	60				
-4	5	549	552	6	9	106	106	7	0	36	50	6	5	67	72	0	0	681	595				
-4	6	168	180	8	0	109	119	7	1	166	178	6	7	59	74	0	4	88	106				
-4	7	157	155	8	1	67	74	7	2	245	250	8	0	75	80	2	1	78	94				
-4	8	380	376	8	2	207	215	7	3	107	106	8	1	53	62	2	2	109	110				
-4	9	129	140	8	4	93	101	7	4	448	455	8	2	158	170	2	6	63	83				
-4	10	121	129	8	5	170	166	7	5	64	65	8	4	84	86	4	0	52	59				
-4	11	195	189	8	6	132	143	7	6	127	130	8	5	146	151	4	1	363	341				
-4	12	113	115	8	7	116	119	7	7	142	140	8	6	114	125	4	2	129	133				
-4	13	214	196	8	8	232	220	7	8	113	117	8	7	107	103	4	4	158	165				
-4	14	201	192	10	0	132	136	7	9	79	72	10	0	95	104	4	5	211	214				
-2	1	144	148	10	1	511	524	9	0	169	177	10	1	437	440	6	0	378	363				
-2	2	376	357	10	2	176	175	9	1	364	367	10	2	141	140	6	3	200	201				
-2	3	335	336	10	5	294	278	9	3	101	120	10	5	249	241	6	4	79	83				
-2	4	337	327	10	7	98	92	9	4	86	92	12	0	98	98	8	2	96	105				

APPENDIX H. CALCULATED AND OBSERVED STRUCTURE FACTOR AMPLITUDES FOR Sc_5Cl_8N

K = -4

H	L	FO	FC
-14	4	185	175
-14	5	122	133
-14	7	103	93
-14	8	106	134
-12	2	123	137
-12	6	422	416
-10	1	143	151
-10	2	185	176
-10	5	88	81
-10	6	49	46
-10	10	57	51
-8	1	60	90
-8	3	124	134
-8	4	130	133
-8	5	191	184
-8	7	339	336
-8	8	203	192
-8	10	162	178
-6	2	108	112
-6	3	122	117
-6	6	288	279
-6	7	75	9
-6	9	112	111
-4	1	127	125
-4	3	82	79
-4	5	221	218
-4	6	79	92
-4	7	71	80
-4	8	180	184
-4	9	75	82
-2	2	110	115
-2	3	109	112
-2	4	133	137
-2	5	213	203
-2	7	338	327
-2	8	155	142

K = -3

H	L	FO	FC
-19	5	136	144
-19	6	86	89
-19	7	56	68
-19	9	70	93
-17	4	80	80
-17	7	292	293
-17	8	102	116
-17	10	260	265
-17	11	87	103
-15	2	96	98
-15	3	126	126
-15	4	98	102
-15	5	204	208
-15	6	145	149
-15	9	238	245
-15	10	88	93
-15	12	62	71
-13	2	427	416
-13	6	78	72
-13	8	176	172
-13	9	214	229
-13	12	133	142
-11	1	167	167
-11	4	77	82
-11	7	96	107
-11	8	107	116
-11	9	149	140
-11	10	435	454
-11	11	124	118
-11	13	57	73
-9	1	97	113
-9	2	97	101
-9	3	499	494
-9	4	191	194
-9	5	177	184
-9	6	231	236
-9	7	103	115
-9	10	66	26
-7	2	295	285
-7	5	165	161
-7	6	72	71
-7	7	58	55
-7	9	248	249
-7	11	217	225
-7	12	173	187
-5	1	372	355
-5	2	79	82
-5	4	467	434
-5	5	121	116
-5	7	146	145
-5	8	120	122
-5	9	143	144
-5	10	283	281
-3	1	228	210
-3	2	114	108
-3	3	624	541
-3	4	228	180
-3	5	97	103
-3	7	153	159
-3	9	176	164
-3	11	61	78
-1	2	52	66
-1	3	134	133
-1	6	112	127
-1	8	159	161
-1	9	219	199
-1	10	71	79

K = -2

H	L	FO	FC
-22	8	246	231
-22	11	156	160
-22	12	92	108
-20	3	77	84
-20	6	106	111
-20	8	87	88
-20	9	120	127
-20	10	128	125
-20	11	170	175
-20	13	205	214
-18	2	129	126
-18	3	275	261
-18	6	327	323
-18	8	64	76
-18	9	143	167
-18	10	86	94
-18	11	73	88
-18	12	131	140
-16	1	240	225
-16	2	188	182
-16	5	217	205
-16	6	78	79
-16	8	100	111
-16	11	276	292
-16	12	184	192
-16	13	128	144
-16	14	187	193
-16	15	71	95
-14	3	154	154
-14	4	259	265
-14	5	197	206
-14	6	54	85
-14	7	129	137
-14	8	203	206
-14	9	130	145
-14	10	148	164
-14	11	151	146
-14	12	79	70
-14	13	246	251
-14	14	146	132
-12	2	204	205
-12	3	95	105
-12	5	69	77
-12	6	658	648
-12	7	109	102
-12	9	64	77
-12	12	71	76
-12	13	199	214
-12	15	50	46
-10	1	253	243
-10	2	271	269
-10	3	54	78
-10	5	131	147
-10	7	66	73
-10	10	64	80
-10	11	71	72
-10	12	162	148
-10	13	201	197
-10	14	302	310
-10	15	93	98
-8	1	142	151
-8	2	102	101
-8	3	249	243
-8	4	231	229
-8	5	335	326
-8	7	531	526
-8	8	327	313
-8	9	84	93
-8	10	264	274
-8	11	149	160
-6	2	188	185
-6	3	143	147
-6	4	96	95
-6	5	116	107
-6	6	483	459
-6	7	98	9
-6	8	41	48
-6	9	173	172
-6	13	198	190
-6	14	55	63
-4	1	233	228
-4	2	43	58
-4	3	166	157
-4	4	47	57
-4	5	410	385
-4	6	140	140
-4	7	127	123
-4	8	297	295
-4	9	94	114
-4	10	98	105
-4	11	165	168
-4	12	105	101
-4	13	183	169
-2	1	96	92
-2	2	263	224
-2	3	246	217
-2	4	212	210
-2	5	389	366
-2	7	523	494
-2	8	252	227
-2	11	168	168

K = -1

H	L	FO	FC
-23	7	207	200
-23	10	97	95
-23	13	59	46
-21	5	223	199
-21	6	95	103
-21	7	79	90
-21	9	264	252
-21	10	158	166
-21	11	105	107
-21	12	264	256
-21	15	73	84
-19	2	271	252
-19	4	70	75
-19	5	181	181
-19	6	121	111
-19	7	90	100
-19	8	70	68
-19	9	105	120
-19	12	138	130
-19	14	73	84
-19	15	232	227
-19	16	94	87
-17	1	116	111
-17	2	88	81
-17	4	112	106
-17	6	54	74
-17	7	409	398
-17	8	146	154
-17	9	104	100
-17	10	361	353
-17	11	134	130
-17	13	149	159
-17	15	118	113
-17	16	151	169
-15	1	58	63
-15	2	136	139
-15	3	163	168
-15	4	144	143
-15	5	296	286
-15	6	190	197
-15	7	91	101
-15	9	327	315
-15	10	144	133
-15	11	75	98
-15	12	82	99
-15	14	103	108
-15	15	176	169
-15	16	154	154
-13	2	576	572
-13	5	83	82
-13	6	102	107
-13	7	100	111
-13	8	234	240
-13	9	312	323
-13	12	203	204
-13	14	168	177
-13	15	162	150
-13	16	106	103
-11	1	242	242
-11	4	145	151
-11	6	72	81
-11	7	182	184
-11	8	171	172
-11	9	210	204
-11	10	631	617
-11	11	170	156
-11	13	88	95
-9	1	176	182
-9	2	180	186
-9	3	749	763
-9	4	326	330
-9	5	285	288
-9	6	331	345
-9	7	190	190
-9	10	119	25
-9	11	85	91
-9	14	129	134
-7	2	485	484
-7	3	75	88
-7	4	67	75
-7	5	255	255
-7	6	127	131
-7	7	99	95
-7	8	175	172
-7	9	374	365
-7	10	62	74
-7	11	300	295
-7	12	245	247
-7	14	263	255
-7	15	115	116
-5	1	610	632
-5	2	116	126
-5	3	60	64
-5	4	758	772
-5	5	197	193
-5	7	168	176
-5	8	182	180
-5	9	223	215
-5	10	380	374
-5	12	76	79
-5	13	80	90
-3	1	402	406
-3	2	217	215
-3	3	1031	976
-3	4	379	347
-3	5	170	167
-3	7	236	242
-3	9	242	236
-3	10	73	91
-3	11	85	100
-3	12	105	111
-1	1	130	111
-1	2	121	115
-1	3	224	226
-1	4	80	92
-1	5	65	62
-1	6	201	208
-1	8	212	211
-1	9	288	276
-1	10	99	103
-1	11	271	261
-1	12	171	149

K = 0

H	L	FO	FC
-24	8	85	87
-24	11	109	105
-24	12	255	235
-22	5	203	191
-22	6	115	125
-22	8	265	262
-22	11	180	186
-22	12	115	122
-22	14	59	64
-20	1	125	130
-20	3	112	99
-20	6	144	130
-20	8	75	88
-20	9	163	147
-20	10	139	143
-20	11	224	205
-20	12	53	53
-20	13	245	241
-20	14	194	193
-20	15	75	90
-20	16	217	214
-18	1	59	69
-18	2	151	143
-18	3	328	302
-18	6	399	377
-18	7	83	88
-18	8	87	83
-18	9	187	188
-18	10	101	108
-18	11	105	109
-18	12	152	158
-18	13	77	103
-18	16	97	93
-16	1	270	260
-16	2	229	208
-16	5	247	234
-16	6	111	100
-16	7	48	53
-16	8	145	138
-16	10	47	53
-16	11	358	345
-16	12	214	221
-16	13	180	166
-16	14	222	221
-16	15	107	105
-16	16	68	65
-14	2	66	67
-14	3	198	191
-14	4	320	316
-14	5	247	253
-14	6	110	115
-14	7	164	170
-14	8	273	257
-14	9	170	173
-14	10	185	190
-14	11	201	180
-14	12	100	83
-14	13	297	282
-14	14	183	152
-14	16	70	79
-12	1	50	57
-12	2	257	246
-12	3	159	147
-12	5	96	97
-12	6	811	811
-12	7	139	129
-12	9	61	86
-12	10	85	67
-12	11	60	60
-12	12	92	90
-12	13	240	249

K = -4

H	L	FO	FC
-14	4	160	169
-12	6	343	344
-8	7	264	304
-6	6	212	216
-4	5	219	223
-2	5	192	190
-2	7	238	287
4	-6	131	96
8	-5	192	173

K = -3

H	L	FO	FC
-17	7	258	261
-15	9	179	191
-13	2	376	369
-13	9	192	231
-11	10	378	390
-9	3	474	471
-9	4	191	180
-9	6	192	219
-7	2	256	246
-7	9	214	247
-7	12	153	172
-5	1	342	336
-5	4	407	410
-5	5	125	118
-5	10	196	236
-3	1	202	208
-3	3	543	512
-3	4	156	179
-1	9	166	181
1	-6	138	111
7	-11	212	190
9	-5	135	153
11	-1	174	156
15	-5	154	176
15	-3	170	135
17	-10	180	234

K = -2

H	L	FO	FC
-18	3	251	227
-18	6	289	300
-16	2	167	175
-16	5	153	162
-16	11	262	273
-14	4	243	254
-14	8	176	201
-12	2	200	195
-12	6	587	595
-12	13	218	227
-10	1	214	222
-10	2	254	252
-10	13	207	201
-10	14	234	270
-8	3	244	236
-8	4	214	234
-8	5	317	329
-8	7	469	496
-8	8	277	303
-8	10	233	265
-6	2	163	180
-6	6	439	419
-6	9	129	158
-4	0	128	131
-4	1	201	202
-4	3	128	167
-4	5	390	394
-4	6	138	154
-4	8	250	267
-2	0	126	135
-2	2	219	202
-2	3	198	214
-2	4	194	184
-2	5	348	357
-2	7	455	464
-2	8	206	221
-2	11	152	165
4	-13	158	171
14	-13	211	210
14	-5	218	214
14	-3	171	163
16	-1	201	207
22	-8	270	216

K = -1

H	L	FO	FC
-21	9	232	206
-19	2	175	233
-19	15	191	230
-17	7	381	370
-17	10	333	339
-15	5	261	271
-15	6	169	197
-15	9	266	267
-13	2	528	532
-13	8	222	237
-13	9	328	351
-11	1	233	251
-11	4	139	178
-11	7	158	183
-11	8	194	178
-11	9	209	214
-11	10	586	581
-9	1	155	180
-9	2	158	186
-9	3	732	747
-9	4	301	316
-9	5	286	286
-9	6	324	344
-9	7	160	188
-9	10	147	49
-9	14	137	152
-7	2	428	454
-7	5	240	235
-7	8	144	174
-7	9	385	380
-7	11	240	250
-7	12	241	247
-7	14	251	243
-5	1	628	633
-5	4	796	770
-5	5	181	204
-5	7	149	169
-5	8	166	170
-5	9	207	230
-5	10	339	360
-3	1	396	411
-3	2	203	200
-3	3	1048	965
-3	4	412	343
-3	7	214	236
-3	9	216	236
-1	3	211	228
-1	6	144	215
-1	8	192	204
-1	9	235	261
-1	11	232	228
-1	12	142	147
1	-2	130	123
1	-1	114	120
7	-6	113	140
11	-11	157	131
13	-12	216	205
15	-3	147	176
15	-2	136	133
17	-15	133	108
17	-8	131	154
19	-5	151	173
21	-12	253	232
21	-5	211	188
23	-10	176	116
23	-7	209	188

K = 0

H	L	FO	FC
-22	8	267	255
-18	3	257	268
-18	6	348	361
-16	1	257	249
-16	2	199	216
-16	11	346	328
-16	14	202	206
-14	3	175	197
-14	4	291	303
-14	5	238	277
-14	8	251	262
-14	9	135	157
-14	13	260	250
-12	2	223	234
-12	6	758	774
-12	13	251	271
-10	1	295	302
-10	2	322	339
-10	12	204	169
-10	13	267	240
-10	14	320	325
-10	-1	482	499
-8	0	121	125
-8	1	180	178
-8	3	321	326
-8	4	296	311
-8	5	480	471
-8	7	700	652
-8	8	446	409
-8	10	351	319
-6	2	247	252
-6	3	225	242
-6	4	133	137
-6	5	211	181
-6	6	676	609
-6	7	169	34
-6	9	232	214
-6	13	208	224
-4	1	331	343
-4	3	257	244
-4	5	596	564
-4	6	182	200
-4	7	188	183
-4	8	346	346
-4	9	123	144
-4	11	166	177
-4	13	201	201
-2	1	131	162
-2	2	417	375
-2	3	348	325
-2	4	325	322
-2	5	550	508
-2	7	541	585
-2	8	306	290
-2	11	167	201
0	1	126	149
0	4	228	233
0	5	149	161
0	12	160	157
2	0	228	227
2	1	252	249
2	2	245	251
2	3	132	137
2	6	126	143
2	7	169	196
2	8	462	448
4	0	200	202
4	1	815	808
4	2	338	347
4	4	297	310
4	5	423	410
6	0	870	891
6	3	390	387
6	4	139	154
6	7	126	88
8	2	160	188
8	5	177	163
8	8	230	209
8	-11	166	185
8	-2	111	142
10	2	177	173
10	5	314	284
10	-15	139	95
10	-11	123	98
10	-5	239	224
12	3	165	177
12	-3	130	136
14	2	292	294
14	-10	178	186
14	-7	175	178
16	-13	152	169
16	-12	254	227
16	-8	160	157
16	-5	195	185
18	-2	161	140
20	-13	203	206
20	-11	228	198
22	-11	216	184
22	-5	151	147
24	-12	253	194

K = 1

H	L	FO	FC
-3	-6	160	142
-1	-8	166	180
1	1	135	166
1	2	235	225
1	3	114	127
1	4	1039	987
1	5	203	191
1	9	145	151
3	0	341	340
3	1	540	515
3	3	188	188
3	4	177	174
5	1	123	142
5	3	146	187
5	5	282	268
5	6	162	191
5	8	234	249
5	9	213	199
7	1	158	172
7	2	228	236
7	4	465	447
9	0	133	157
9	1	370	368
11	2	230	212
11	5	230	217
13	2	180	203
15	0	187	180
15	1	198	187

K = 2

H	L	FO	FC
-10	-2	142	132
-6	-4	126	136
-2	-7	188	150
0	0	1109	1076
0	4	141	183
2	1	126	138
2	2	140	167
2	8	381	375
4	1	547	550
4	2	225	229
4	4	247	241
4	5	352	322
6	0	613	610
6	3	315	293
8	2	125	149
8	5	148	138
10	1	418	417
10	5	230	241
14	2	217	253

K = 3

H	L	FO	FC
-11	-2	158	135
-7	-2	140	165
-1	-9	192	113
-1	-8	140	139
1	4	625	588
3	1	286	279
5	5	202	209
7	4	341	307
9	1	241	246

K = 4

H	L	FO	FC
0	0	597	539
4	1	292	322
4	5	202	194
6	0	321	329
10	1	305	275

APPENDIX I. CALCULATED AND OBSERVED STRUCTURE FACTOR AMPLITUDES (x10) FOR 1T-Sc_2Cl_2C

H = -1

K	L	FO	FC
-2	4	27	30
2	-8	24	31

H = 0

K	L	FO	FC
0	1	174	178
0	2	174	170
0	3	27	27
0	4	293	290
0	5	191	192
0	6	264	253
0	7	168	161
0	8	39	39
0	9	123	112
0	10	63	62
1	0	239	240
1	2	279	282
1	3	107	105
1	4	359	376
1	5	179	188
1	7	78	86
1	8	113	119
1	9	174	173
1	10	43	49
2	0	164	163
2	2	358	354
2	3	134	132
2	4	22	35
2	5	33	38
2	6	147	150
2	7	157	154
2	8	104	99
3	0	269	256
3	1	49	52
3	2	70	70
3	4	135	134
3	5	98	98

H = 1

K	L	FO	FC
0	2	551	535
0	3	198	194
0	4	35	42
0	5	37	49
0	6	188	190
0	7	190	189
0	8	126	121
0	9	102	100
0	10	26	36
1	0	451	437
1	1	99	96
1	2	112	109
1	4	206	206
1	5	139	144
1	6	195	192
1	7	127	125
1	9	99	92
2	0	129	126
2	2	156	154
2	3	60	63
2	4	214	217
2	5	113	111

H = 2

K	L	FO	FC
0	1	26	28
0	2	203	197
0	3	82	78
0	4	262	271
0	5	139	138
0	7	72	70
0	8	100	99
1	2	272	273
1	3	103	100
1	5	31	30
1	6	127	125
2	0	222	213
2	1	34	43

H = 3

K	L	FO	FC
0	1	48	52
0	2	70	70
0	4	135	134
0	5	84	97

APPENDIX J. CALCULATED AND OBSERVED STRUCTURE FACTOR AMPLITUDES (x10) FOR 1T-Sc_2Cl_2N

H = -3

K	L	FO	FC
2	-1	20	15

H = 0

K	L	FO	FC
-2	6	20	20
0	1	195	-191
0	2	170	-153
0	3	52	-43
0	4	327	-292
0	5	249	216
0	6	287	252
0	7	190	-175
0	8	60	53
0	9	172	-149
0	10	62	-53
1	2	259	-279
1	3	111	115
1	4	361	379
1	5	192	-204
1	6	31	31
1	7	115	-114
1	8	112	-118
1	9	197	208
1	10	33	38
1	-1	12	-13
2	2	336	358
2	3	138	-142
2	4	25	-24
2	5	52	-53
2	6	146	-153
2	7	174	180
2	8	93	94
3	1	58	-55
3	2	69	-66
3	4	139	-138
3	5	114	113

H = 1

K	L	FO	FC
0	0	222	-231
0	2	510	541
0	3	205	-212
0	4	28	-24
0	5	63	-70
0	6	187	-193
0	7	212	220
0	8	112	114
0	9	104	-106
0	10	37	44
1	0	461	442
1	1	103	-105
1	2	98	-98
1	4	204	-209
1	5	162	163
1	6	195	191
1	7	137	-135
1	8	42	41
1	9	121	-123
2	2	154	-155
2	3	72	72
2	4	216	219
2	5	115	-120
2	6	19	15

H = 2

K	L	FO	FC
0	0	150	-158
0	1	16	21
0	2	197	-197
0	3	87	87
0	4	271	274
0	5	143	-150
0	7	92	-93
0	8	95	-99
1	0	127	-125
1	2	285	277
1	3	109	-108
1	4	25	-22
1	5	45	-43
1	6	126	-128

H = 3

K	L	FO	FC
0	0	286	261
0	1	59	-55
0	2	67	-66
0	4	145	-138
0	5	115	113

APPENDIX K. CALCULATED AND OBSERVED STRUCTURE FACTOR AMPLITUDES FOR 3R-$ScClH_{1.0}$ (ZrCl-type)

H = 0

K	L	FO	FC
-2	32	14	17
0	3	65	59
0	6	131	147
0	9	17	18
0	12	178	187
0	15	104	103
0	18	152	156
0	21	81	79
0	27	40	39
0	30	58	53
0	33	85	76
0	36	17	19
1	2	47	44
1	5	18	12
1	8	210	244
1	11	83	91
1	14	139	159
1	17	53	58
1	20	31	35
1	23	56	60
1	26	75	80
1	29	81	80
1	32	17	21
2	1	23	20
2	4	204	208
2	7	49	53
2	10	102	109
2	13	25	28
2	16	63	69
2	19	56	64
2	22	84	91
2	25	61	67
2	28	9	13
3	0	162	147
3	3	25	22
3	6	60	52
3	9	8	10
3	12	94	83
3	15	57	50
3	18	92	82
3	21	48	45
4	8	70	79
4	11	31	31

H = 1

K	L	FO	FC
0	1	31	21
0	4	311	313
0	7	66	76
0	10	145	153
0	13	40	39
0	16	87	90
0	19	72	79
0	22	107	112
0	25	76	80
0	28	14	17
0	34	28	28
1	0	322	249
1	3	53	39
1	6	103	86
1	9	20	18
1	12	151	130
1	15	88	75
1	18	137	120
1	21	73	62
1	27	39	32
1	30	56	45
1	33	82	65
2	2	22	21
2	5	11	8
2	8	128	132
2	11	51	52
2	14	91	96
2	17	33	36
2	20	20	23
2	23	40	41
2	26	54	57
2	29	60	59
3	1	10	10
3	4	104	109
3	7	25	28
3	10	56	60
3	13	11	17
3	16	37	41
3	19	34	37

H = 2

K	L	FO	FC
0	2	29	28
0	5	16	13
0	8	161	170
0	11	64	66
0	14	110	119
0	17	41	44
0	20	24	28
0	23	48	49
0	26	63	67
0	29	69	68
1	1	14	14
1	4	158	159
1	7	38	40
1	10	84	86
1	13	18	22
1	16	53	56
1	19	49	52
1	22	73	77
1	25	53	57
2	0	141	122
2	3	22	19
2	6	50	44
2	12	80	71
2	15	49	42
2	18	79	69
2	21	42	39

H = 3

K	L	FO	FC
0	3	27	22
0	6	58	52
0	9	8	10
0	12	95	83
0	15	58	50
0	18	93	82
0	21	50	45
1	2	15	14
1	8	87	92
1	11	37	36
1	14	66	68
1	17	23	28

H = 4

K	L	FO	FC
-4	2	13	12
0	4	82	93
0	7	20	25
0	10	47	51

APPENDIX L. PARAMETERS USED IN MOLECULAR ORBITAL AND BAND CALCULATIONS WITH EXTENDED HUCKEL METHOD

Table L1. VALENCE ORBITAL IONIZATION ENERGIES AND ZETAS OF ATOMS USED IN EXTENDED HUCKEL CALCULATIONS

ATOM	NS[a]	EXPS[b]	COULS[c]	NP[d]	EXPP[e]	COULP[f]	ND[g]	EXPD[h]	COULD[i]	C1[j]	EXPD2[k]	C2[l]
Sc	4	1.40	-7.18	4	1.40	-4.52	3	4.35	-7.03	0.4050	1.50	0.7708
Cl	3	2.36	-30.00	3	2.04	-15.00						
B	2	1.30	-15.20	2	1.30	8.50						
C	2	1.625	-21.50	2	1.625	-11.40						
N	2	1.950	-26.00	2	1.95	-13.40						

[a]Principal quantum number of the valence s orbital. [b]Zeta of the valence s orbital. [c]s valence orbital ionization energy (eV). [d]Principal quantum number of the valence p orbitals. [e]Zeta of the valence p orbitals. [f]p valence orbital ionization energy (eV). [g]Principal quantum number of the valence d orbitals. [h]First zeta of the valence d orbital double zeta expansion. [i]d valence orbital ionization energy (eV). [j]Coefficient of the first zeta. [k]Second zeta of the valence d orbital double zeta expansion. [l]Coefficient of the second zeta.

Table L2. Geometries of clusters used for extended Hückel calculations

Cluster	Point group	Atom	x	y	z
$Sc_6Cl_{18}B^{9-}$	D_{3d}				
		Sc	-1.9012	0.0000	1.3366
		Sc	0.9506	1.6465	1.3366
		Cl	0.0000	3.6230	0.0000
		Cl	-3.1376	1.8115	0.0000
		Cl	2.0543	0.0000	3.0037
		Cl	-1.0272	1.7791	3.0037
		Cl	2.0673	3.5806	2.9067
		Cl	-4.1345	0.0000	2.9067
$Sc_6Cl_{18}N^{3-}$	D_{3d}				
		Sc	-1.8799	0.0000	1.3182
		Sc	0.9399	1.6280	1.3182
		Cl	0.0000	3.6220	0.0000
		Cl	-3.1367	1.8110	0.0000
		Cl	2.1051	0.0000	2.9524
		Cl	-1.0526	1.8231	2.9524
		Cl	2.0633	3.5737	2.8936
		Cl	-4.1266	0.0000	2.8936
Sc_2Cl_2C	(one slab, 2-dimensional condensed cluster)				
		Sc	0.0000	1.9628	1.6635
		Sc	0.0000	0.0000	4.0924
		Cl	0.0000	0.0000	0.0000
		Cl	0.0000	1.9628	5.7559